AD A137256

AD F200 371

MEMORANDUM REPORT ARBRL-MR-03329

(Supersedes IMR No. 787)

FURTHER ANALYSIS OF YAWSONDE DATA FROM SOME LIQUID PAYLOAD PROJECTILES

Russell L. Pope
Defense Research Center
Australia

December 1983

US ARMY ARMAMENT RESEARCH AND DEVELOPMENT CENTER

BALLISTIC RESEARCH LABORATORY

ABERDEEN PROVING GROUND, MARYLAND

Approved for public release; distribution unlimited.

Destroy this report when it is no longer needed.
Do not return it to the originator.

Additional copies of this report may be obtained from the National Technical Information Service, U. S. Department of Commerce, Springfield, Virginia 22161.

The findings in this report are not to be construed as an official Department of the Army position, unless so designated by other authorized documents.

The use of trade names or manufacturers' names in this report does not constitute indorsement of any commercial product.

UNCLASSIFIED

SECURITY CLASSIFICATION OF THIS PAGE (When Data Entered)

REPORT DOCUMENTATION PAGE		READ INSTRUCTIONS BEFORE COMPLETING FORM
1. REPORT NUMBER MEMORANDUM REPORT ARBRL-MR-03329	2. GOVT ACCESSION NO. AD-A137 256	3. RECIPIENT'S CATALOG NUMBER
4. TITLE (and Subtitle) FURTHER ANALYSIS OF YAWSONDE DATA FROM SOME LIQUID PAYLOAD PROJECTILES		5. TYPE OF REPORT & PERIOD COVERED Final 6. PERFORMING ORG. REPORT NUMBER
7. AUTHOR(s) Russell L. Pope*		8. CONTRACT OR GRANT NUMBER(s)
9. PERFORMING ORGANIZATION NAME AND ADDRESS U.S. Army Ballistic Research Laboratory, ARDC ATTN: DRSMC-BLL(A) Aberdeen Proving Ground, Maryland 21005		10. PROGRAM ELEMENT, PROJECT, TASK AREA & WORK UNIT NUMBERS RDT&E 1L162618AH80
11. CONTROLLING OFFICE NAME AND ADDRESS US Army AMCCOM, ARDC Ballistic Research Laboratory, ATTN:DRSMC-BLA-S(A) Aberdeen Proving Ground, Maryland 21005		12. REPORT DATE December 1983 13. NUMBER OF PAGES 82
14. MONITORING AGENCY NAME & ADDRESS(if different from Controlling Office)		15. SECURITY CLASS. (of this report) Unclassified 15a. DECLASSIFICATION/DOWNGRADING SCHEDULE

16. DISTRIBUTION STATEMENT (of this Report)

Approved for public release; distribution unlimited.

17. DISTRIBUTION STATEMENT (of the abstract entered in Block 20, if different from Report)

18. SUPPLEMENTARY NOTES

This report supersedes IMR 787, dated August 1983.
*Dr. Pope is on detail to the Ballistic Research Laboratory from the Defense Research Center, Australia.

19. KEY WORDS (Continue on reverse side if necessary and identify by block number)

Data Analysis
Liquid Payload
Unstable Projectiles
Yawsondes

20. ABSTRACT (Continue on reverse side if necessary and identify by block number) (bja)

Theoretical methods have recently been developed for predicting side moments and rolling moments created by a liquid payload on a spinning, coning projectile. A substantial amount of flight data is available from liquid payload projectiles fitted with yawsondes. There is also considerable data available from laboratory gyroscopes. To facilitate comparisons of flight measurements with theoretical results and with the experimental data base obtained from gyroscope experiments, data from some of the unstable liquid payload rounds have been analyzed in some detail.

DD FORM 1 JAN 73 1473 EDITION OF 1 NOV 65 IS OBSOLETE

UNCLASSIFIED

SECURITY CLASSIFICATION OF THIS PAGE (When Data Entered)

TABLE OF CONTENTS

		Page
	LIST OF ILLUSTRATIONS	5
I.	INTRODUCTION	9
II.	DATA ANALYSIS	10
	A. Interpretation of Yawsonde Data	10
	B. Processing the Data	12
III.	RESULTS	13
	A. High Reynolds Number	14
	B. Low Reynolds Number	14
	C. Felt Wedge Rounds	15
IV.	SUMMARY	15
	REFERENCES	77
	LIST OF SYMBOLS	79
	DISTRIBUTION LIST	81

LIST OF ILLUSTRATIONS

Figure		Page
1a	Roll Acceleration - BRL 404	17
1b	Coning Amplitude - BRL 404	18
1c	Nondimensional Coning Frequency - BRL 404	19
1d	Liquid Roll Moment Coefficient - BRL 404	20
1e	Equivalent Side Moment Coefficient - BRL 404	21
2a	Roll Acceleration - BRL 1339	22
2b	Coning Amplitude - BRL 1339	23
2c	Nondimensional Coning Frequency - BRL 1339	24
2d	Liquid Roll Moment Coefficient - BRL 1339	25
2e	Equivalent Side Moment Coefficient - BRL 1339	26
3a	Roll Acceleration - BRL 1866	27
3b	Coning Amplitude - BRL 1866	28
3c	Nondimensional Coning Frequency - BRL 1866	29
3d	Liquid Roll Moment Coefficient - BRL 1866	30
3e	Equivalent Side Moment Coefficient - BRL 1866	31
4a	Roll Acceleration - BRL 1867	32
4b	Coning Amplitude - BRL 1867	33
4c	Nondimensional Coning Frequency - BRL 1867	34
4d	Liquid Roll Moment Coefficient - BRL 1867	35
4e	Equivalent Side Moment Coefficient - BRL 1867	36
5a	Roll Acceleration - BRL 1868	37
5b	Coning Amplitude - BRL 1868	38
5c	Nondimensional Coning Frequency - BRL 1868	39
5d	Liquid Roll Moment Coefficient - BRL 1868	40
5e	Equivalent Side Moment Coefficient - BRL 1868	41

LIST OF ILLUSTRATIONS (Continued)

Figure		Page
6a	Roll Acceleration - BRL 1955	42
6b	Coning Amplitude - BRL 1955	43
6c	Nondimensional Coning Frequency - BRL 1955	44
6d	Liquid Roll Moment Coefficient - BRL 1955	45
6e	Equivalent Side Moment Coefficient - BRL 1955	46
7a	Roll Acceleration - BRL 1293	47
7b	Coning Amplitude - BRL 1293	48
7c	Nondimensional Coning Frequency - BRL 1293	49
7d	Liquid Roll Moment Coefficient - BRL 1293	50
7e	Equivalent Side Moment Coefficient - BRL 1293	51
8a	Roll Acceleration - BRL 1313	52
8b	Coning Amplitude - BRL 1313	53
8c	Nondimensional Coning Frequency - BRL 1313	54
8d	Liquid Roll Moment Coefficient - BRL 1313	55
8e	Equivalent Side Moment Coefficient - BRL 1313	56
9a	Roll Acceleration - BRL 1585	57
9b	Coning Amplitude - BRL 1585	58
9c	Nondimensional Coning Frequency - BRL 1585	59
9d	Liquid Roll Moment Coefficient - BRL 1585	60
9e	Equivalent Side Moment Coefficient - BRL 1585	61
10a	Roll Acceleration - BRL 1587	62
10b	Coning Amplitude - BRL 1587	63
10c	Nondimensional Coning Frequency - BRL 1587	64
10d	Liquid Roll Moment Coefficient - BRL 1587	65
10e	Equivalent Side Moment Coefficient - BRL 1587	66

LIST OF ILLUSTRATIONS (Continued)

Figure		Page
11a	Roll Acceleration - BRL 1588	67
11b	Coning Amplitude - BRL 1588	68
11c	Nondimensional Coning Frequency - BRL 1588	69
11d	Liquid Roll Moment Coefficient - BRL 1588	70
11e	Equivalent Side Moment Coefficient - BRL 1588	71
12a	Roll Acceleration - BRL 1693	72
12b	Coning Amplitude - BRL 1693	73
12c	Nondimensional Coning Frequency - BRL 1693	74
12d	Liquid Roll Moment Coefficient - BRL 1693	75
12e	Equivalent Side Moment Coefficient - BRL 1693	76

I. INTRODUCTION

A 155mm liquid payload shell which was fired in 1974 and carried a yawsonde telemetry package developed a coning motion with an amplitude of forty to fifty degrees.[1] At this large amplitude the projectile was subject to rapid roll deceleration far in excess of any which might be produced by aerodynamic effects. Since then, one other round containing a low viscosity liquid.[2] several containing high viscosity liquids[3-5] and some rounds with felt wedge-type payloads[6] have exhibited similar behaviour.

Recently, theoretical techniques for predicting the side moment[7] and rolling moment[8] due to the liquid payload have been developed and a substan-

---

1. *W. P. D'Amico, V. Oskay, W. H. Clay, "Flight Tests of the 155mm XM687 Binary Projectile and Associated Design Modification Prior to the Nicolet Winter Test 1974-1975," U.S. Ballistic Research Laboratory, Aberdeen Proving Ground, Maryland, BRL Memorandum Report ARBRL-MR-2746, May 1977 (AD B019969L).*

2. *W. P. D'Amico, W. H. Clay, and A. Mark, "Yawsonde Data for M687-Type Projectiles with Application to Rapid Spin Decay and Stewartson-Type Spin-Up Instabilities," U.S. Ballistic Research Laboratory, Aberdeen Proving Ground, Maryland, BRL Memorandum Report ARBRL-MR-03027, June 1980 (AD A089646).*

3. *W. P. D'Amico, W. H. Clay, and A. Mark, "Diagnostic Tests for Wick-Type Payloads and High-Viscosity Liquids," U.S. Ballistic Research Laboratory, Aberdeen Proving Ground, Maryland, BRL Memorandum Report ARBRL-MR-02913, April 1979 (AD A072812).*

4. *W. P. D'Amico and W. H. Clay, "High Viscosity Liquid Payload Yawsonde Data for Small Launch Yaws," U.S. Ballistic Research Laboratory, Aberdeen Proving Ground, Maryland, BRL Memorandum Report ARBRL-MR-03029, June 1980 (AD A088411).*

5. *W. P. D'Amico and R. J. Yalamanchili, "Yawsonde Tests of the 8-Inch XM877 Binary Projectile: Phase I," U.S. Ballistic Research Laboratory, Aberdeen Proving Ground, Maryland, BRL Memorandum Report in preparation.*

6. *W. P. D'Amico, "Aeroballistic Testing of the XM825 Projectile: Phase III, High Muzzle Velocity and High Quadrant Elevation," U.S. Ballistic Research Laboratory, Aberdeen Proving Ground, Maryland, BRL Memorandum Report ARBRL-MR-03196, September 1982 (AD B068511L).*

7. *C. H. Murphy, "Angular Motion of a Spinning Projectile With a Viscous Liquid Payload," U.S. Ballistic Research Laboratory, Aberdeen Proving Ground, Maryland, BRL Memorandum Report ARBRL-MR-03194, August 1982 (AD A118676). (See also Journal of Guidance, Control, and Dynamics, Vol. 6, No. 4, July-August 1983, pp. 280-286.)*

8. *C. H. Murphy, "Liquid Payload Roll Moment Induced by a Spinning and Coning Projectile," U.S. Ballistic Research Laboratory, Aberdeen Proving Ground, Maryland, BRL Technical Report ARBRL-TR-02521, September 1983 (AD A133684).*

tial experimental data base assembled from gyroscope experiments.[9,10] In order to facilitate comparisons of flight data with theory and gyroscope results, further analysis of the flight data from the unstable liquid payload rounds has been undertaken. Comparison of flight data with theory and gyroscope results is not altogether satisfactory because of gaps in the flight data and large transient effects which violate the basic assumptions in the theory. However, some of the comparisons are useful, particularly where amplitude growth is slow and steady state assumptions are reasonable. The low viscosity, high Reynolds number cases fail to satisfy any such conditions, but the steady state approximation is quite good for some of the high viscosity (low Reynolds number) cases. The Reynolds number (Re) is defined as $a^2\dot{\phi}/\nu$, where a is the radius of the cylinder, $\dot{\phi}$ is the projectile spin rate, and ν is the kinematic viscosity of the liquid.

During the analysis, it was necessary to interpret yawsonde measurements from projectiles exhibiting large amplitude coning motion. The initial reduction of the yawsonde data was carried out using a five point data reduction method developed for use with data from large amplitude coning motion.[11] However, interpretation of spin frequency and coning frequency still presents problems due to the residual spin of the axes system used in the data reduction. Before presenting the derived results for the liquid payload moments we will look at the effects of a spinning axes system.

II. DATA ANALYSIS

A. Interpretation of Yawsonde Data.

A method was outlined within Reference 11 to establish liquid moment coefficients. Yawsonde data from rounds undergoing large amplitude high frequency motion in Reference 12 were reduced using the methods within Reference 11, but the techniques were not automated and did not utilize all of the flight data. The coning rate and spin rate obtained from the yawsonde are

---

9. *M. C. Miller, "Flight Instabilities of Spinning Projectiles Having Nonrigid Payloads," Journal of Guidance, Control, and Dynamics, Vol. 5, March-April 1982, pp. 151-157.*

10. *W. P. D'Amico and M.C. Miller, "Flight Instability Produced by a Rapidly Spinning, Highly Viscous Liquid," Journal of Spacecraft and Rockets, Vol. 16, January-February 1979, pp. 62-64.*

11. *C. H. Murphy, "Effect of Large High-Frequency Angular Motion of a Shell on the Analysis of Its Yawsonde Records," U.S. Ballistic Research Laboratory, Aberdeen Proving Ground, Maryland, BRL Memorandum Report ARBRL-MR-2581, February 1976 (AD B009421L).*

12. *W. P. D'Amico, "Yawsonde Tests for Prototype 155mm Shell Using High Viscosity and Non-Newtonian Liquids," U.S. Ballistic Research Laboratory, Aberdeen Proving Ground, Maryland, BRL Memorandum Report in preparation.*

with respect to a sun fixed reference system. The sun fixed system has a non-zero roll rate with respect to the inertial axes frame. Before considering results for the yawsonde data, we look briefly at the effect of the rolling axes system. The characteristic instability of liquid-filled rounds is always to excite the high frequency mode so that we are concerned with simple high frequency coning motion. The interpretation and use of yawsonde data in this report makes use of two different coordinate systems. The first is an earth fixed or inertial coordinate system, OXYZ, with OX along the velocity vector of the projectile, OZ in the vertical plane, and OY completing an orthogonal system, where the velocity direction is assumed constant over the time period for which the system is used. The second coordinate system is a sun fixed coordinate system, OX'Y'Z', which has OX' along the missile axis, OY' normal to the plane defined by the missile axis and the sun direction, and OZ' such that OX'Z' contains both the missile axis and the sun. Then the yawsonde measures coning rate, $\dot{\gamma}$, and spin rate, $\dot{\phi}$, in the sun fixed coordinate system. The sun fixed coordinate system has spin rate, $\dot{\phi}_A$, relative to the inertial axes system. If p is the spin rate of the projectile relative to the inertial axes OXYZ and $\dot{\phi}_1$ is the coning rate relative to OXYZ, then the spin rate measured by the yawsonde is

$$\dot{\phi} = p - \dot{\phi}_A \tag{2.1}$$

and the coning rate is

$$\dot{\gamma} = \dot{\phi}_1 - \dot{\phi}_A. \tag{2.2}$$

The expression given in Reference 11 for $\dot{\phi}_A$ is valid only for relatively small amplitude coning motion. Following a similar method, but avoiding small angle approximations, it follows that

$$\dot{\phi}_A = 1/2\ \dot{\phi}_1 \tan\alpha \left\{ \sin\sigma_{NT} \sin\alpha - \cos\sigma_{NT} \cos\alpha \sin\Gamma \right\} \times \left\{ \frac{1}{1 - \sin\sigma_{NT}\cos\alpha - \cos\sigma_{NT}\sin\alpha\sin\Gamma} - \frac{1}{1 + \sin\sigma_{NT}\cos\alpha + \cos\sigma_{NT}\sin\alpha\sin\Gamma} \right\} \tag{2.3}$$

where σ_{NT} is the complement of the angle between the sun direction and the velocity vector of the shell, which can be assumed constant over the coning cycle; α is the total incidence or semi-angle of the cone and the equation is uniformly valid for all values of α; $\Gamma = \phi_1 + \phi_A + \phi^*$. The phase angle ϕ^* is a

function of sun position relative to the velocity vector and therefore varies with the velocity. The expression for $\dot{\phi}_A$ can be averaged over one cycle of Γ to give

$$\bar{\dot{\phi}}_A = \dot{\phi}_1 \left[1 - (\cos \alpha)^{-1}\right] \tag{2.4}$$

for $\alpha + \sigma_{NT} < \pi/2$. Thus, the spin rate of the shell

$$p = \dot{\phi} - \dot{\phi}_1 \left[1 - (\cos \alpha)^{-1}\right], \tag{2.5}$$

and the coning rate,

$$\dot{\phi}_1 = \dot{\gamma} \cos \alpha \,. \tag{2.6}$$

B. Processing the Data.

We are interested in estimating the liquid moment coefficients described in References 7 and 8. They are defined by the relations

$$\dot{p}\ I_x = m_L a^2 p^2\ \tau\ K_1\ C_{LRM} + M_{aero} \tag{2.7}$$

for the liquid roll moment coefficient, C_{LRM},

$$\varepsilon = \left(m_L a^2/I_x\right)\left[((2\tau/\sigma)\ -1)\right]^{-1}\left\{C_{LSM} + \sigma_L{}^{-1}\left[\tau^{-1}\ C_{M_{p\alpha}} + C_{M_q} + C_{M_{\dot{\alpha}}}\right]\right\}, \tag{2.8}$$

for the liquid side moment coefficient, C_{LSM},

where $\sigma_L = 2\ m_L a^2 p/\rho S \ell^2 V$.

The yaw growth rate ε is defined by

$$K_1 = K_{10}\ e^{\varepsilon p \tau t} \tag{2.9}$$

so that if aerodynamic effects are negligible,

$$\varepsilon = (m_L a^2/I_x)\ (2\tau/\sigma - 1)^{-1}\ C_{LSM}. \tag{2.10}$$

Then processing of the reduced yawsonde data, that is, measurements of $\dot{\phi}$ and σ_N along the trajectory has been undertaken in four steps.

1. Determine amplitude and frequency of the coning motion by fitting a quadratic to the three points closest to each peak and trough in σ_N. The cone angle 2α is the difference between peaks and troughs and the amplitude $K_1 = \sin\alpha$. The frequency determined by the time delay between two adjacent peaks or troughs is converted to coning frequency using Equation (2.6).

2. The second step is to determine spin rate and acceleration. A moving least squares straight line fit, centered on each point successively, is used to smooth the cyclic variation introduced by the axes spin of Equation (2.3) and Equation (2.5) is used to remove the bias effect.

3. Equation (2.7) can now be used to evaluate C_{LRM} using data from steps 1 and 2. In general, an estimate of the aerodynamic roll damping can be obtained from the estimated roll deceleration at times preceding the onset of the liquid payload instability. The estimate can be used to remove the M_{aero} term from Equation (2.7). In any case, the moment is small compared with the liquid roll moment, once the amplitude becomes large.

4. Finally, by using a least squares logarithmic fit to the amplitude data, we can estimate ε using Equation (2.9). This can be converted to an equivalent total side moment coefficient

$$C_{SMEQ} = C_{LSM} + C_{SMA} \tag{2.11}$$

using Equation (2.8), where

$$C_{SMA} = \sigma_L^{-1}\left[\tau^{-1}\, C_{M_{p\alpha}} + C_{M_q} + C_{M_{\dot{\alpha}}}\right] \tag{2.12}$$

represents the aerodynamic contributions to the side moments. Rough estimates of C_{SMA} are included in Table 2 as a guide to the relative magnitudes of the two side moments. However, the estimates are unreliable and indicate signs and relative magnitudes only. All results show total equivalent side moment. Any interpretation of the results should take this into consideration.

III. RESULTS

The rounds which showed liquid payload instabilities can be divided into three categories, according to the types of liquid used. First, there are the high Reynolds number, low viscosity payloads. Only two examples of instability are available from flight data because it is difficult to generate the exact conditions to produce unstable behaviour for high Reynolds number payloads. Both examples will be discussed in some detail. Next, there are a

number of cases where high viscosity liquids (thus producing low Reynolds numbers) were used in the payload, either corn syrup or silicone oils. Thirdly, there are the cases where the Reynolds number concept is not applicable where solids both fixed and free are included with the liquid payload. These rounds contain liquid white phosphorous and felt wedges in the payload cylinders. Descriptive constants for each round are given in Table 1.

A. High Reynolds Number.

The results for round 7254 are given in Figures 1a-1e and those for 9387 in Figures 2a-2e. The initial behaviour of the rounds is quite different. The first round, an XM687 with 0.5 calibre boattail, was given a large launch disturbance and showed signs of the Magnus instability characteristic of the 0.5 calibre boattail shape. It was also subject to high initial roll deceleration caused by the nonlinear spin-up of the liquid so that the liquid was probably fully spun up after 2 seconds. Coning amplitude grew steadily until a little past 6 seconds, when there was a substantial pulse in the side moment and the amplitude increased rapidly to about 45° where it stabilized. Liquid roll moment was negligible until the very large amplitude was attained, C_{LRM} then grew rapidly to around -0.05. The second round had no initial yaw disturbance. Liquid spin-up was slow and steady and was not completed until around 20 seconds. Near 7 seconds from launch τ corresponded to an eigenvalue of the partially spun-up liquid and coning motion began to grow. (See Reference 2.) Side moment and rolling moment history from then on are similar to those for the first round except for the large pulse in the rolling moment which occurred near 11 seconds.

B. Low Reynolds Number.

Nine rounds containing high viscosity liquid have been analyzed--a group of three 8-inch XM877 rounds, 10-B, 11-B, and 12-B, for which results are shown in Figures 3, 4, and 5; a single 155mm M687-type round for which results are shown in Figure 6; and a group of five M687-type rounds for which results are shown in Figures 7 through 11. The first four rounds contained silicon oil with viscosity of 100,000 centi-stoke and the remaining five rounds were filled with corn syrup at 170,000 centi-stoke.

All the silicon oil-filled shells show similar behaviour--an initial steady yaw growth with C_{SMEQ} around 0.05 with no significant despin, then a short spin-up at only a few degrees coning amplitude (equivalent to quite a large positive roll moment coefficient) together with a significant increase in side moment. These short pulses are followed by a return to C_{SMEQ} near 0.05, this time with C_{LRM} approximately -0.05, leading to large amplitude motion and rapid despin.

The behaviour of the five corn syrup rounds is much less consistent than that of the silicon oil rounds. The data is noisier and the onset of large amplitude motion is far more rapid so that the interpretation of the results is more difficult. In general, the levels for liquid side moment and liquid roll moment are slightly smaller and there are traces of the spin-up behaviour exhibited by the other rounds, but the results are much less definite.

Table 1. Physical Characteristics of Projectiles

Round No.	Figure	Yawsonde No.	Reference	c/a	a	$m_L a^2 / I_x$	σ	Re	ν_L
7254*	1	404	1	4.39	0.0537	0.0767	0.0968	2×10^6	100
9387	2	1339	2	4.97	0.0537	0.0861	0.0941	1.8×10^6	135
10-B	3	1866	5	4.23	0.0692	0.0675	0.1171	45.2	375
11-B	4	1867	5	4.23	0.0692	0.0675	0.1171	45.2	375
12-B	5	1868	5	4.23	0.0692	0.0675	0.1171	45.2	375
----	6	1955	12	5.20	0.0514	0.0719	0.0944	20	175
9394	7	1293	3	4.32	0.0587	0.1615	0.1020	10	200
9391	8	1313	3	4.32	0.0587	0.1615	0.1020	10	200
9540	9	1585	4	4.32	0.0587	0.1615	0.1012	10	200
9542	10	1587	4	4.32	0.0587	0.1615	0.1017	10	200
9543	11	1588	4	4.32	0.0587	0.1615	0.1015	10	200
YPG219	12	1693	6	4.32	0.0587	0.1153	0.1020	----	734

* Fill ratio for 7254 was 87%, all others were 100%.

C. Felt Wedge Rounds.

Figures 12a - 12e show the results of analysis of the data from a liquid white phosphorous-felt wedge round. The results are generally similar to those for the high viscosity liquids, although there is clearly a measurable despin moment before the spin-up pulse as well as after it. Around 3-4 degrees amplitude, we have $C_{LRM} = -0.025$, $C_{SMEQ} = 0.02$. The positive roll moment pulse shows up very clearly.

IV. SUMMARY

A summary of results for the rounds analyzed is given in Table 2. The values of C_{LRM} and C_{SMEQ} have been obtained when possible for moderate amplitudes of several degrees where the coefficients have remained fairly constant over a range of conditions. The results appear to be generally consistent with the result, $C_{LRM} = -C_{LSM}$ from Reference 8. Growth rate for the coning motion on some of the high viscosity rounds is sufficiently slow for the steady state assumption of Reference 8 to be reasonable. Most of the rounds exhibited a characteristic spin-up behaviour at small coning amplitudes just prior to or possibly coincident with rapid increases in coning amplitudes.

Table 2. Summary of Results.

Yawsonde	Re	τ	C_{LRM}	C_{SMEQ}	C_{SMA}
404	2×10^6	0.090	-0.05	0.05	<0.01
1339	1.8×10^6	0.090	-0.02	0.04	-0.005
1866	45.2	0.123	-0.055	0.050	-0.004
1867	45.2	0.123	-0.055	0.050	-0.004
1868	45.2	0.123	-0.060	0.053	-0.004
1955	20	0.087	-0.04	0.04	-0.010
1293	10	0.090	-0.03	0.02	-0.008
1313	10	0.088	-0.02	0.025	-0.008
1585	10	0.091	-0.025	0.02	-0.008
1587	10	0.093	-0.04	0.02	-0.008
1588	10	0.095	-0.03	0.02	-0.008
1693	----	0.094	-0.025	0.025	-0.005

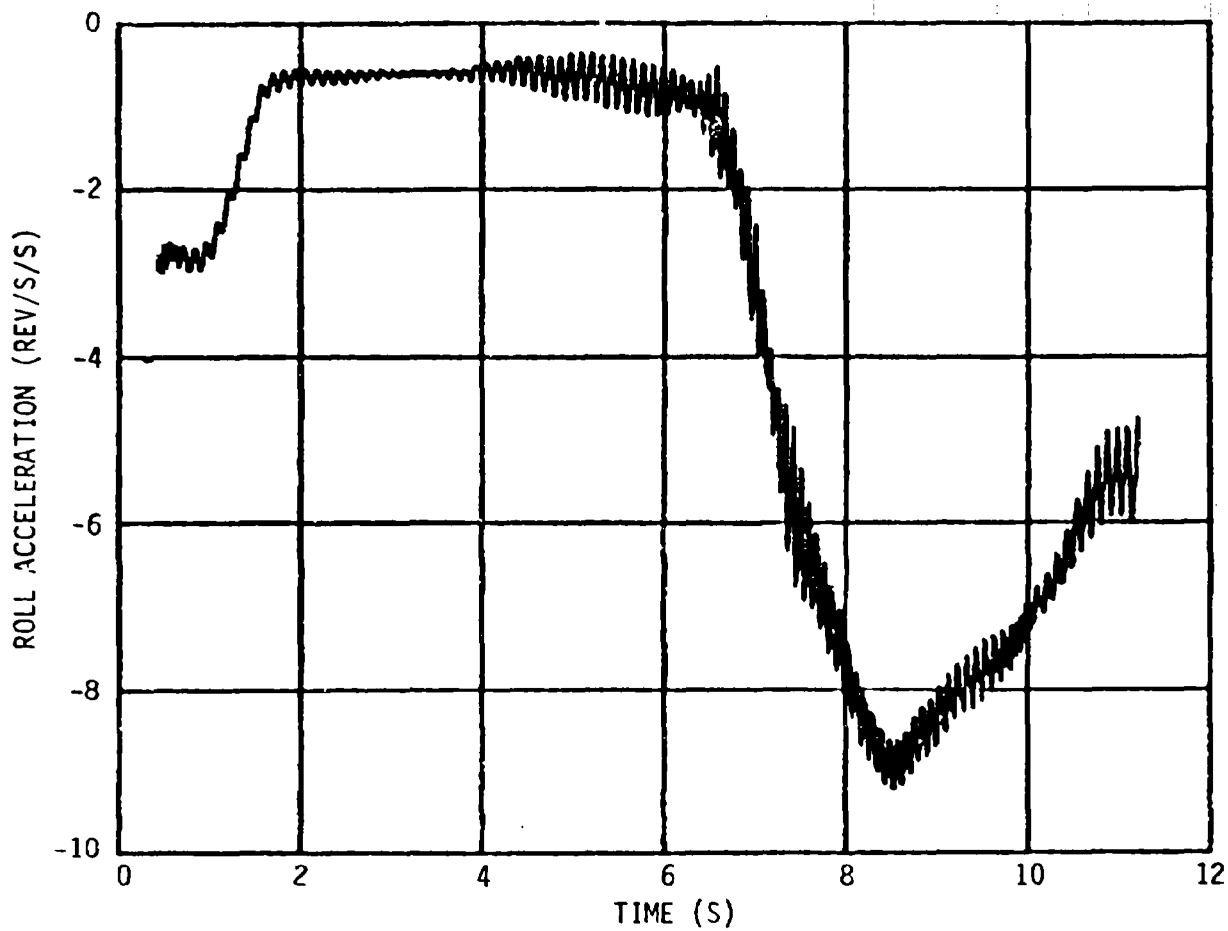

Figure 1a. Roll Acceleration - BRL 404.

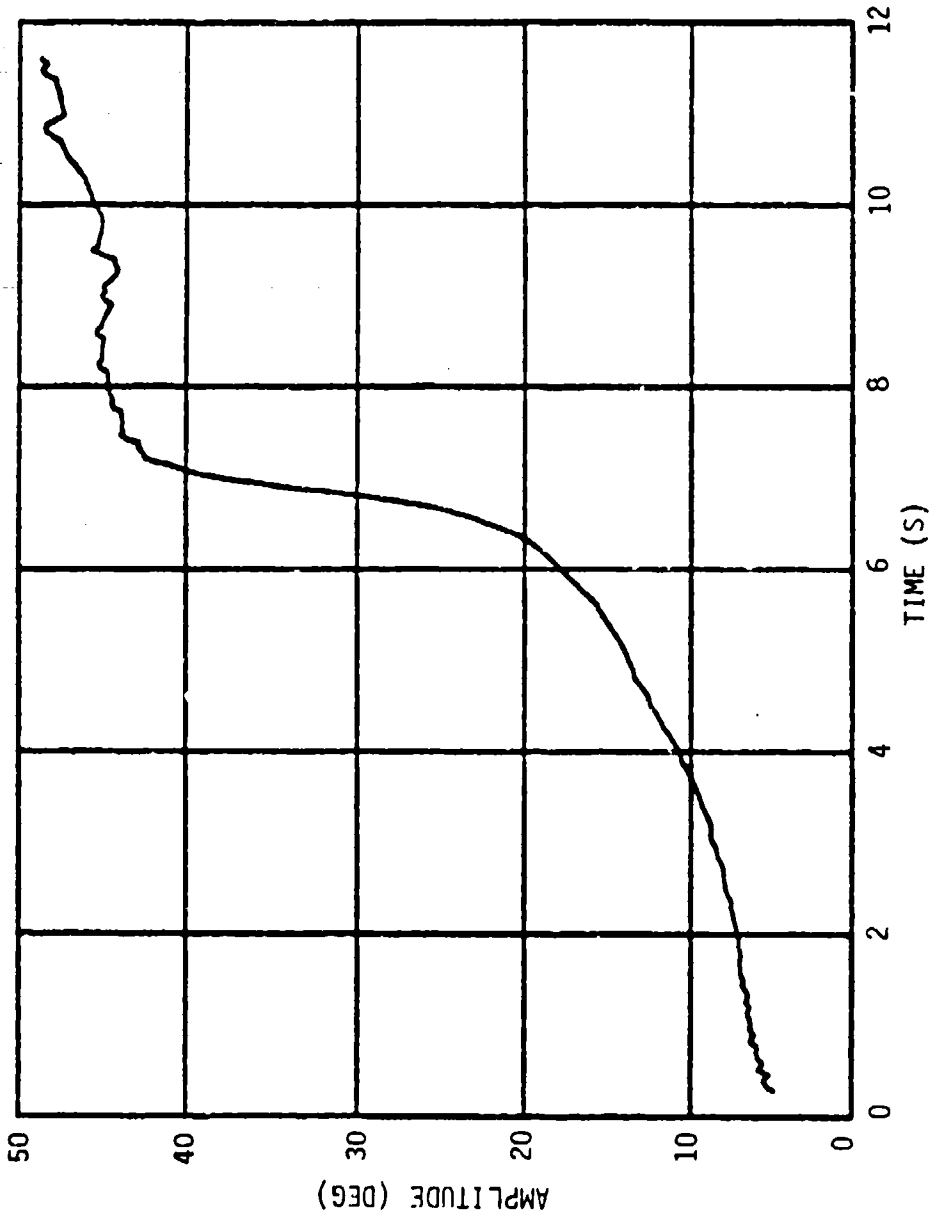

Figure 1b. Coning Amplitude - BRL 404.

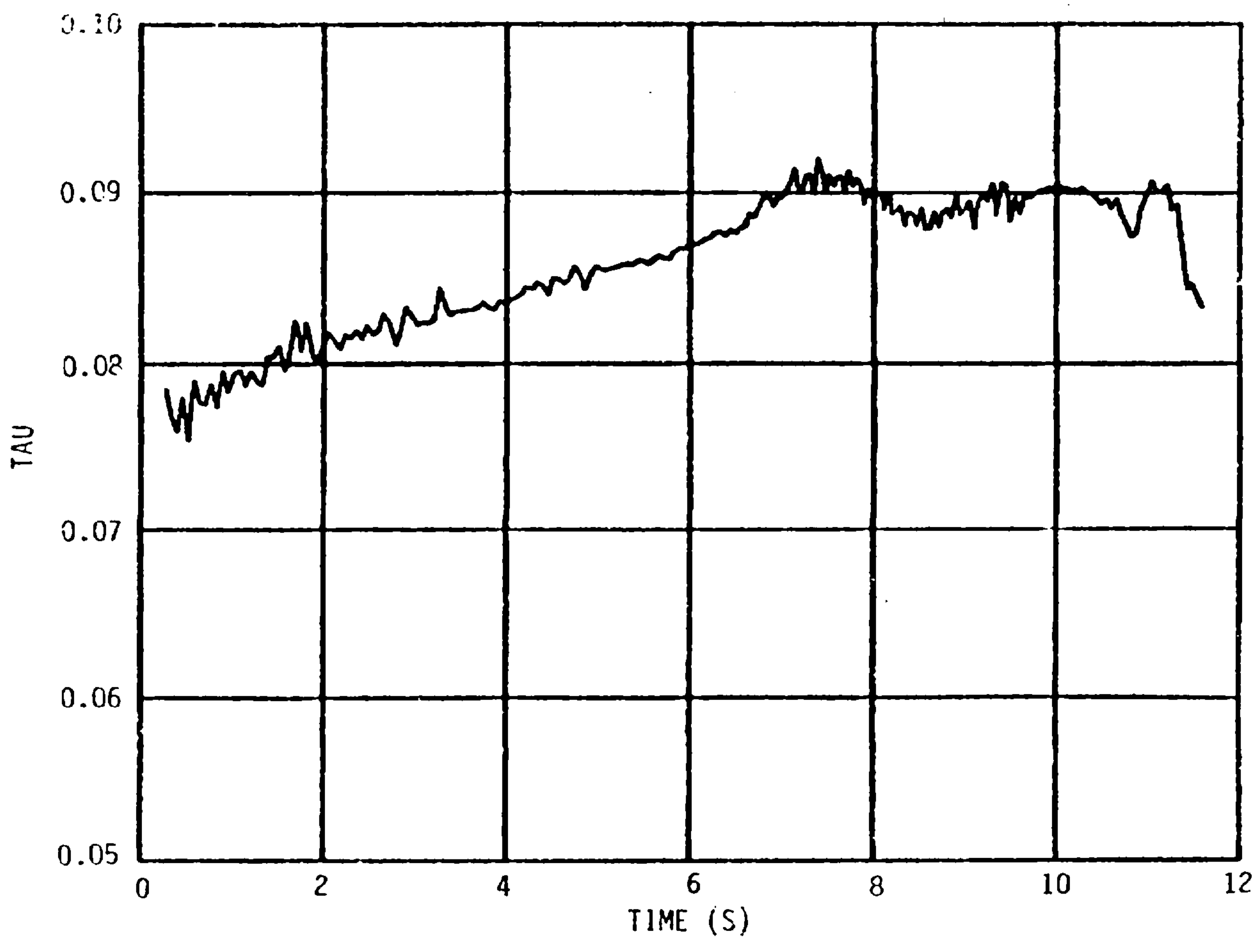

Figure 1c. Nondimensional Coning Frequency - BRL 401.

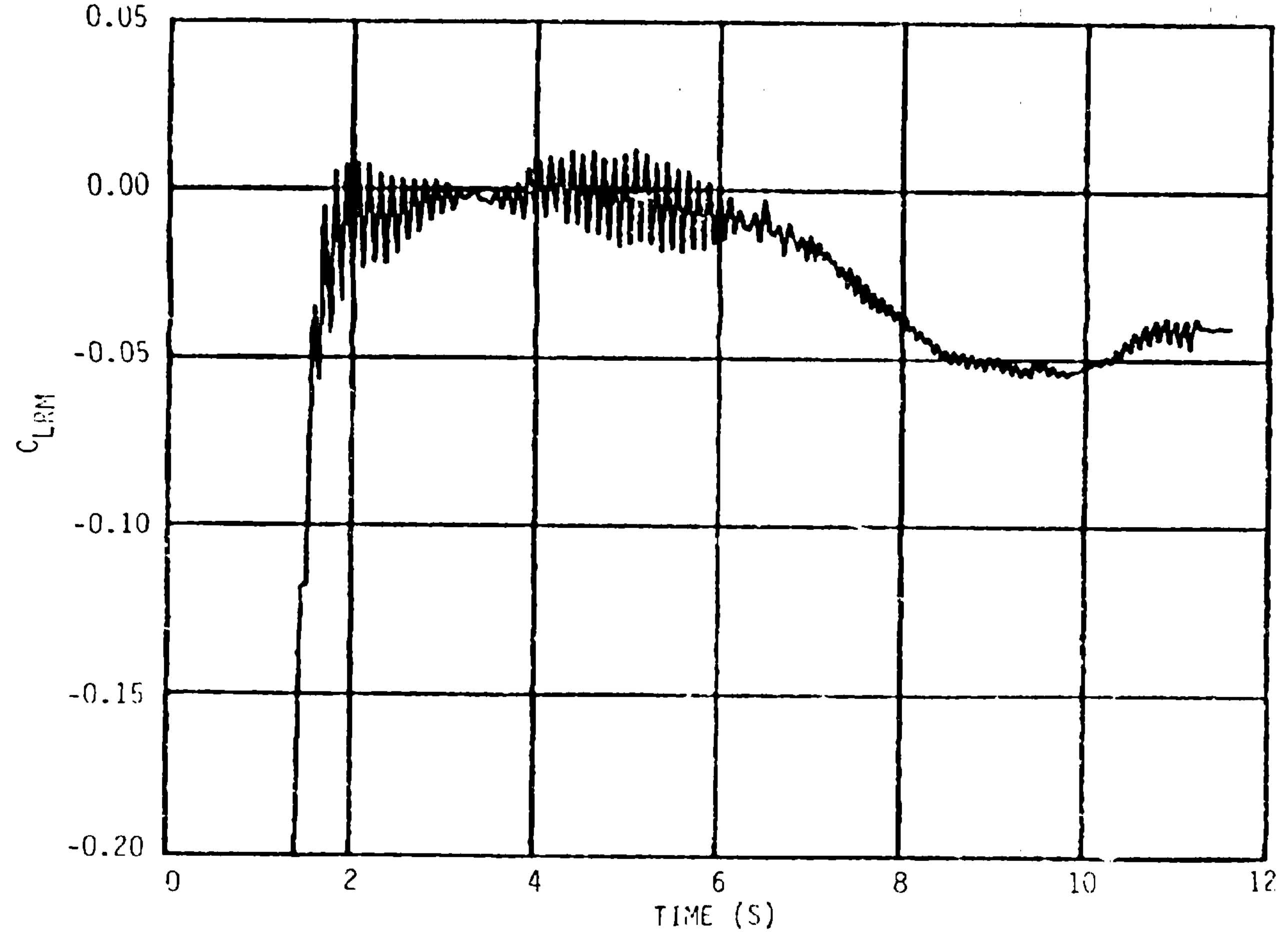

Figure 1d. Liquid Roll Moment Coefficient - BRL 404.

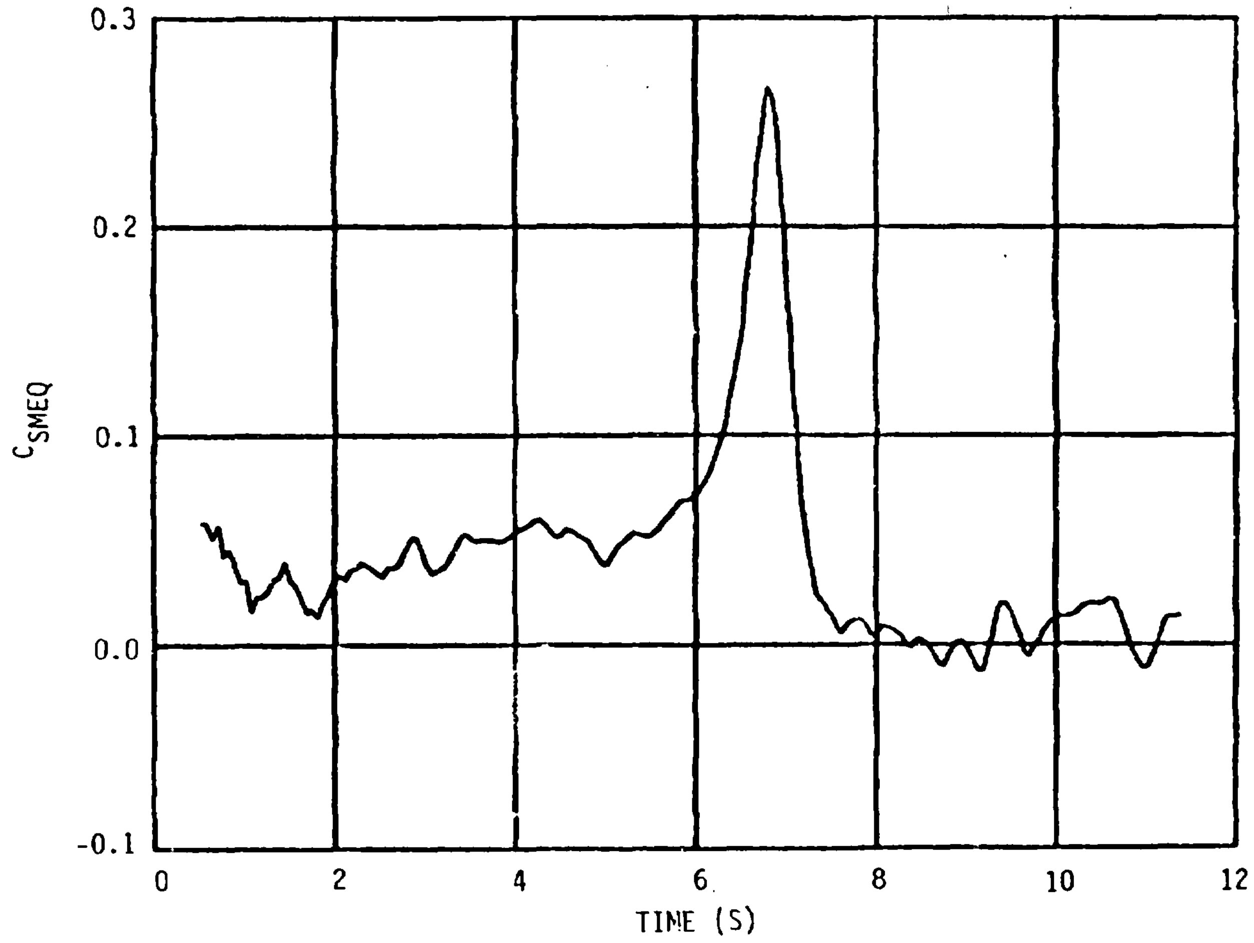

Figure 1e. Equivalent Side Moment Coefficient - BRL 404.

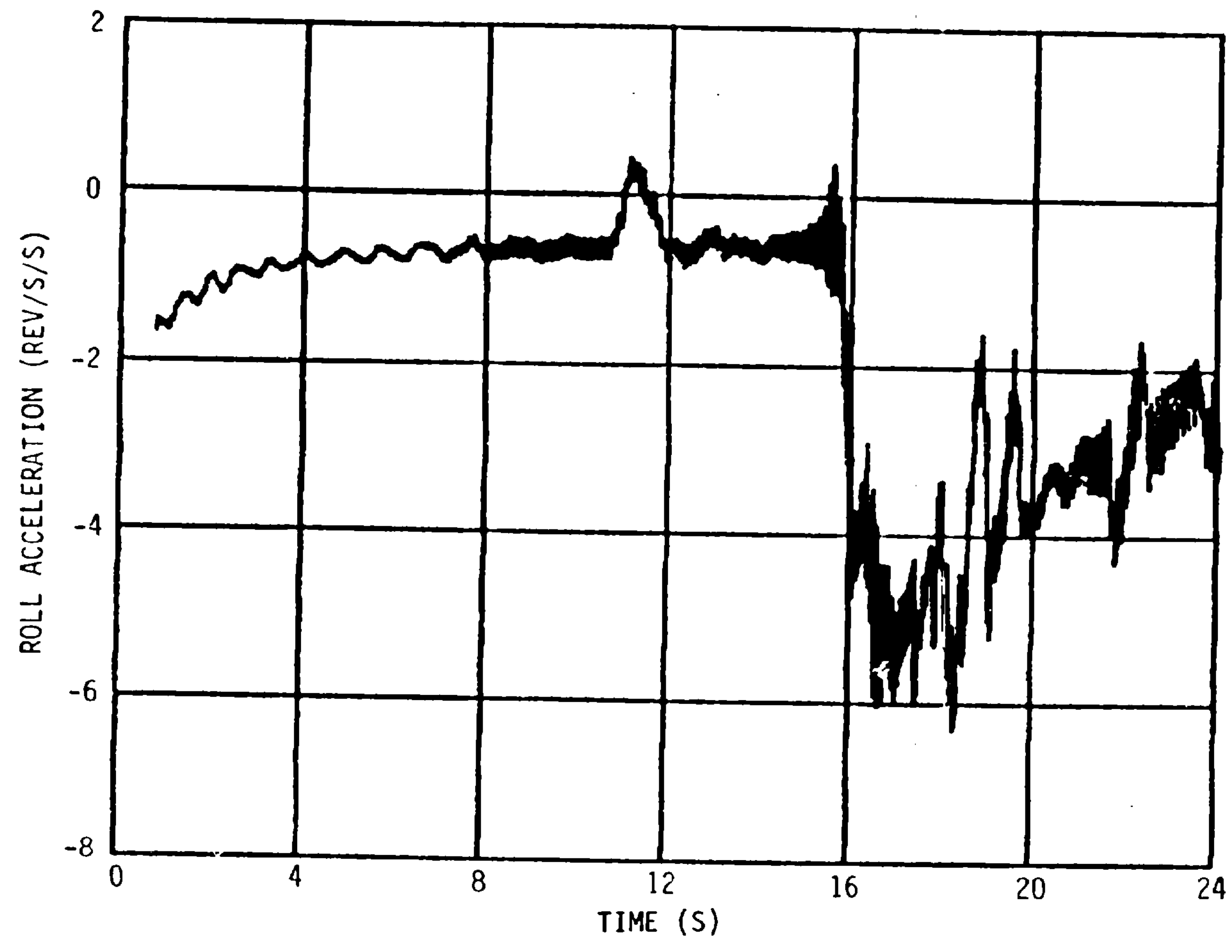

Figure 2a. Roll Acceleration - BRL 1339.

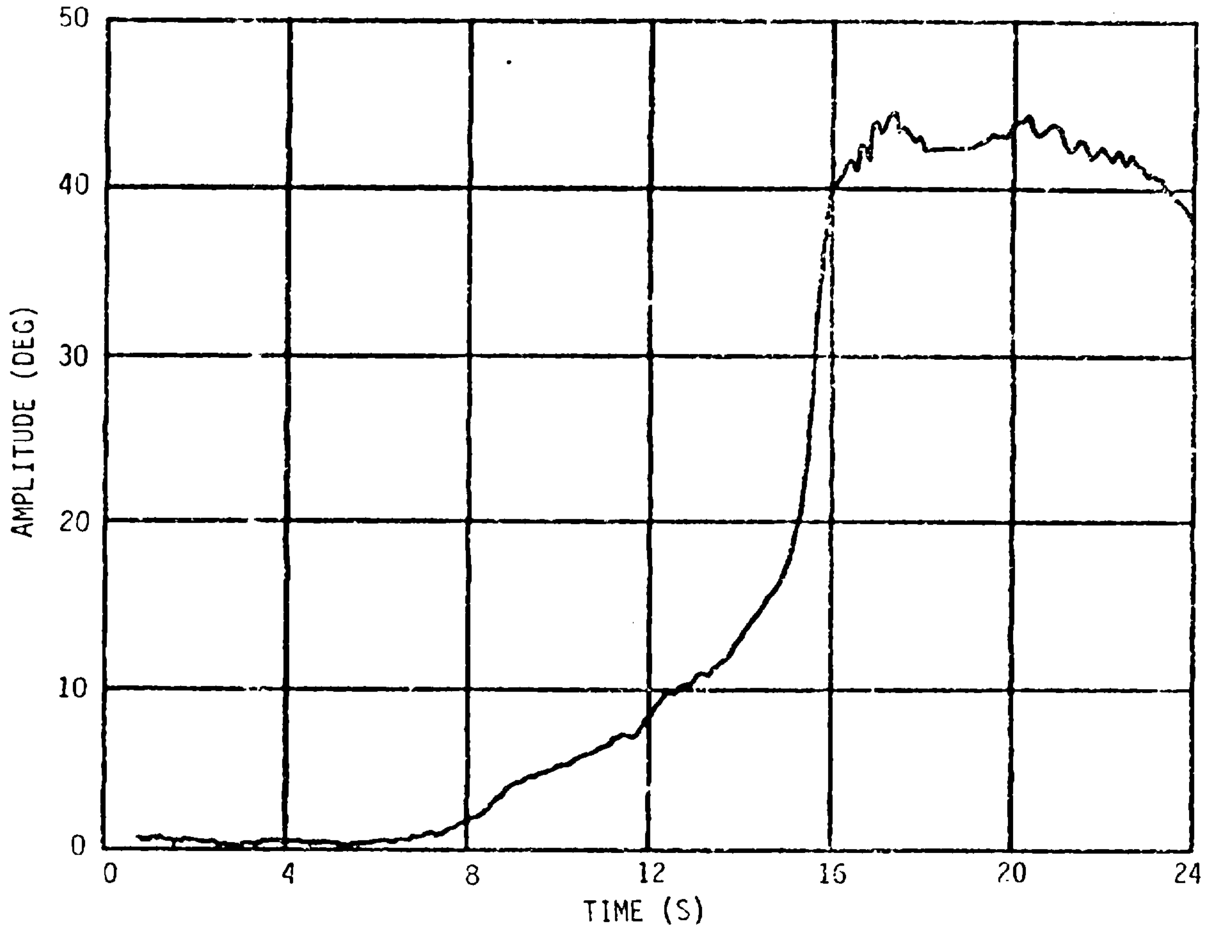

Figure 2b. Coning Amplitude - BRL 1329.

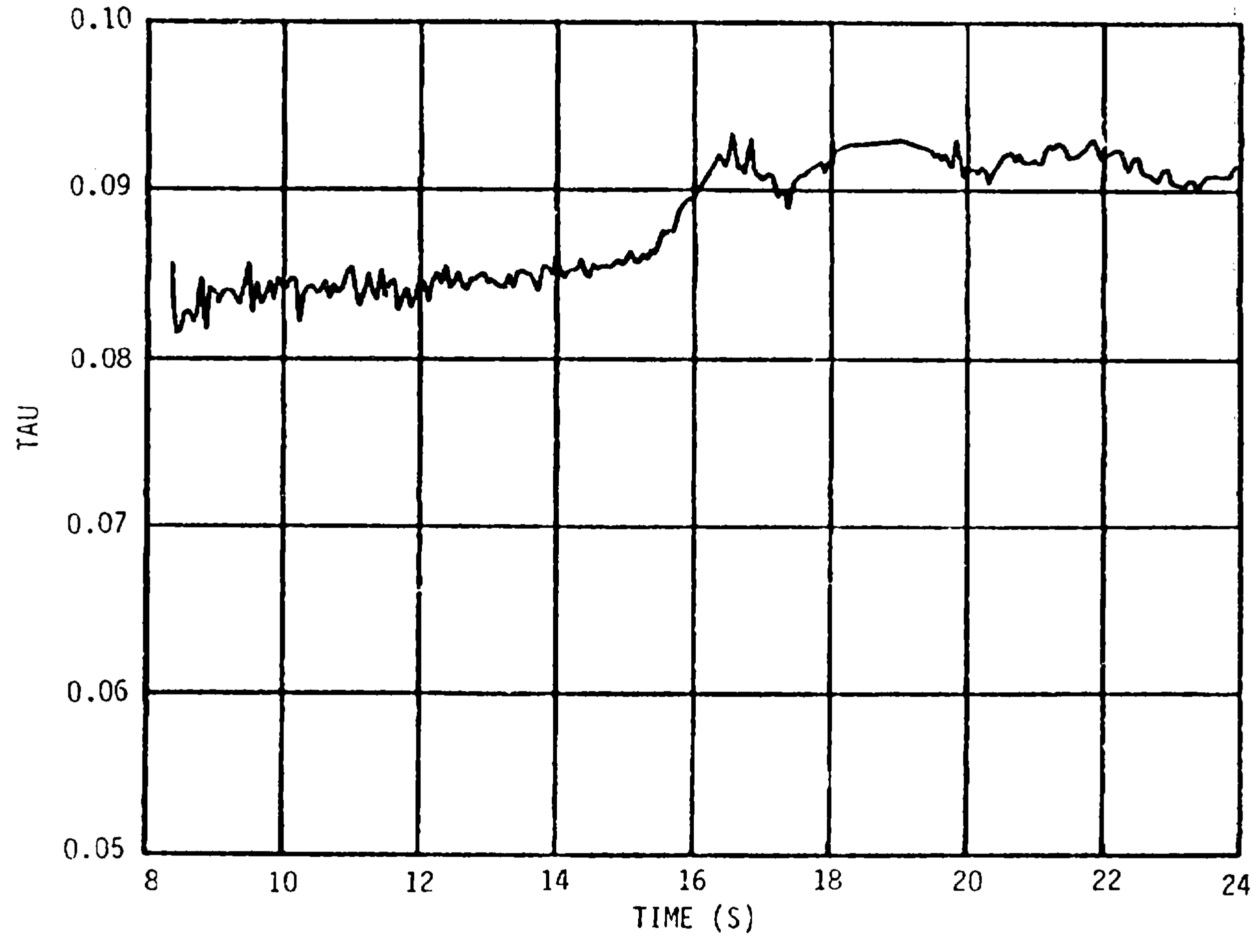

Figure 2c. Nondimensional Coning Frequency - BRL 1339.

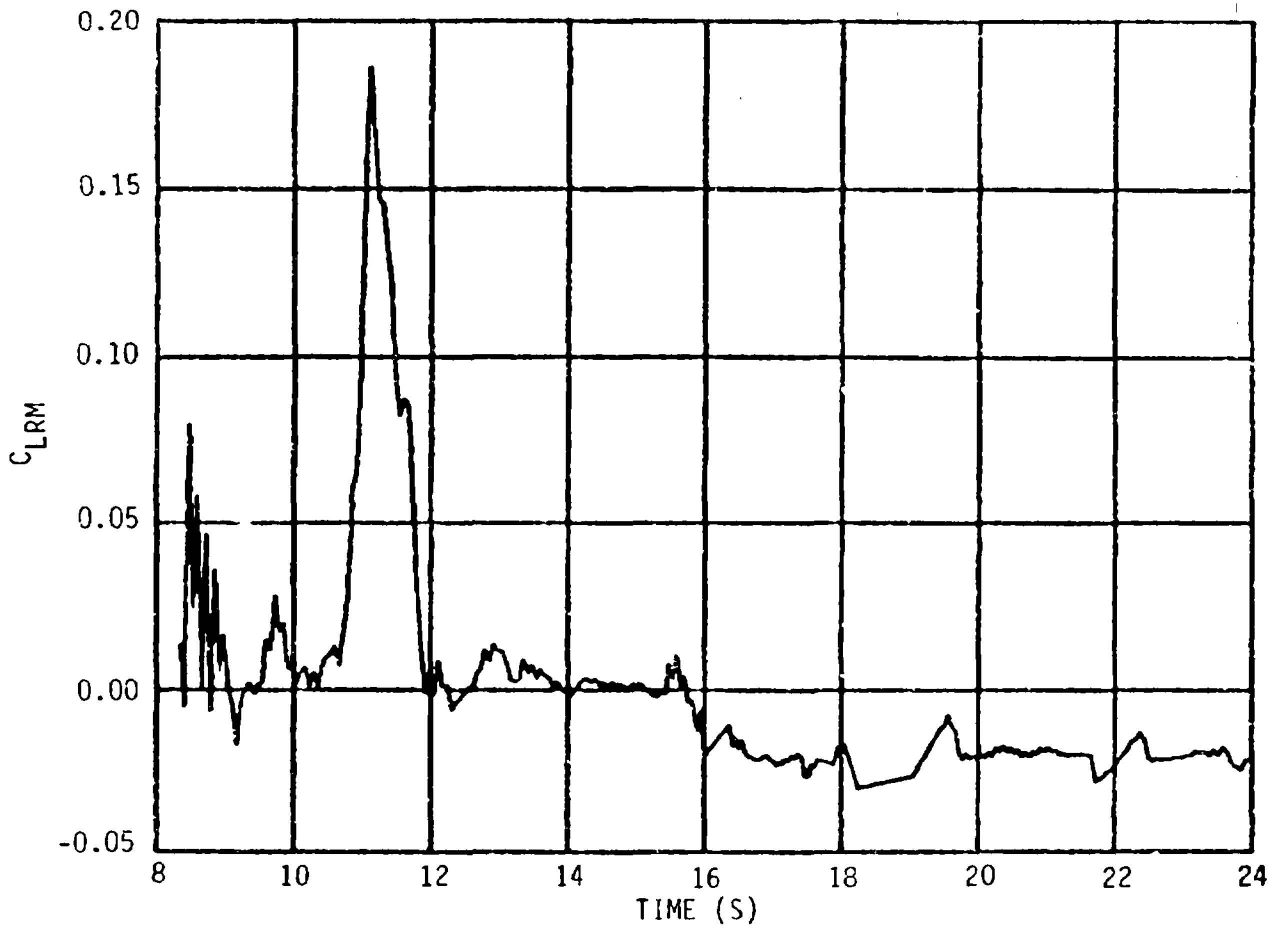

Figure 2d. Liquid Roll Moment Coefficient - BRL 1339.

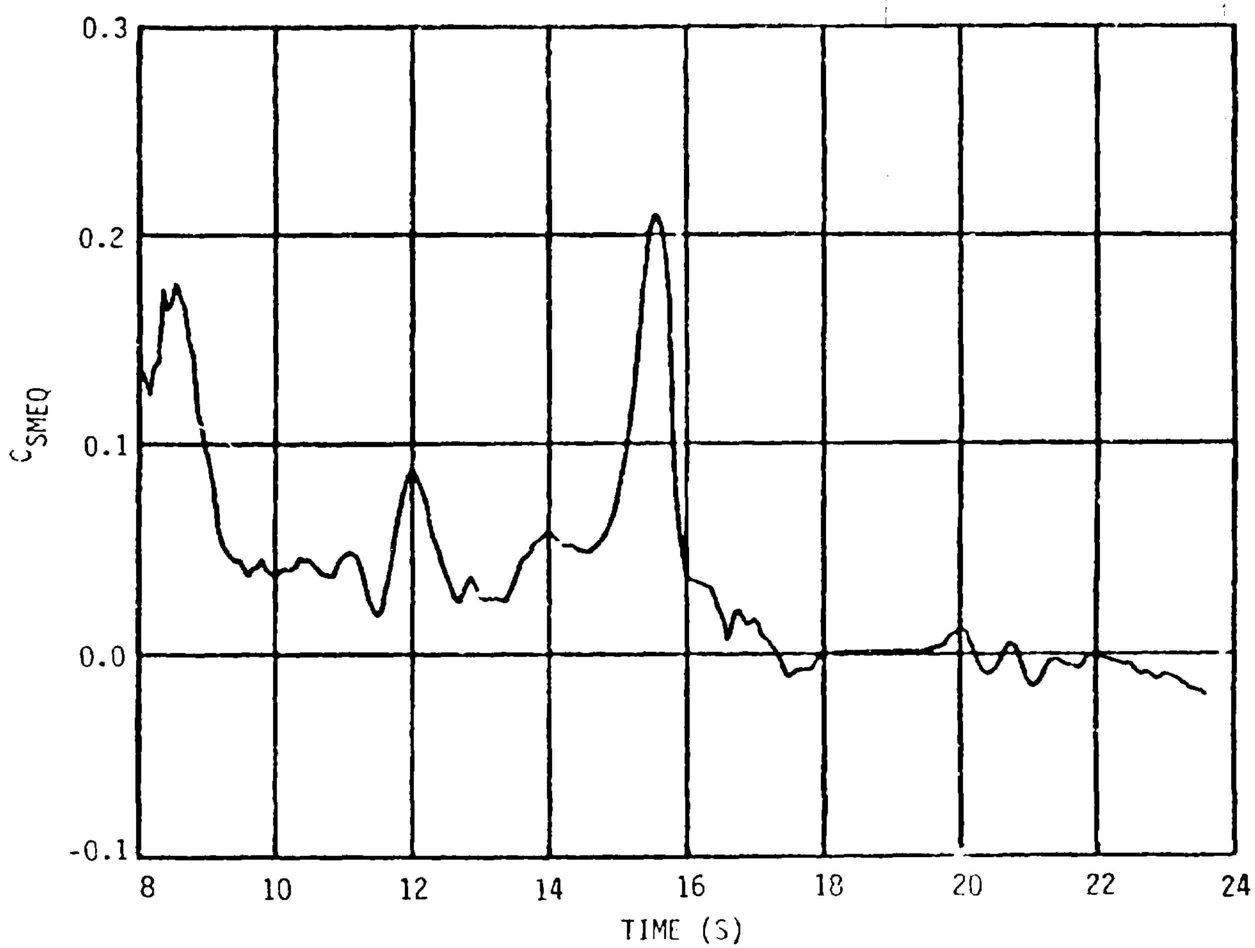

Figure 2e. Equivalent Side Moment Coefficient - BRL 1339.

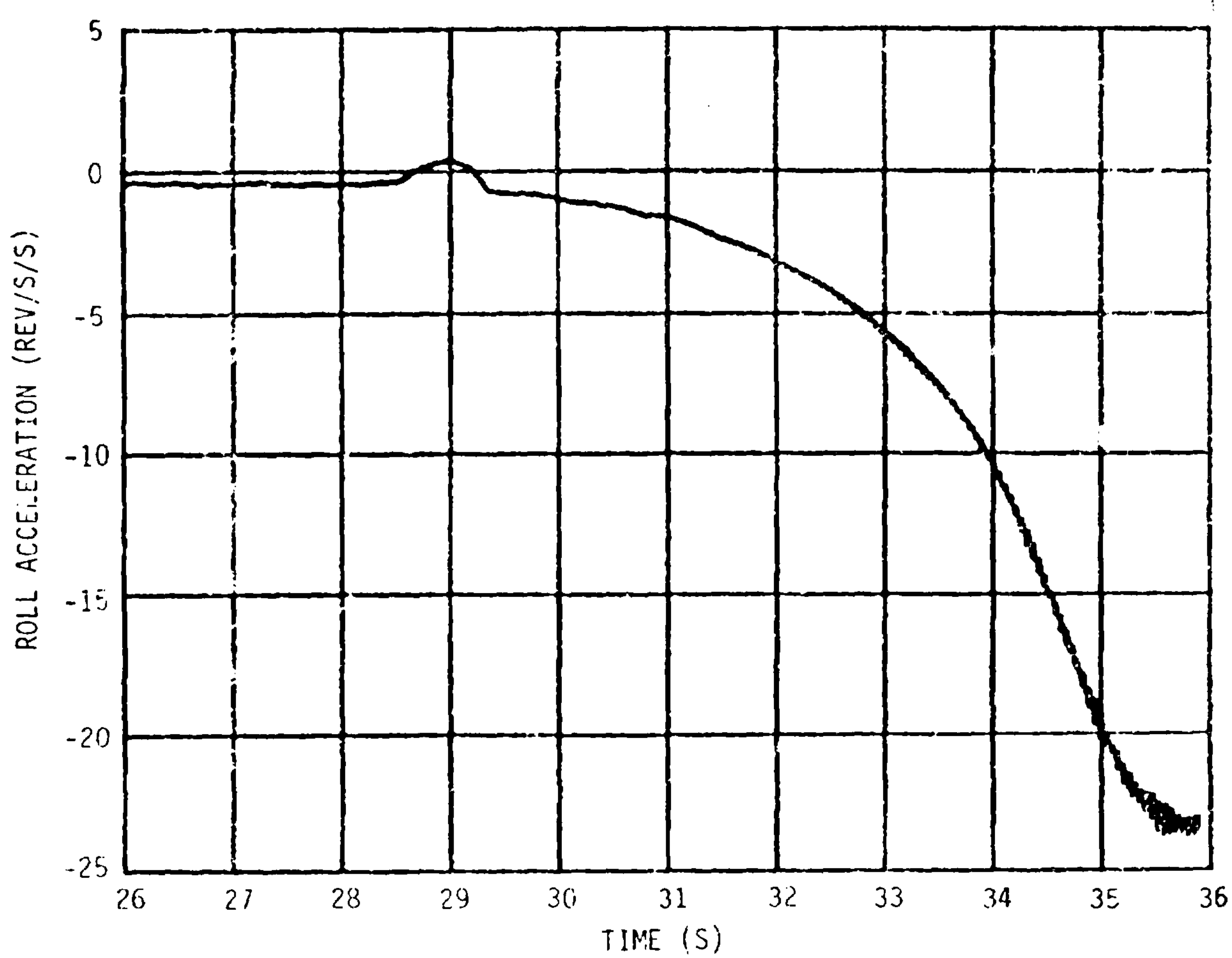

Figure 3a. Roll Acceleration - BRL 1866.

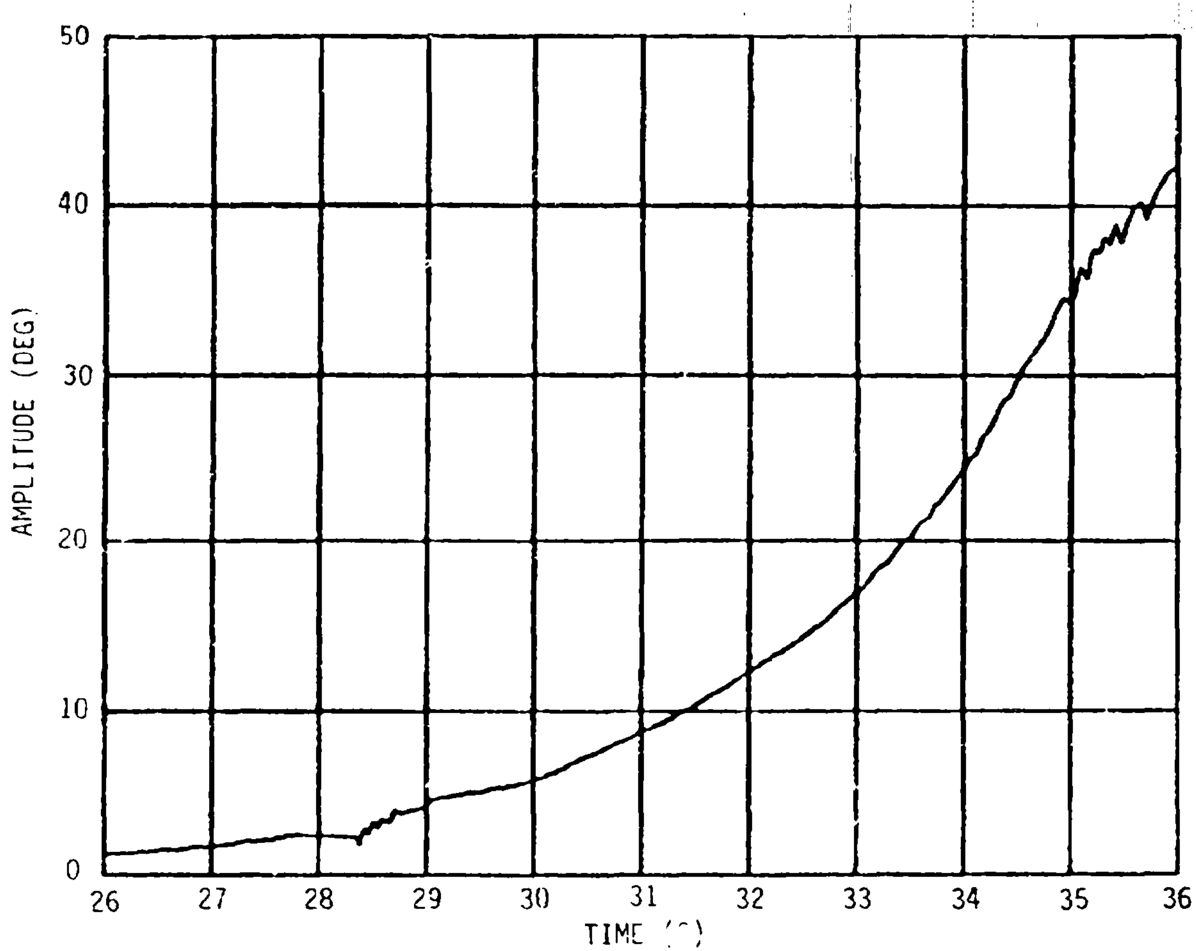

Figure 3b. Coning Amplitude - BRL 1866.

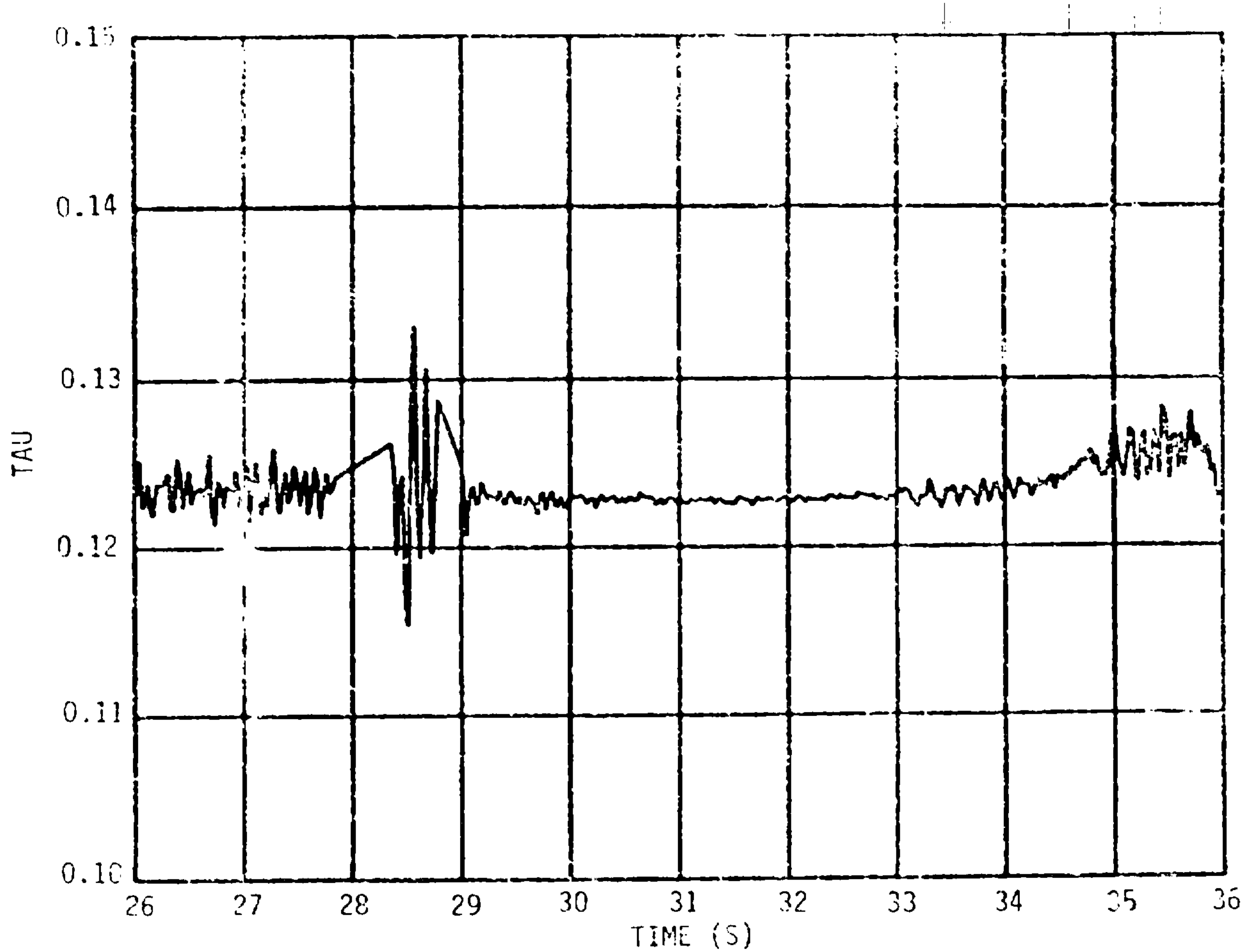

Figure 3c. Nondimensional Coning Frequency - BRL 1866.

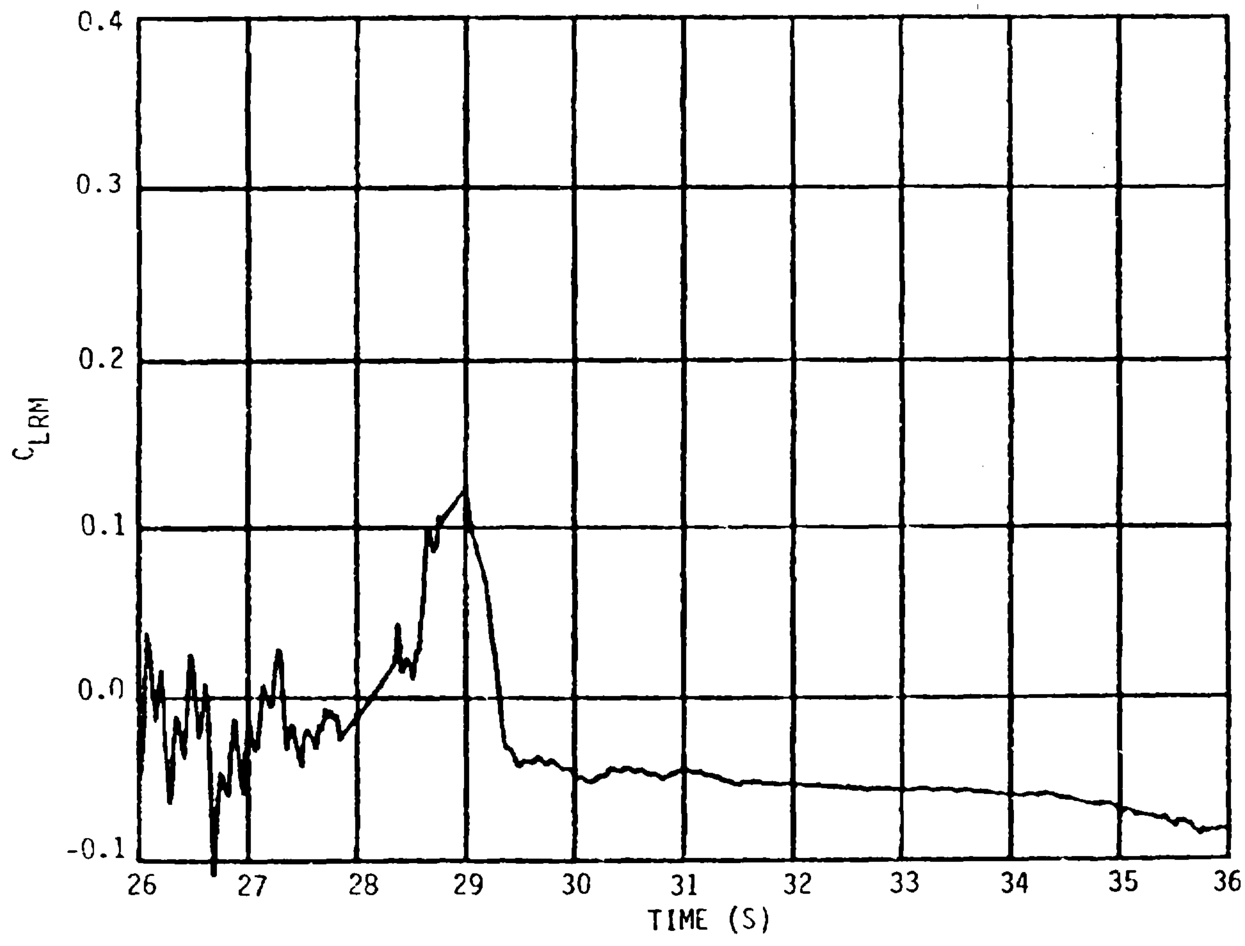

Figure 3d. Liquid Roll Moment Coefficient - BRL 1866.

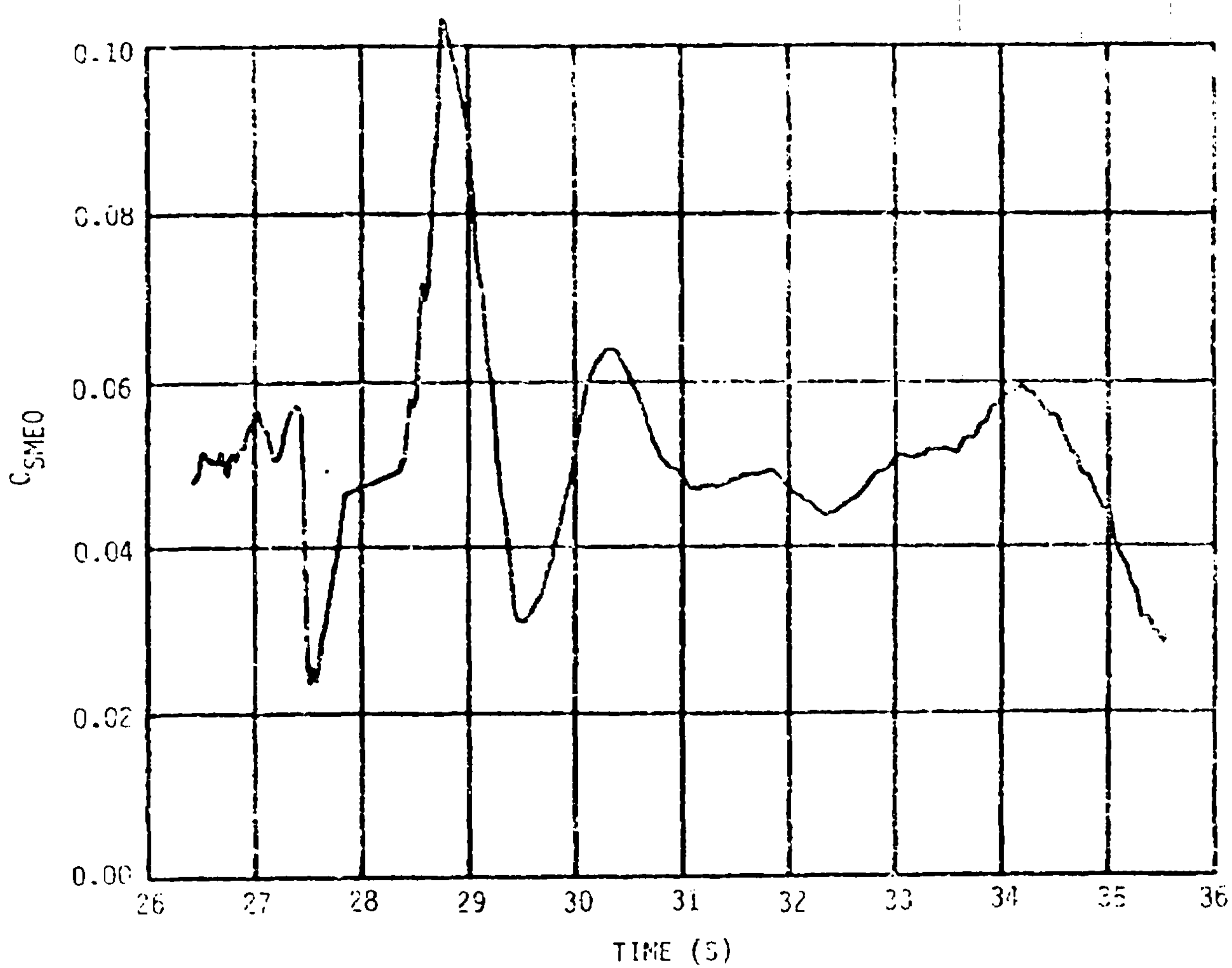

Figure 3e. Equivalent Side Moment Coefficient - BRL 12G..

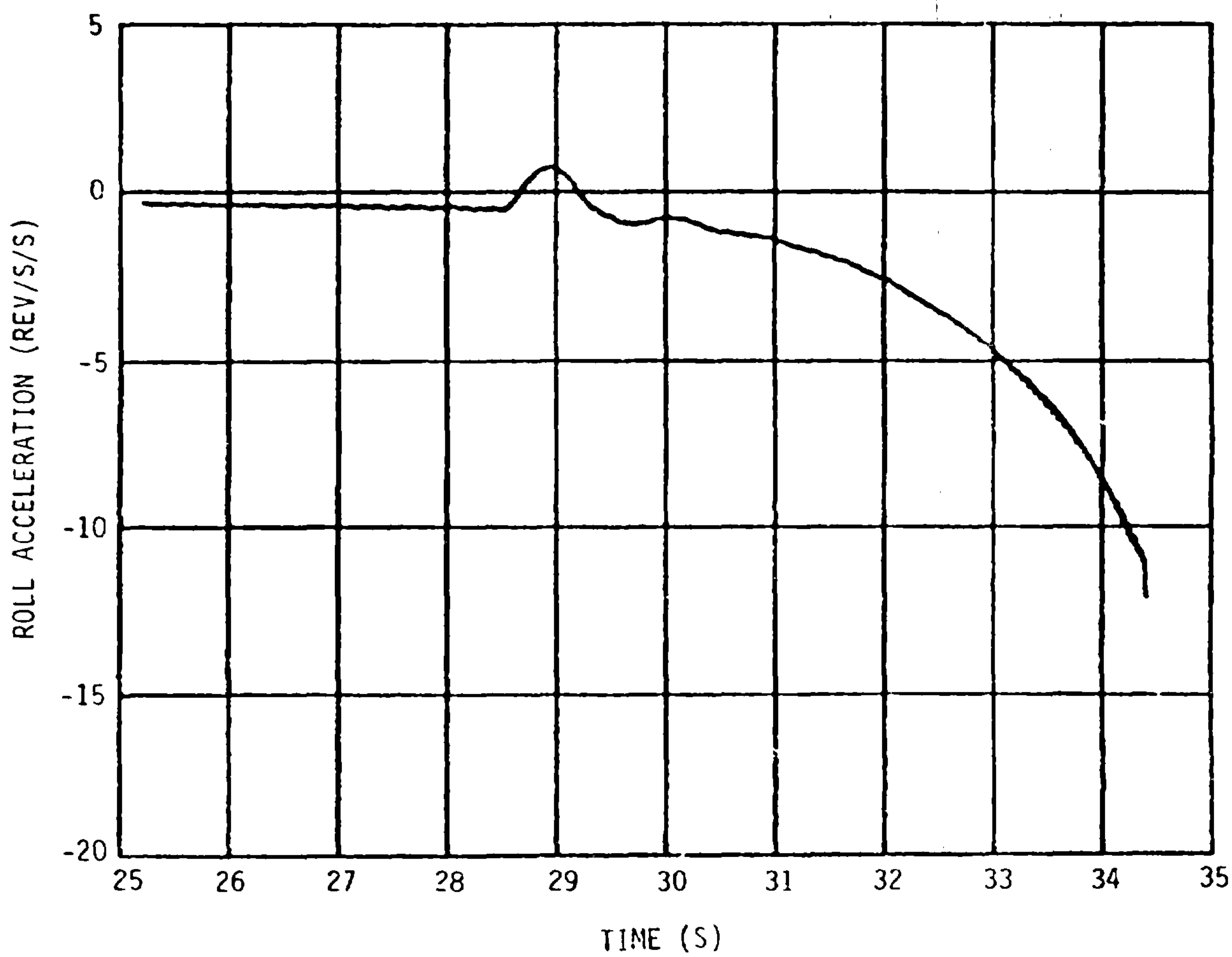

Figure 4a. Roll Acceleration - BRL 1867.

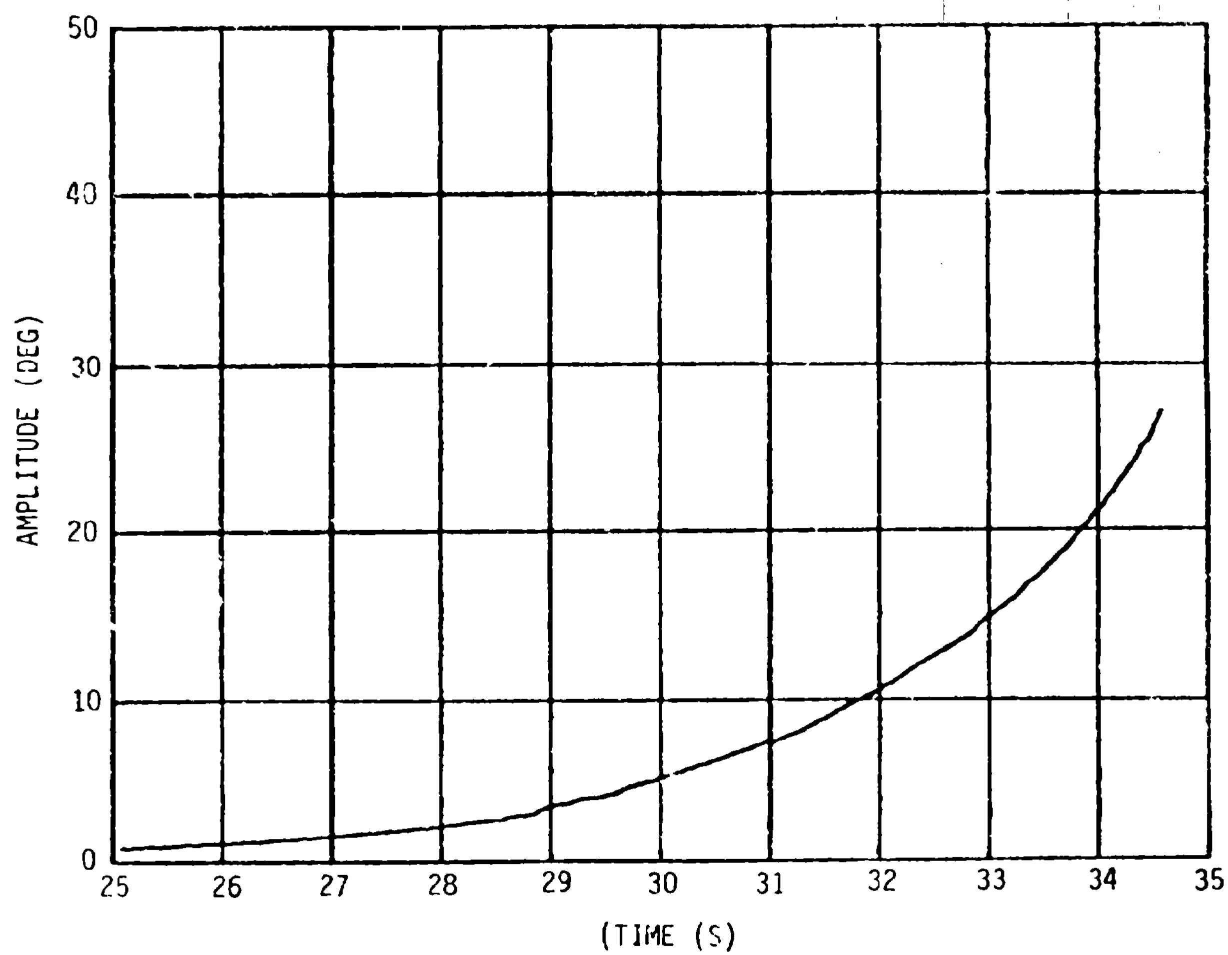

Figure 4b. Coning Amplitude - BRL 1867.

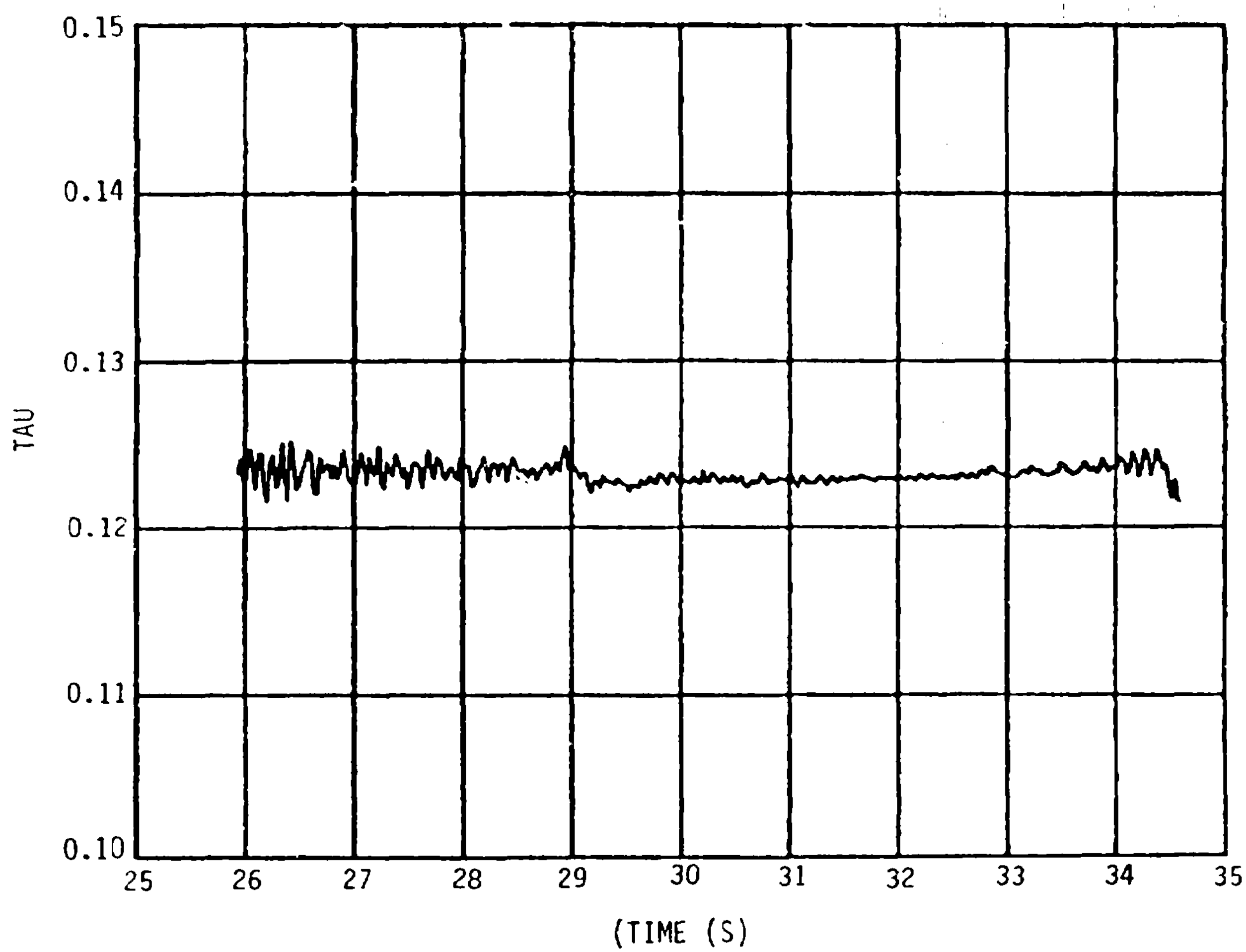

Figure 4c. **Nondimensional** Coning Frequency - BRL 1867.

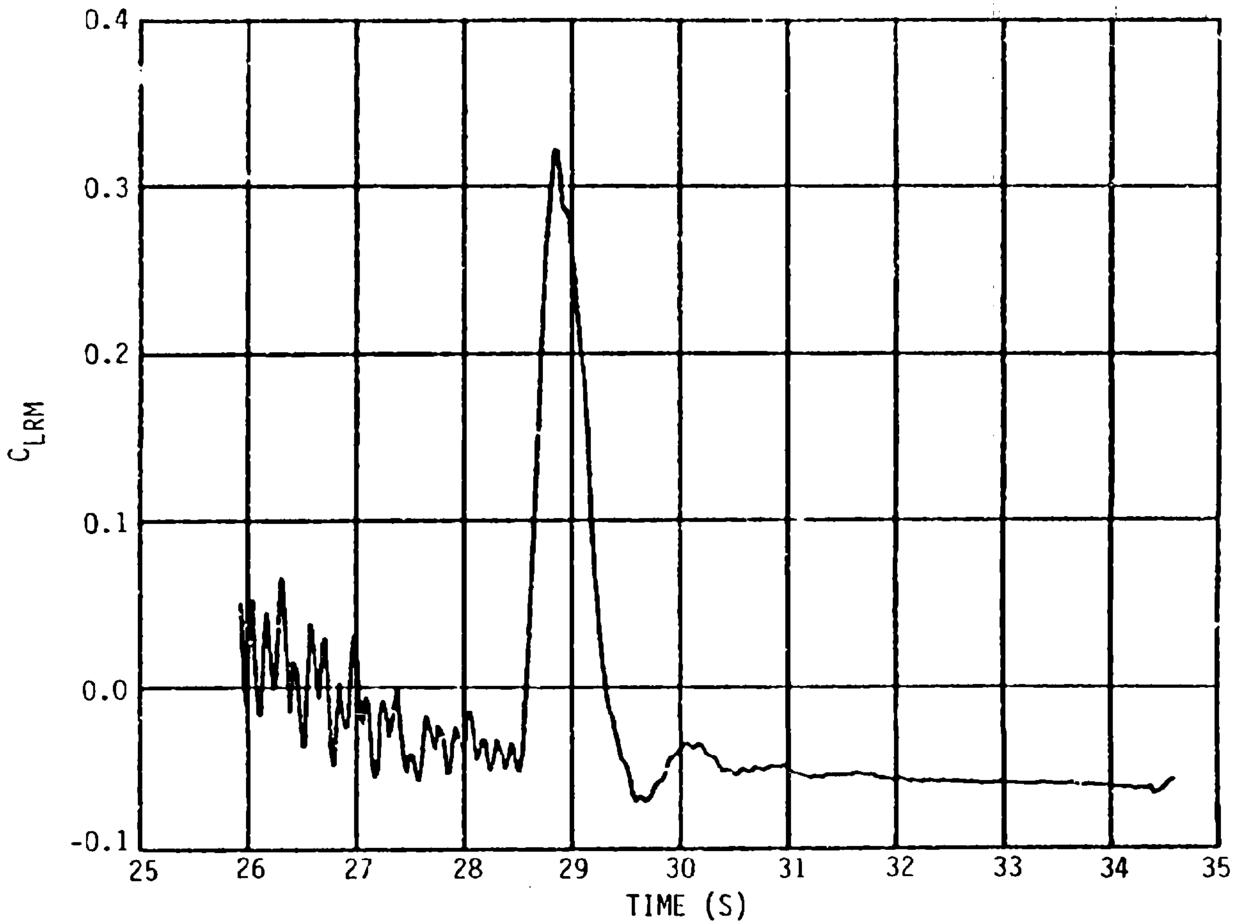

Figure 4d. Liquid Roll Moment Coefficient - BRL 1867.

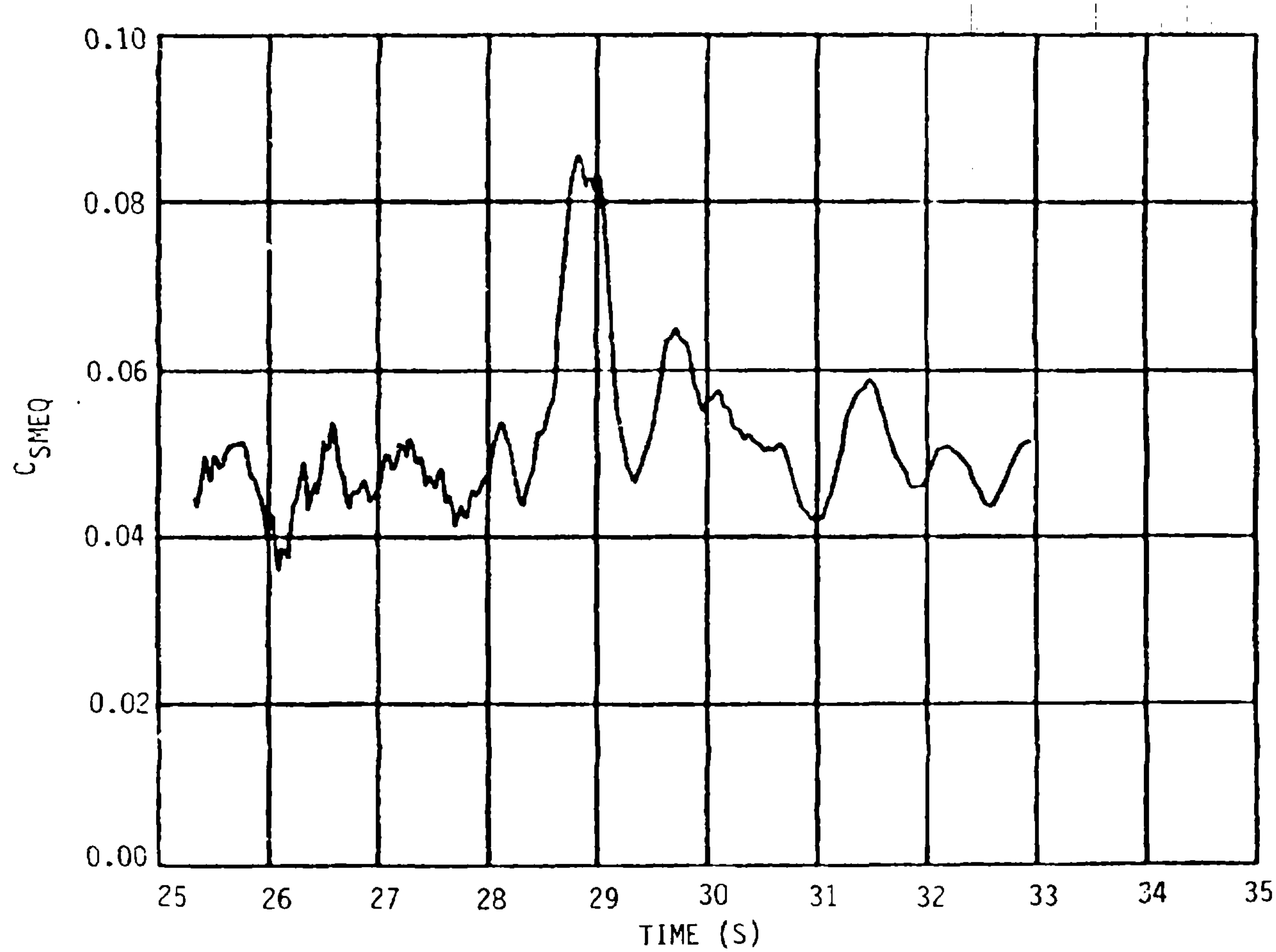

Figure 4e. Equivalent Side Moment Coefficient - BRL 1867.

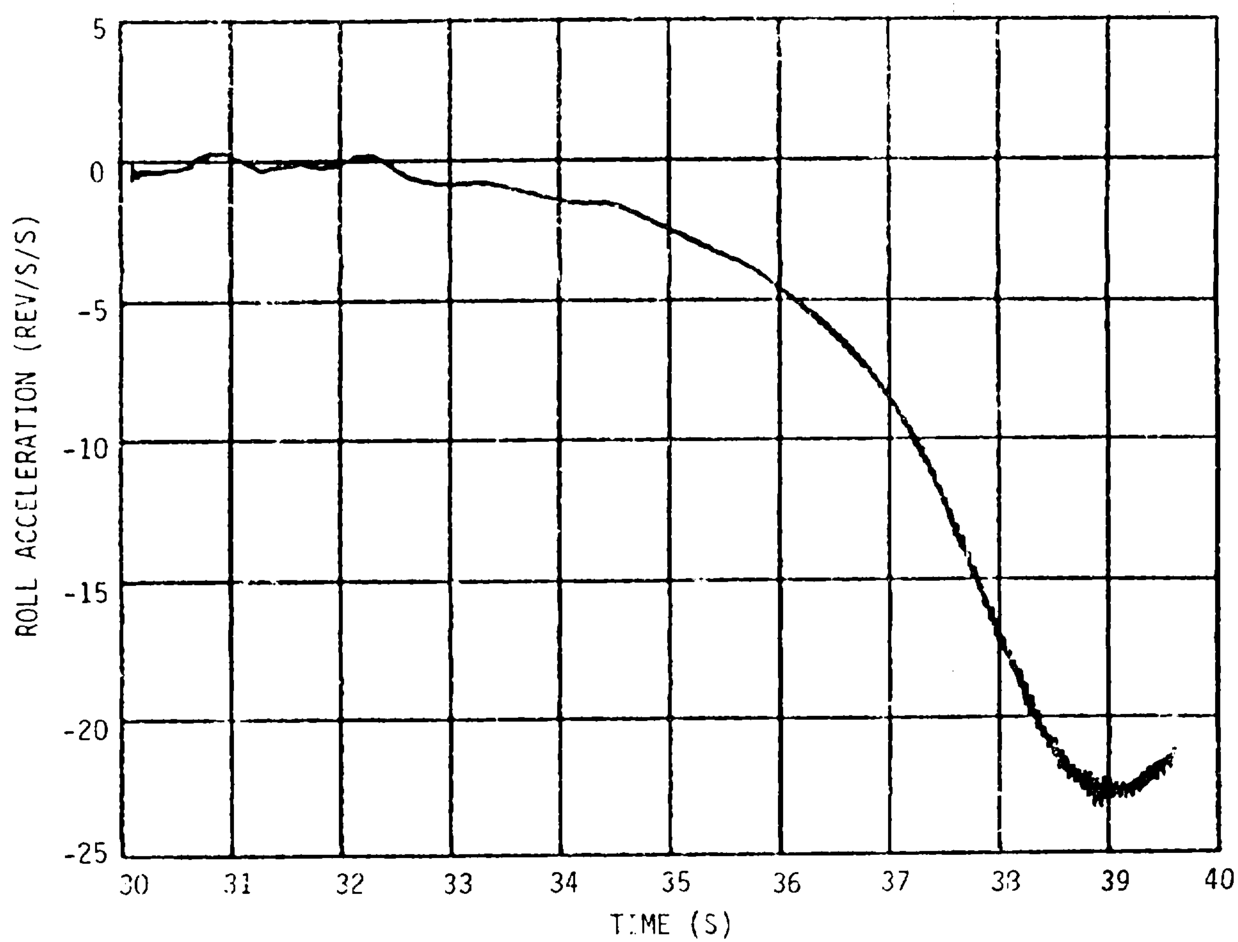

Figure 5a. Roll Acceleration - BRL 1868.

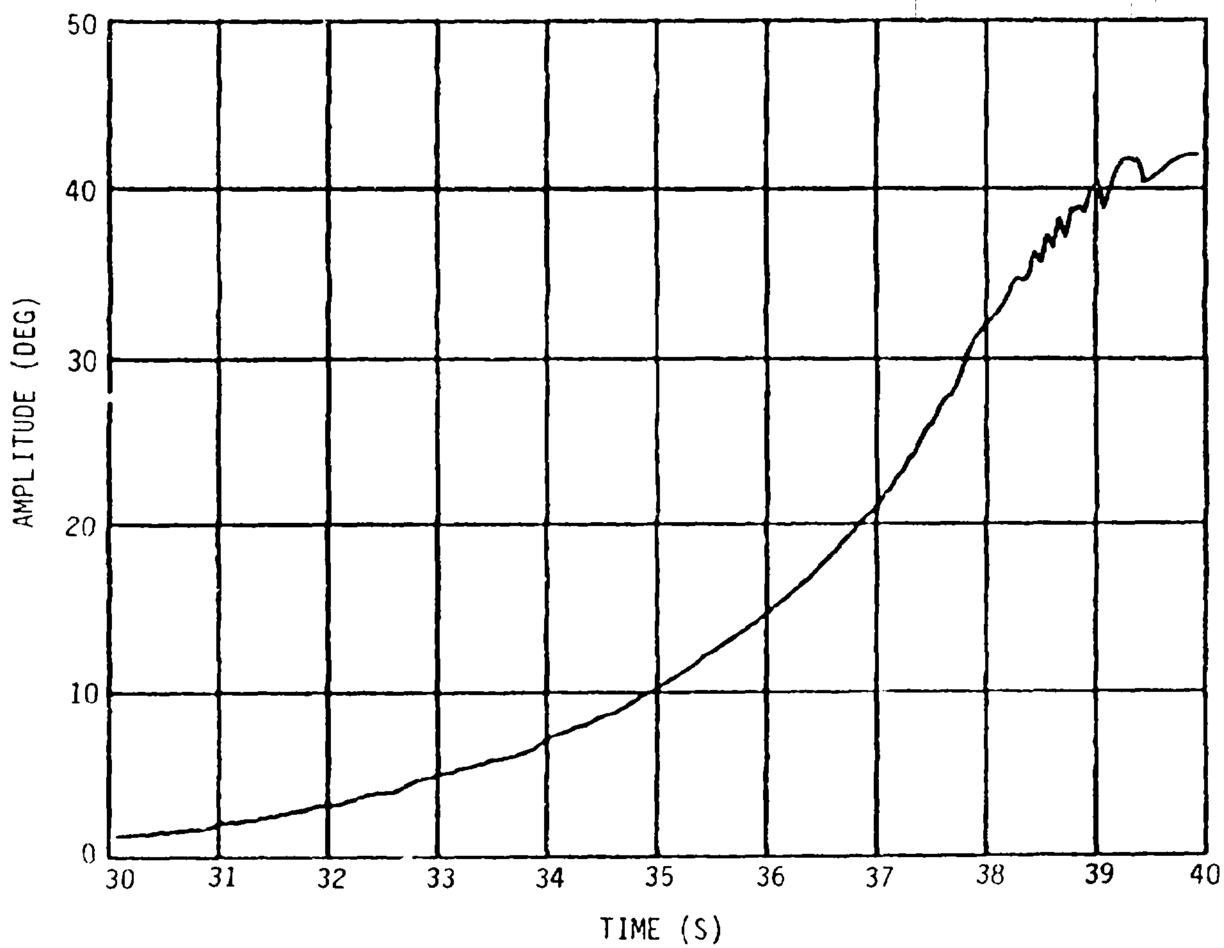

Figure 5b. Coning Amplitude - BRL 1868.

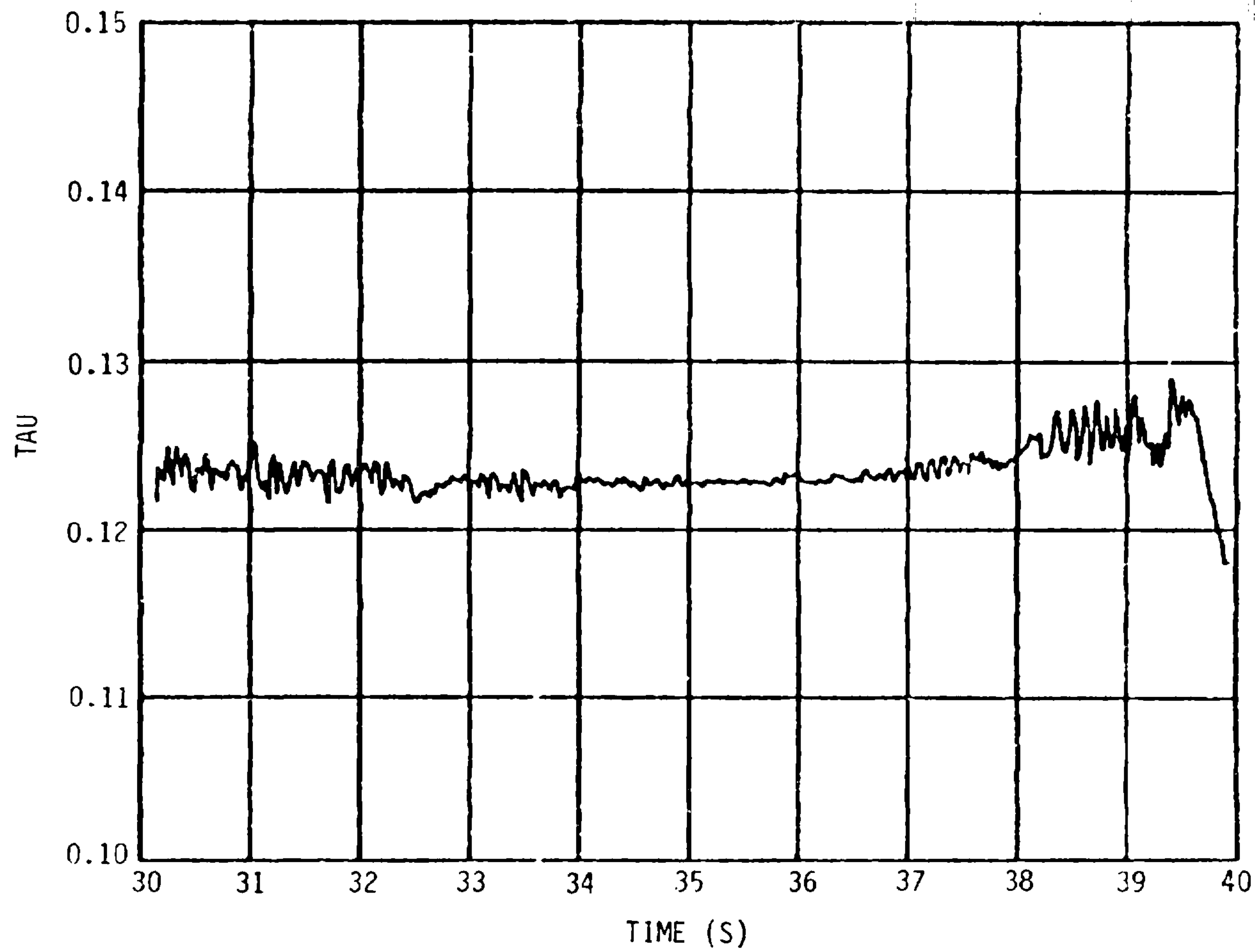

Figure 5c. **Nondimensional** Coning Frequency - BRL 1868.

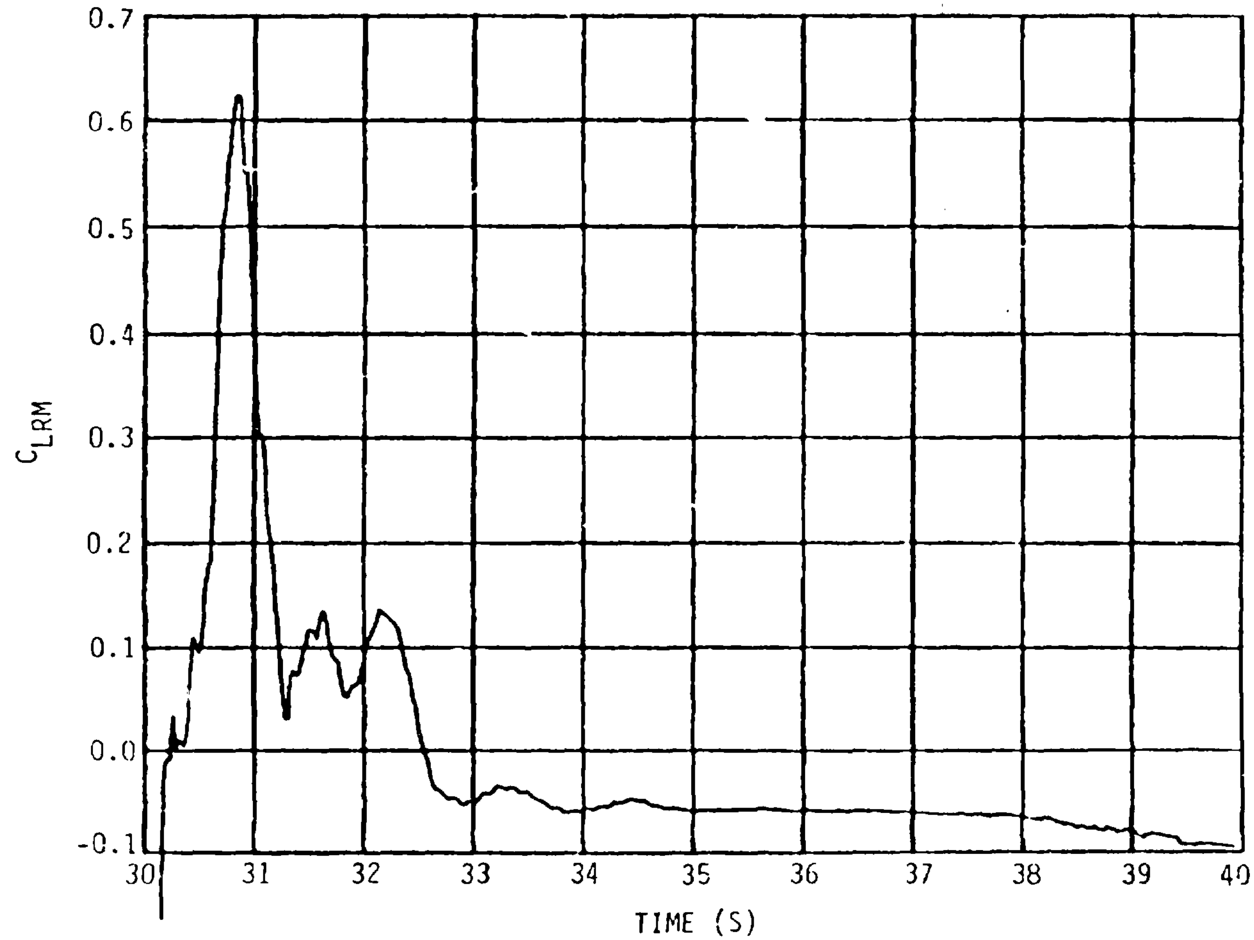

Figure 5d. Liquid Roll Moment Coefficient - BRL 1868.

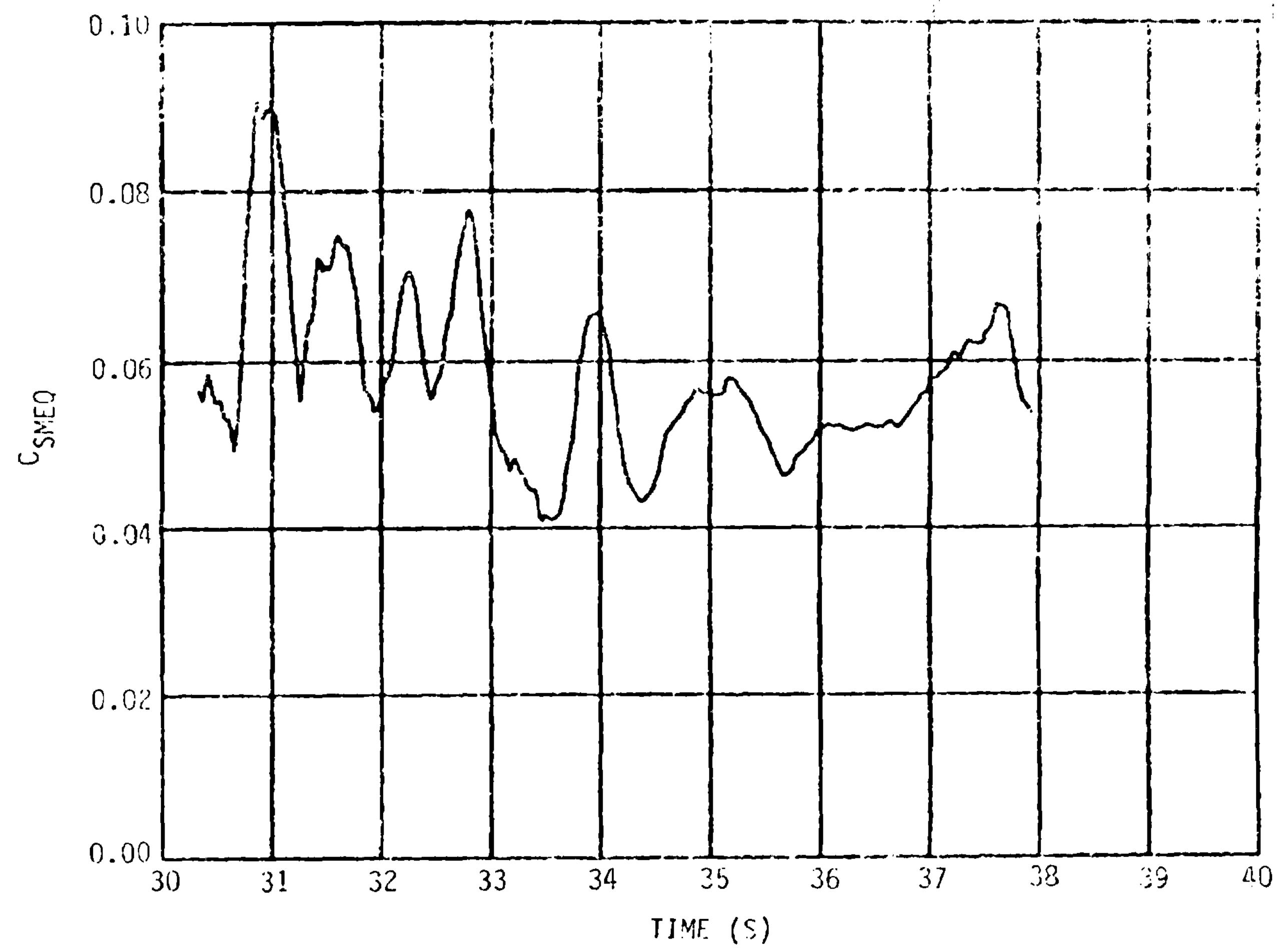

Figure 5e. Equivalent Side Moment Coefficient - BRL 1868.

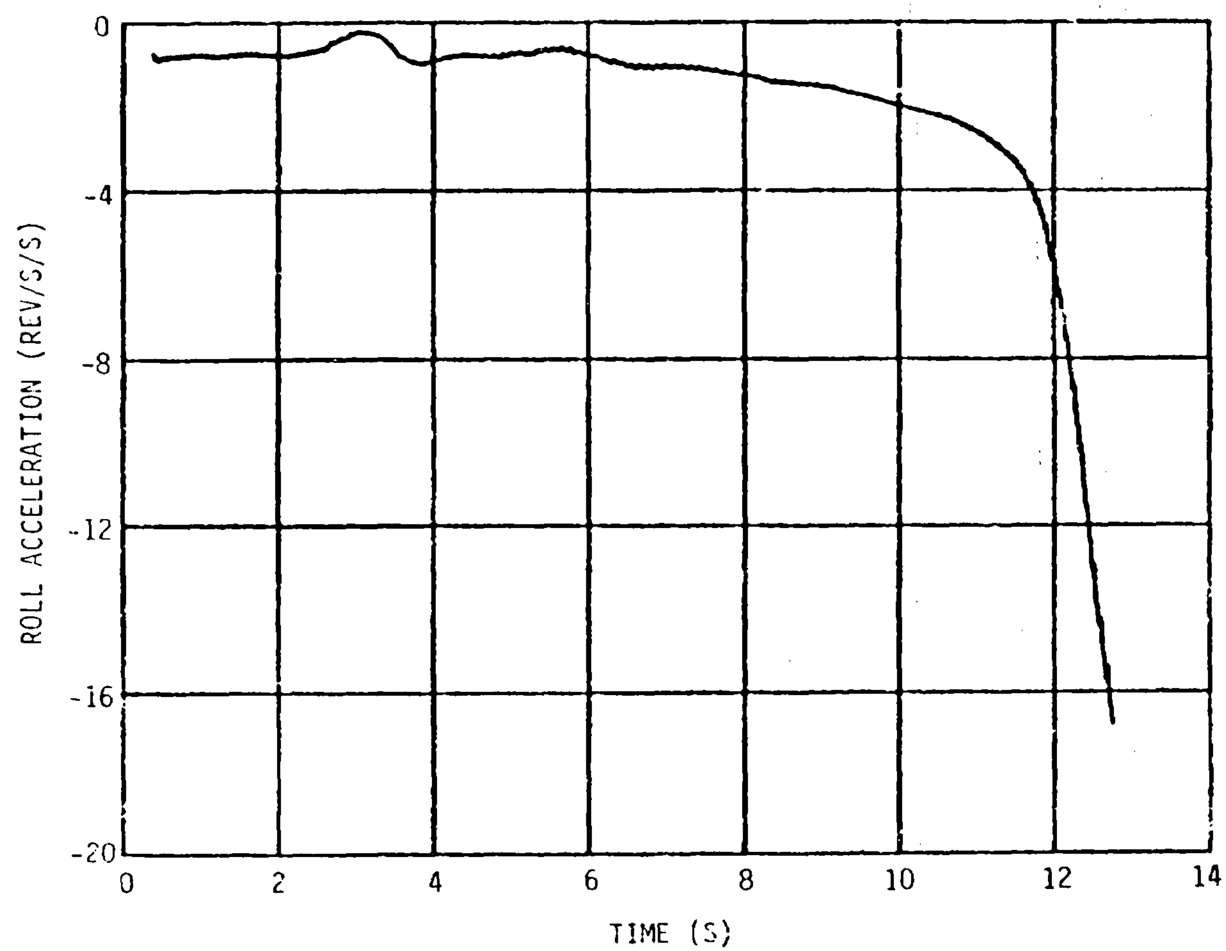

Figure 6a. Roll Acceleration - BRL 1955.

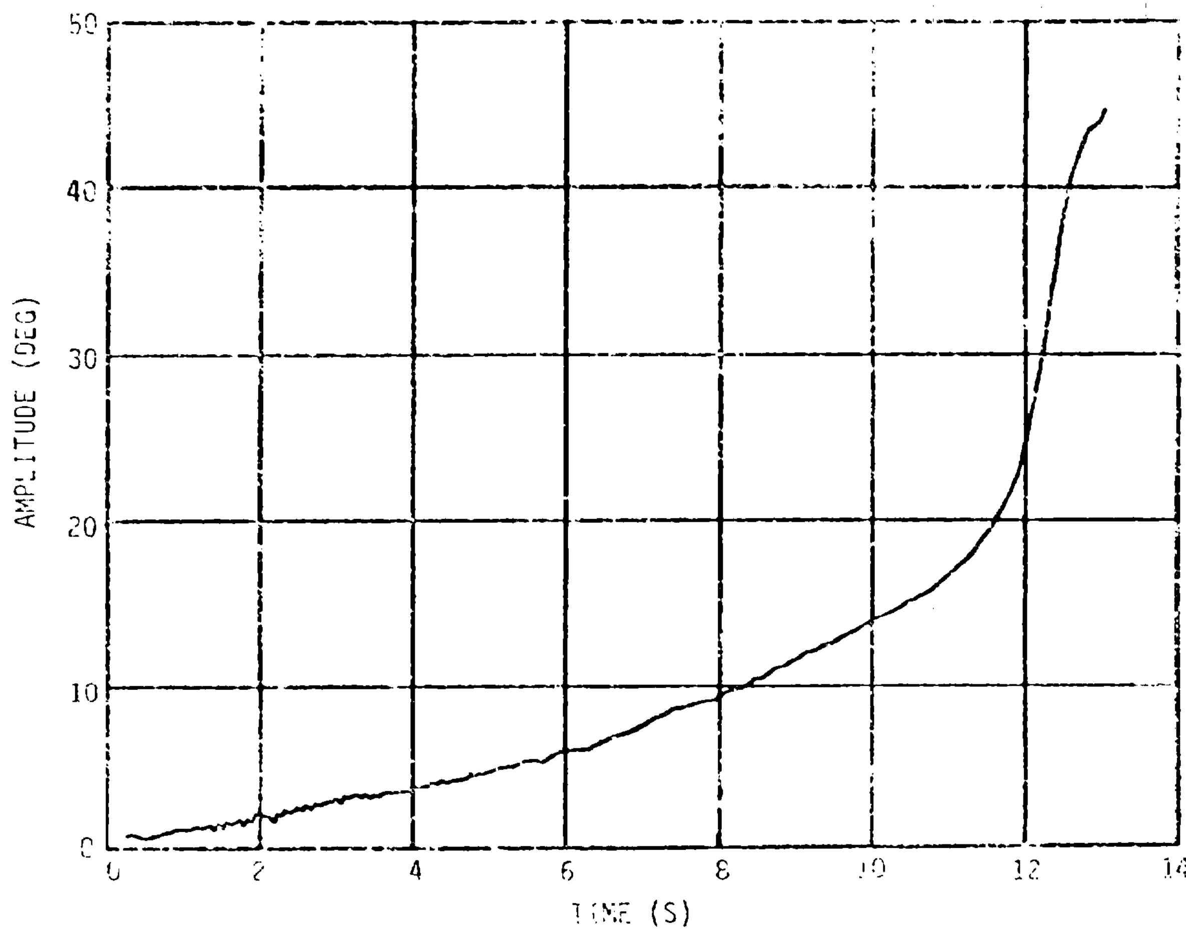

Figure 6b. Coning Amplitude - BRL 1955.

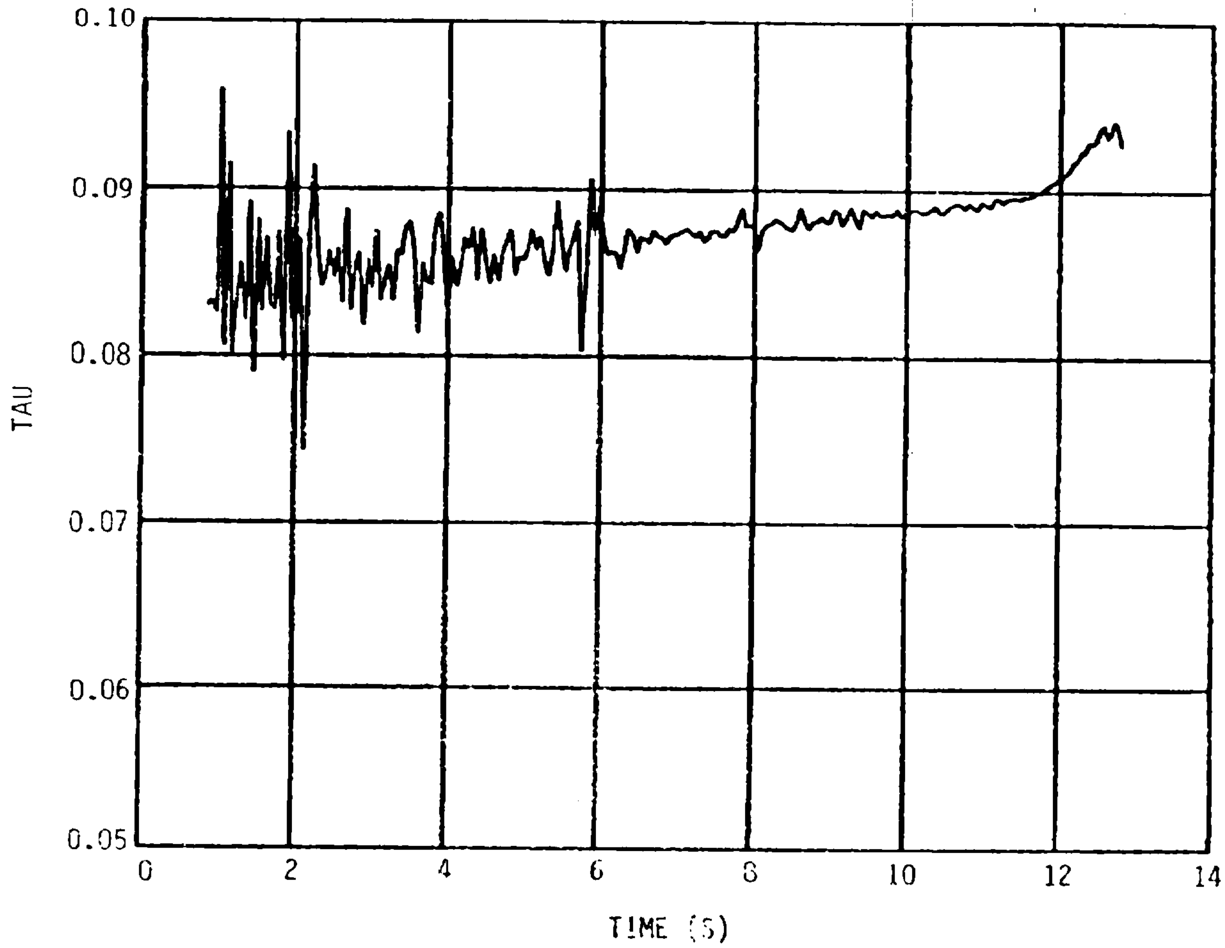

Figure 6c. Nondimensional Coning Frequency - BRL 1955.

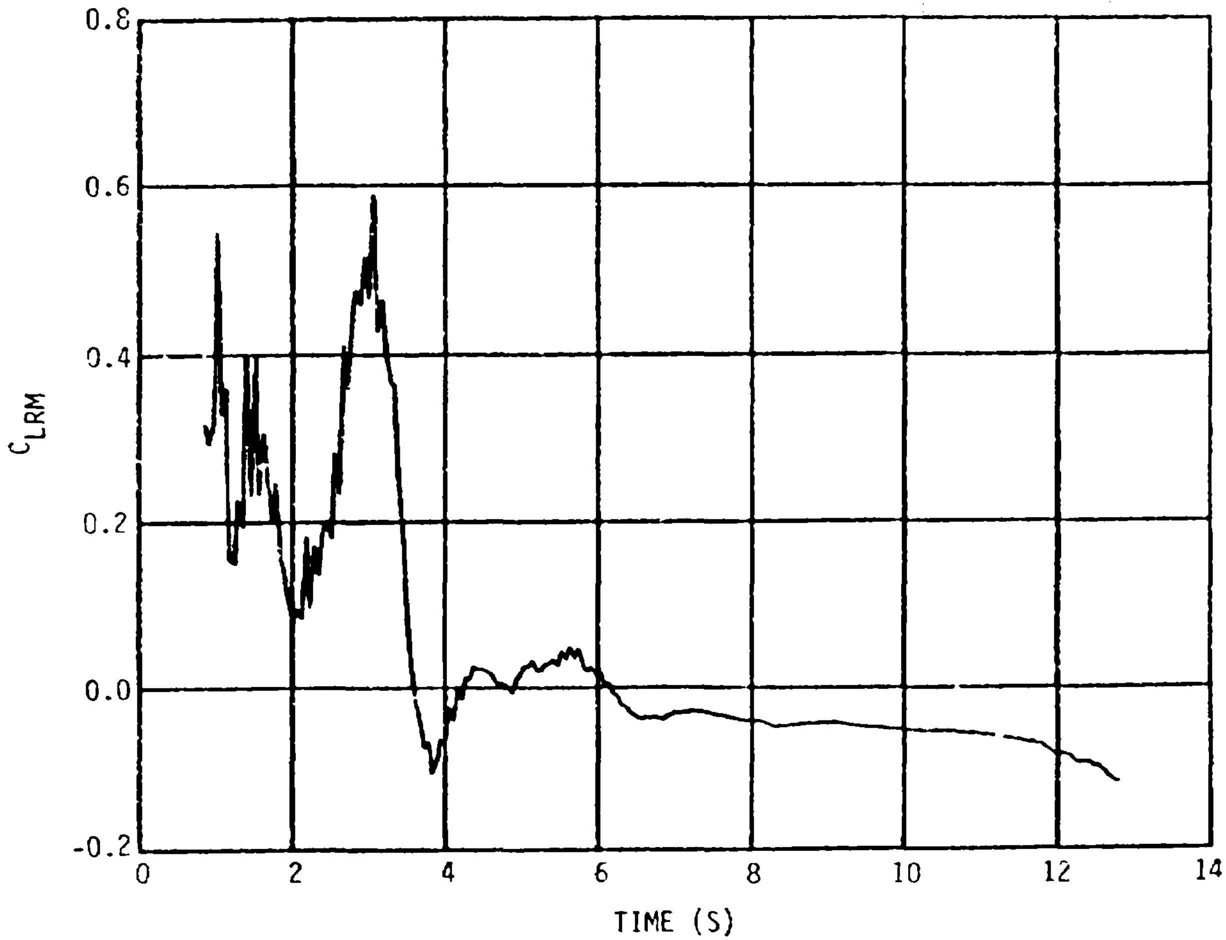

Figure 6d. Liquid Roll Moment Coefficient - BRL 1955.

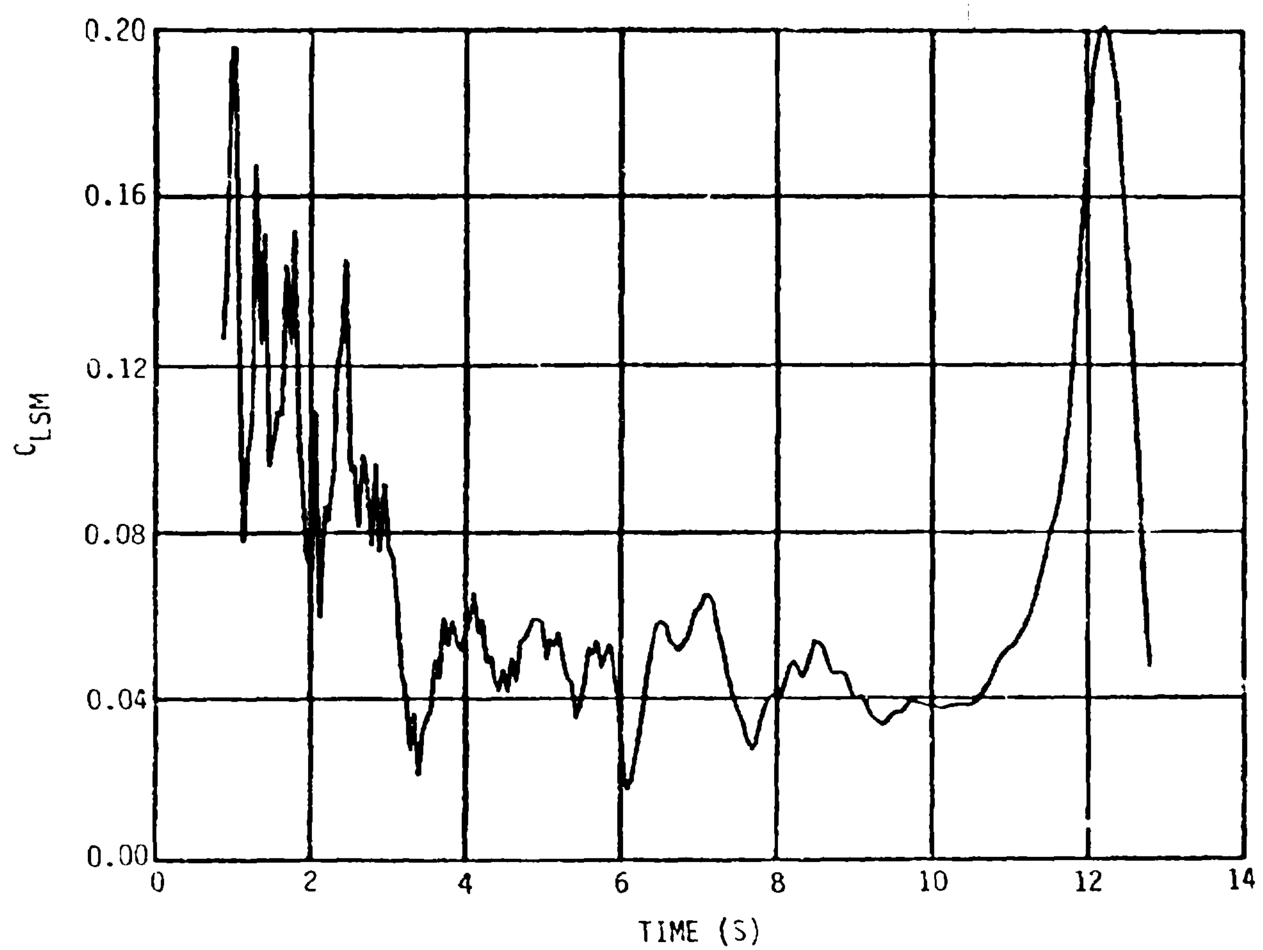

Figure 6e. Equivalent Side Moment Coefficient - BRL 1955.

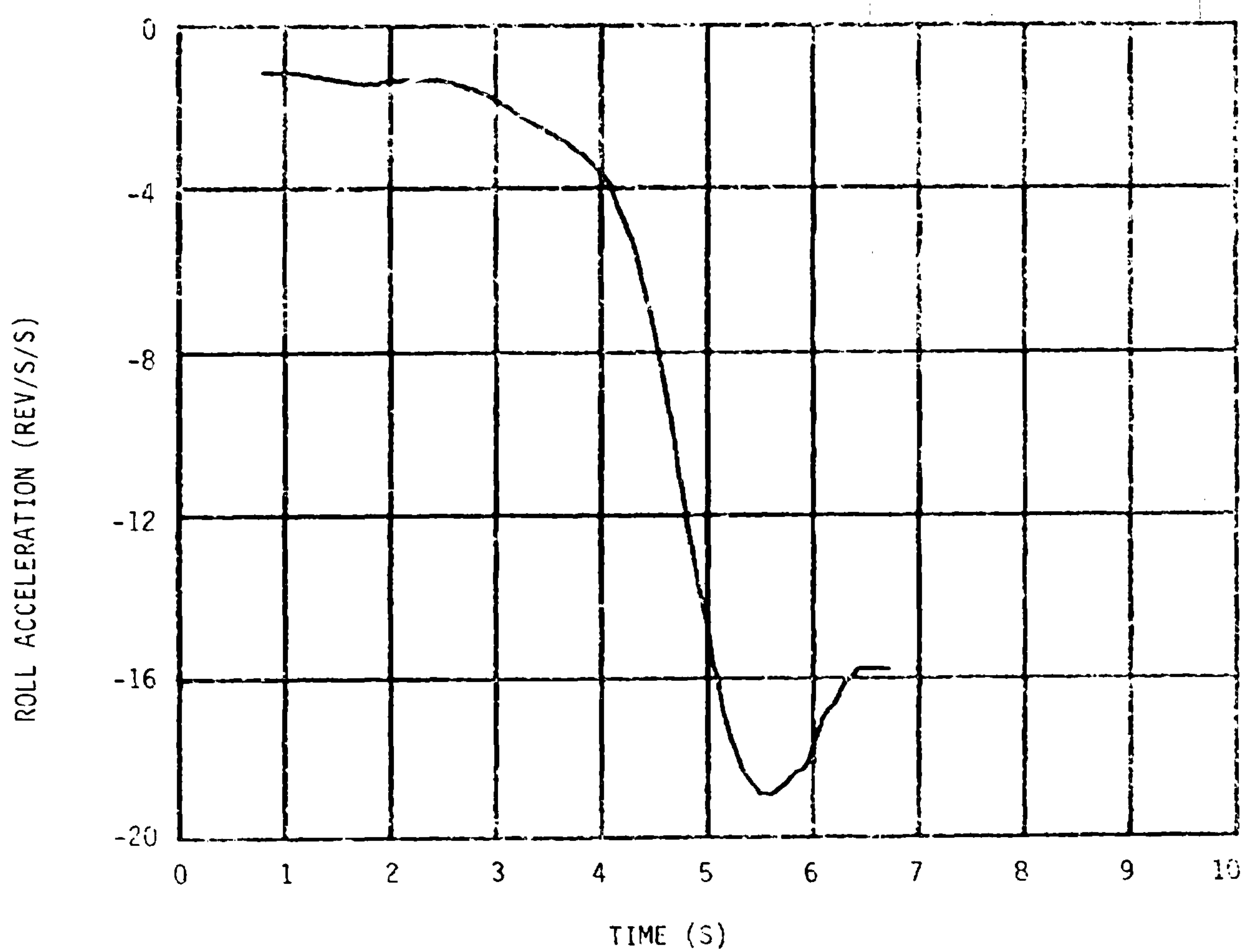

Figure 7a. Roll Acceleration - BRL 1293.

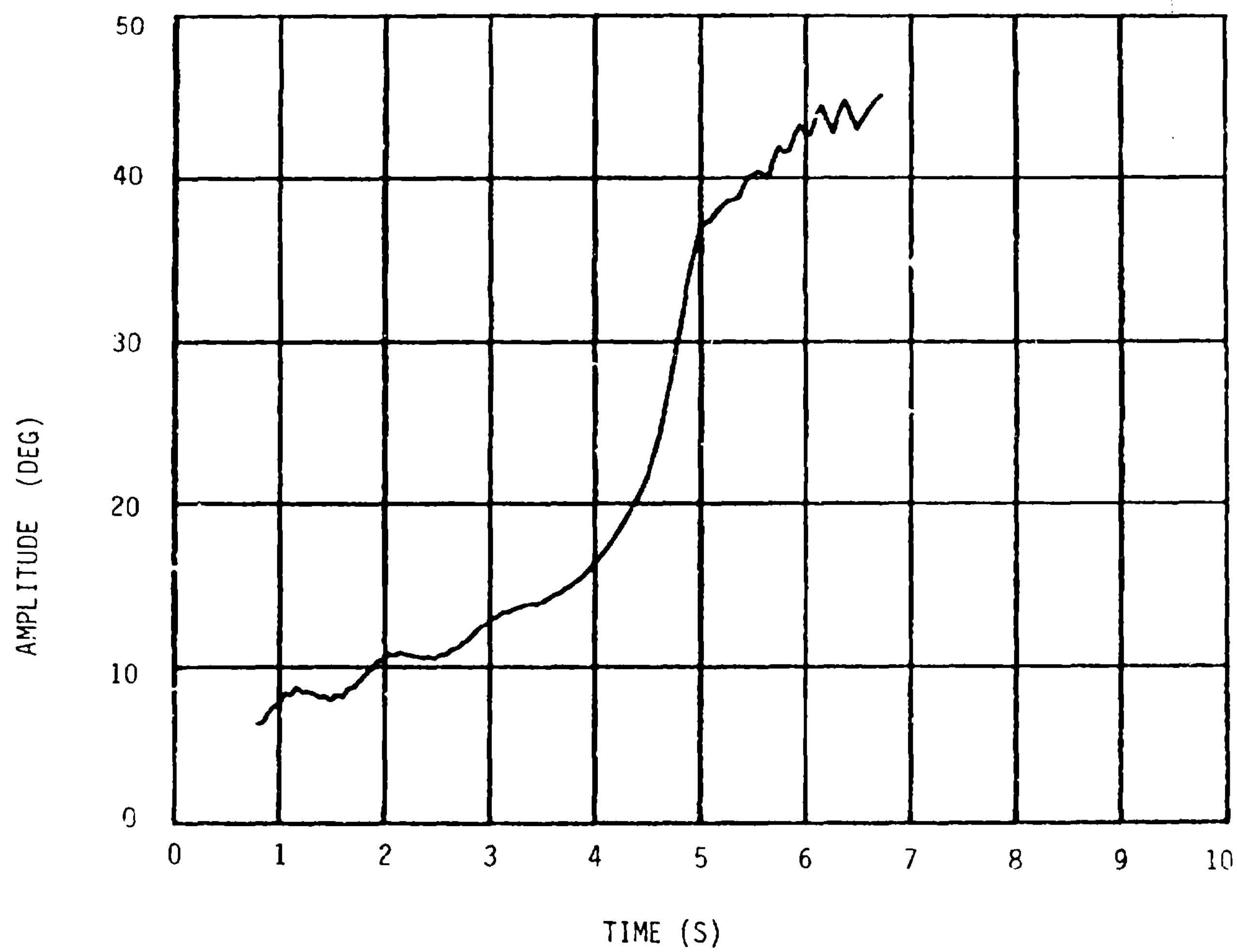

Figure 7b. Coning Amplitude - BRL 1293.

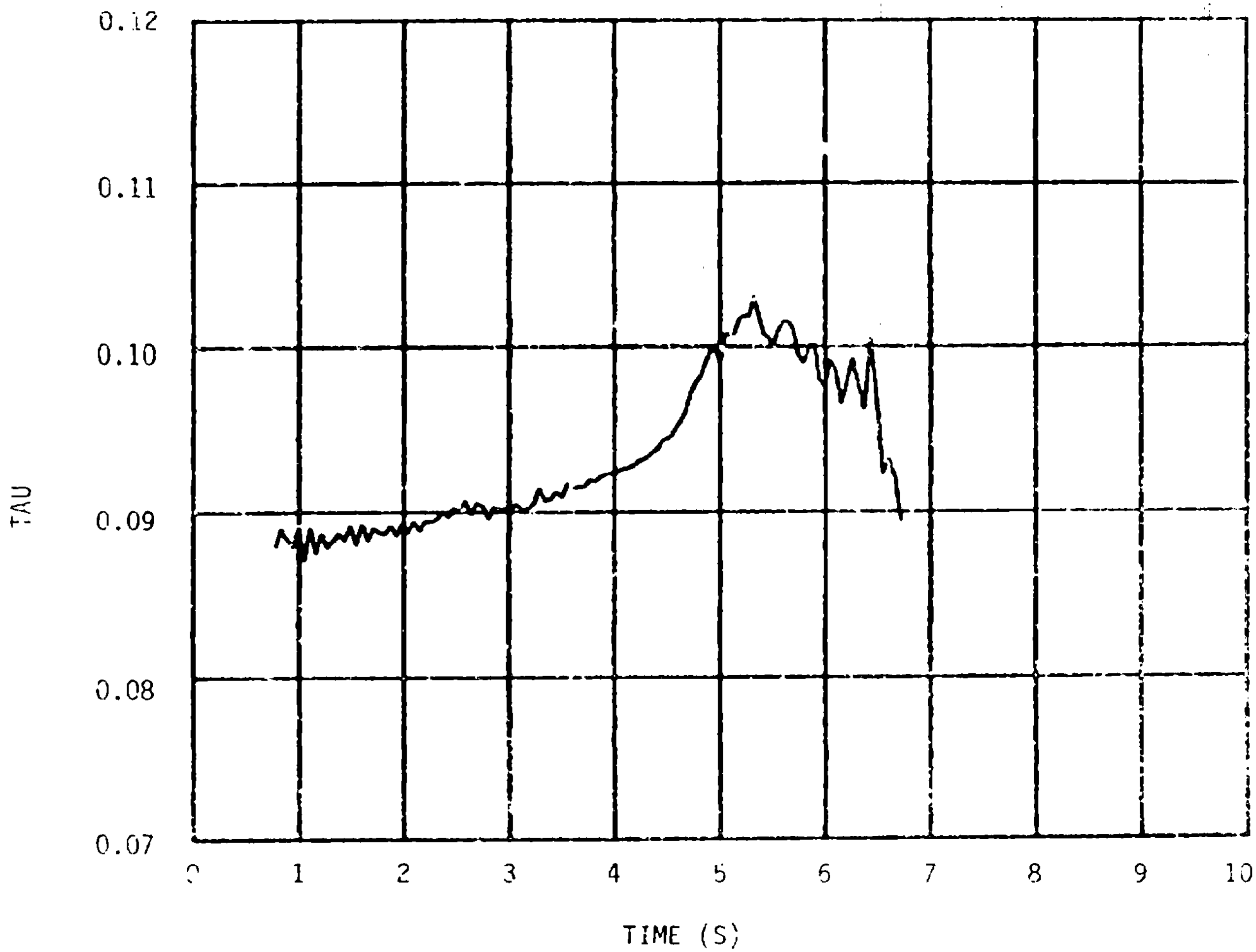

Figure 7c. Nondimensional Coning Frequency - BRL 1293.

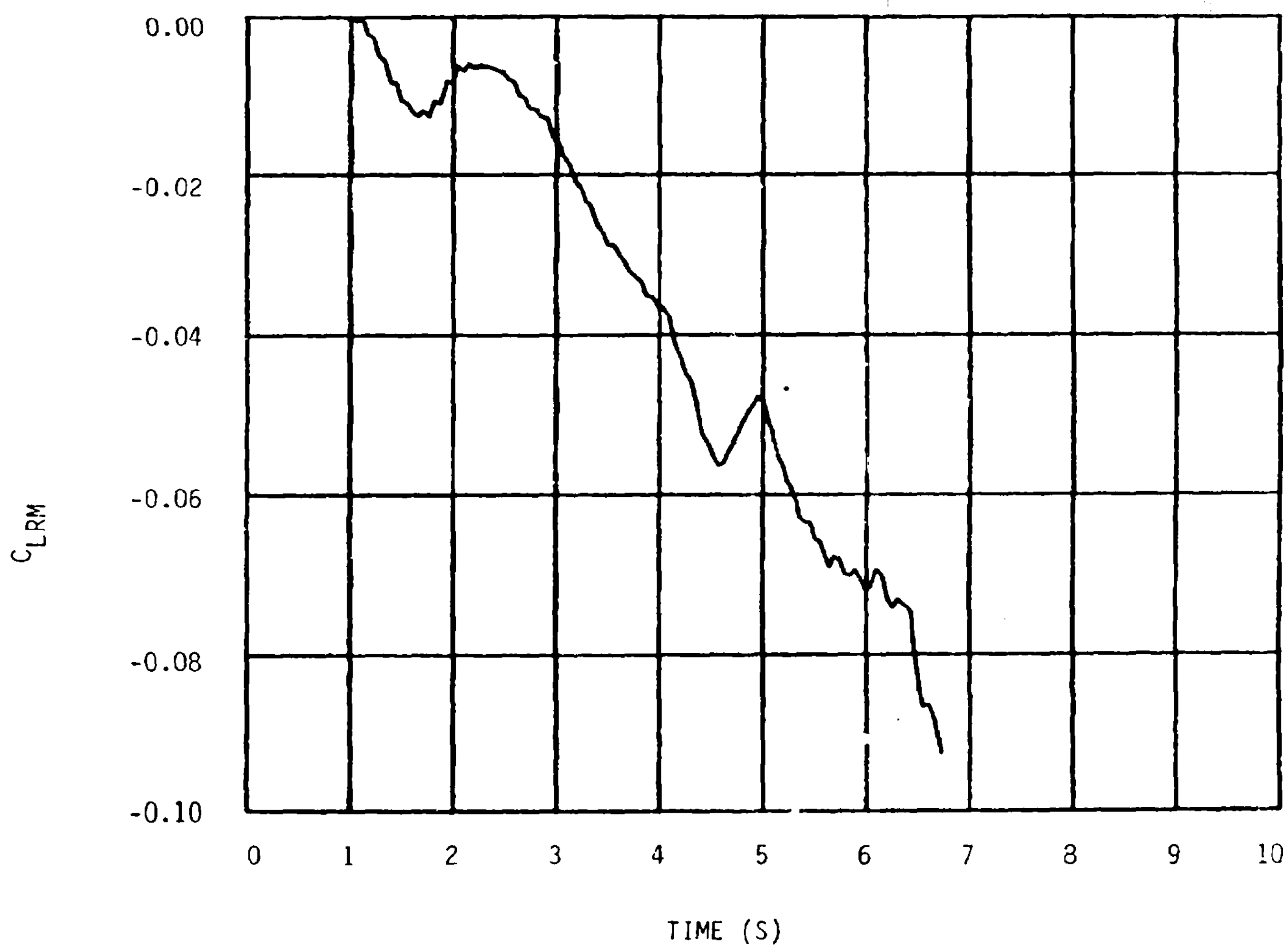

Figure 7d. Liquid Roll Moment Coefficient - BRL 1293.

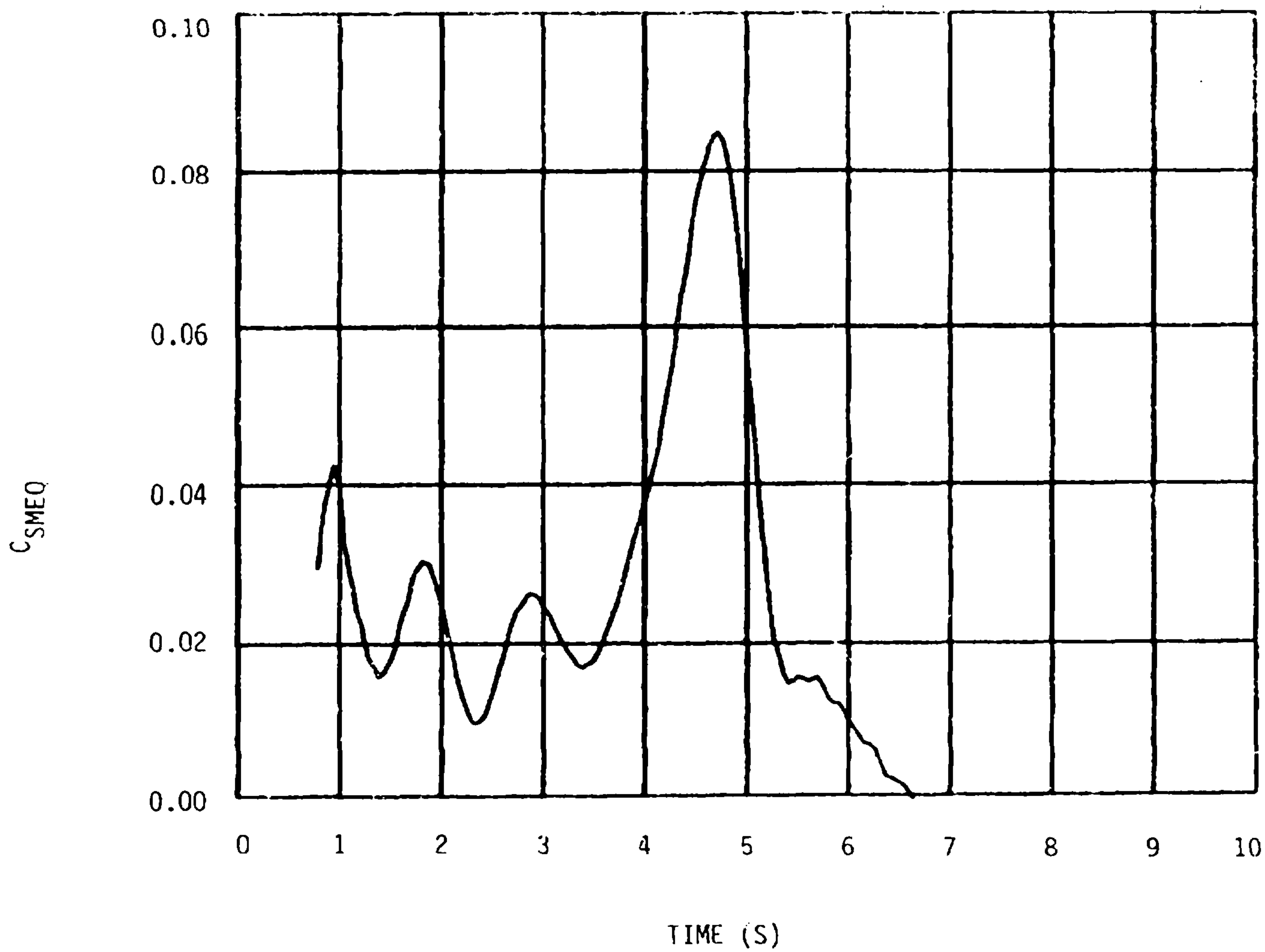

Figure 7e. Equivalent Side Moment Coefficient - BRL 1293.

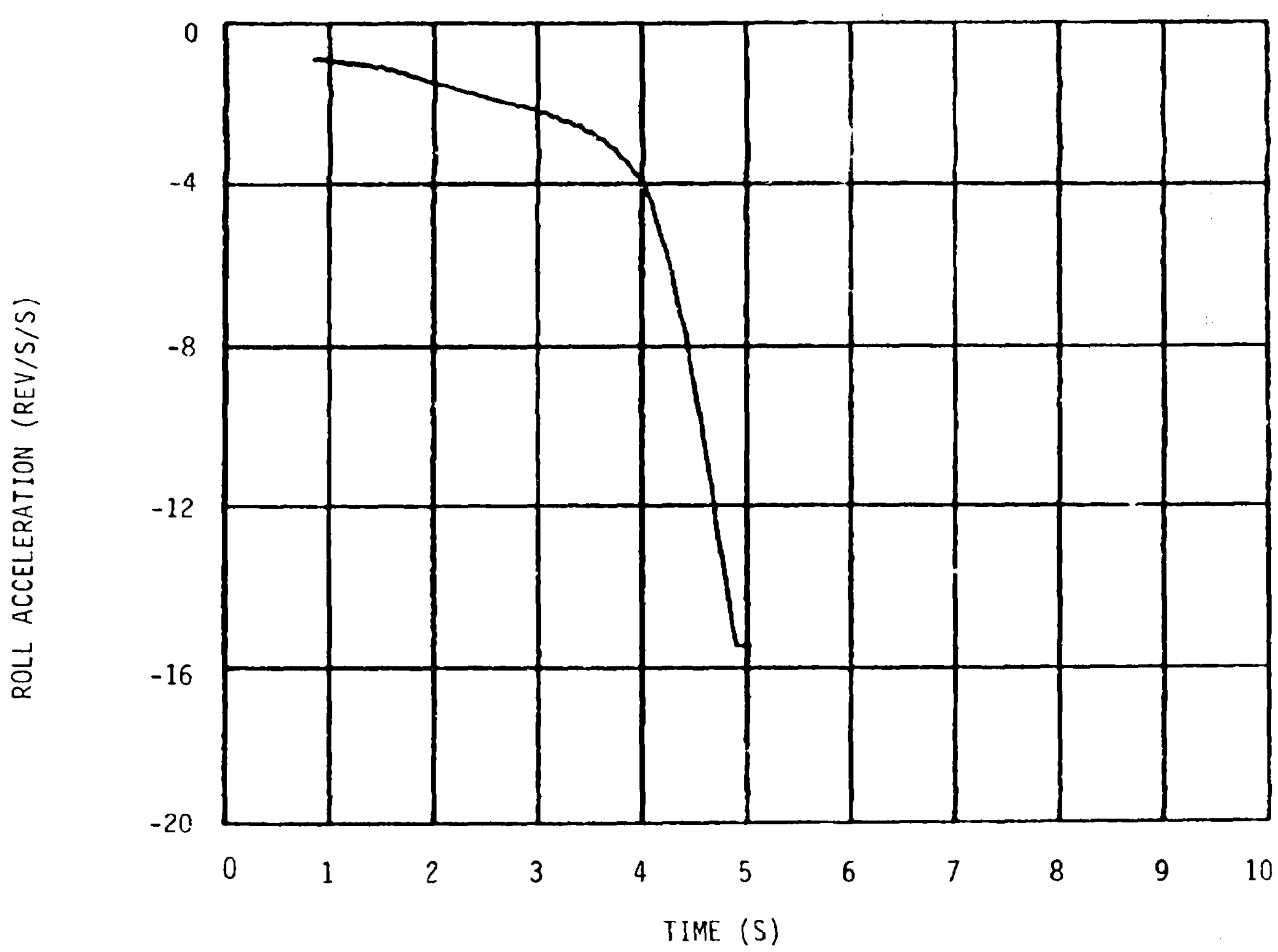

Figure 8a. Roll Acceleration - BRL 1313.

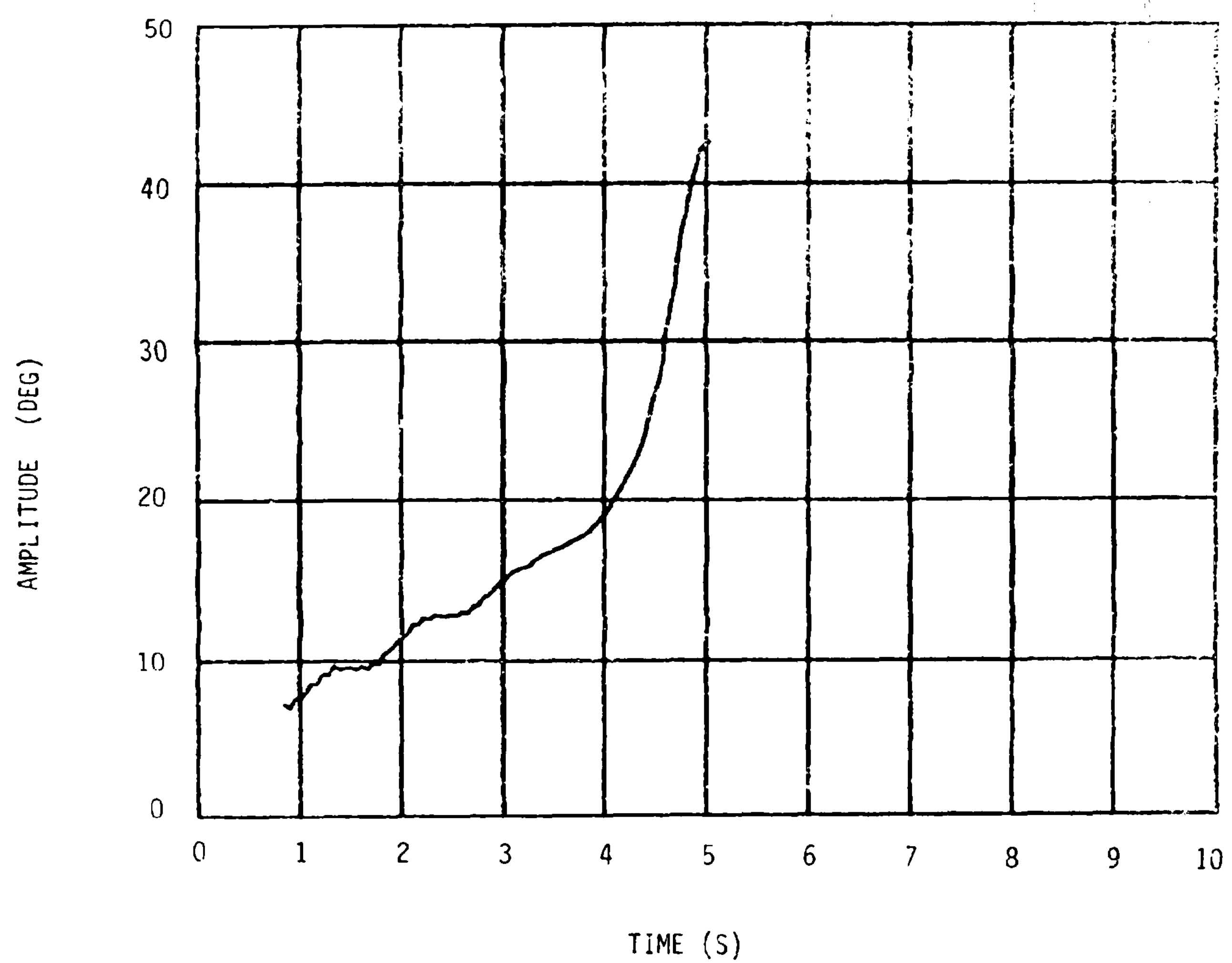

Figure 8b. Coning Amplitude - BRL 1313.

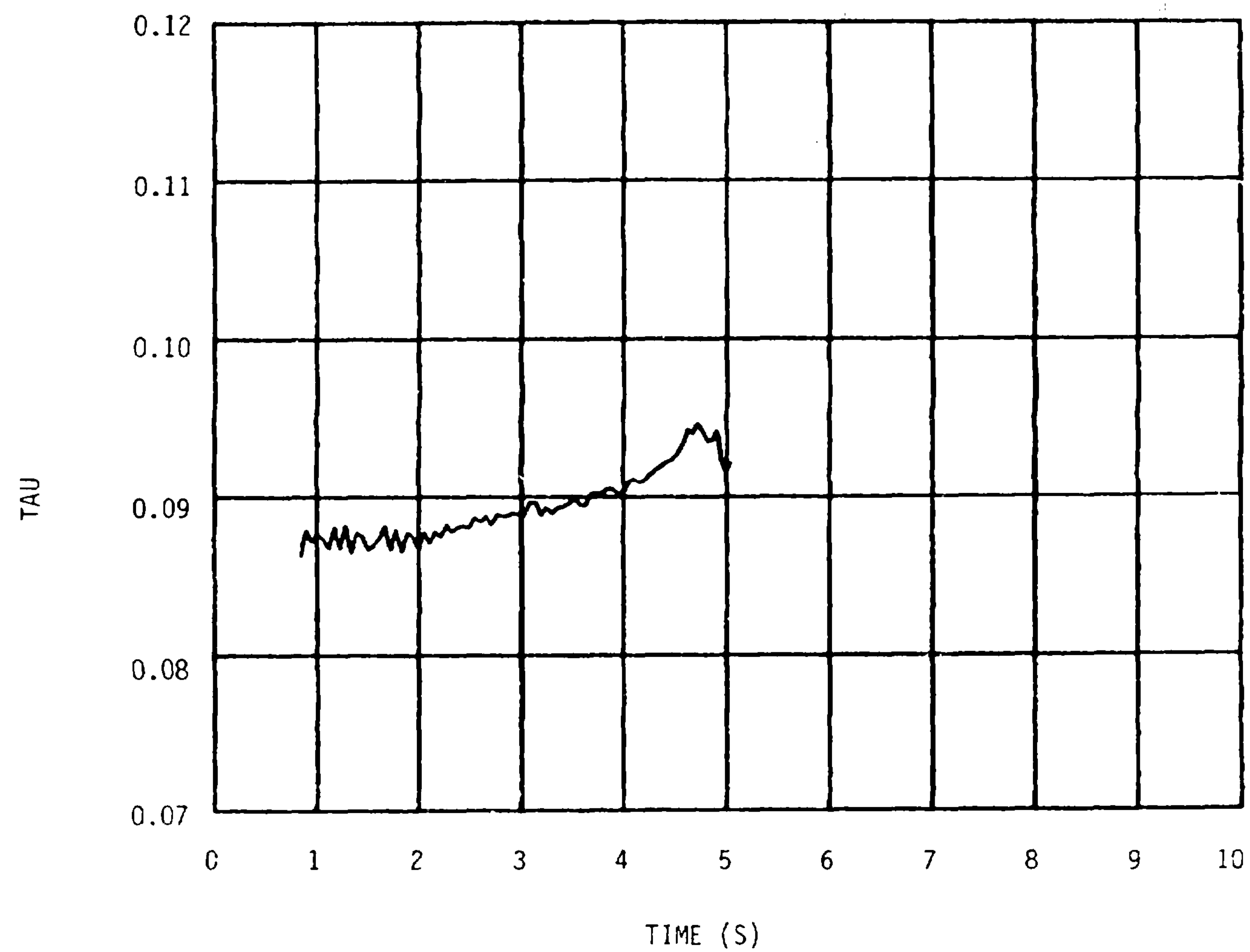

Figure 8c. Nondimensional Coning Frequency - BRL 1313.

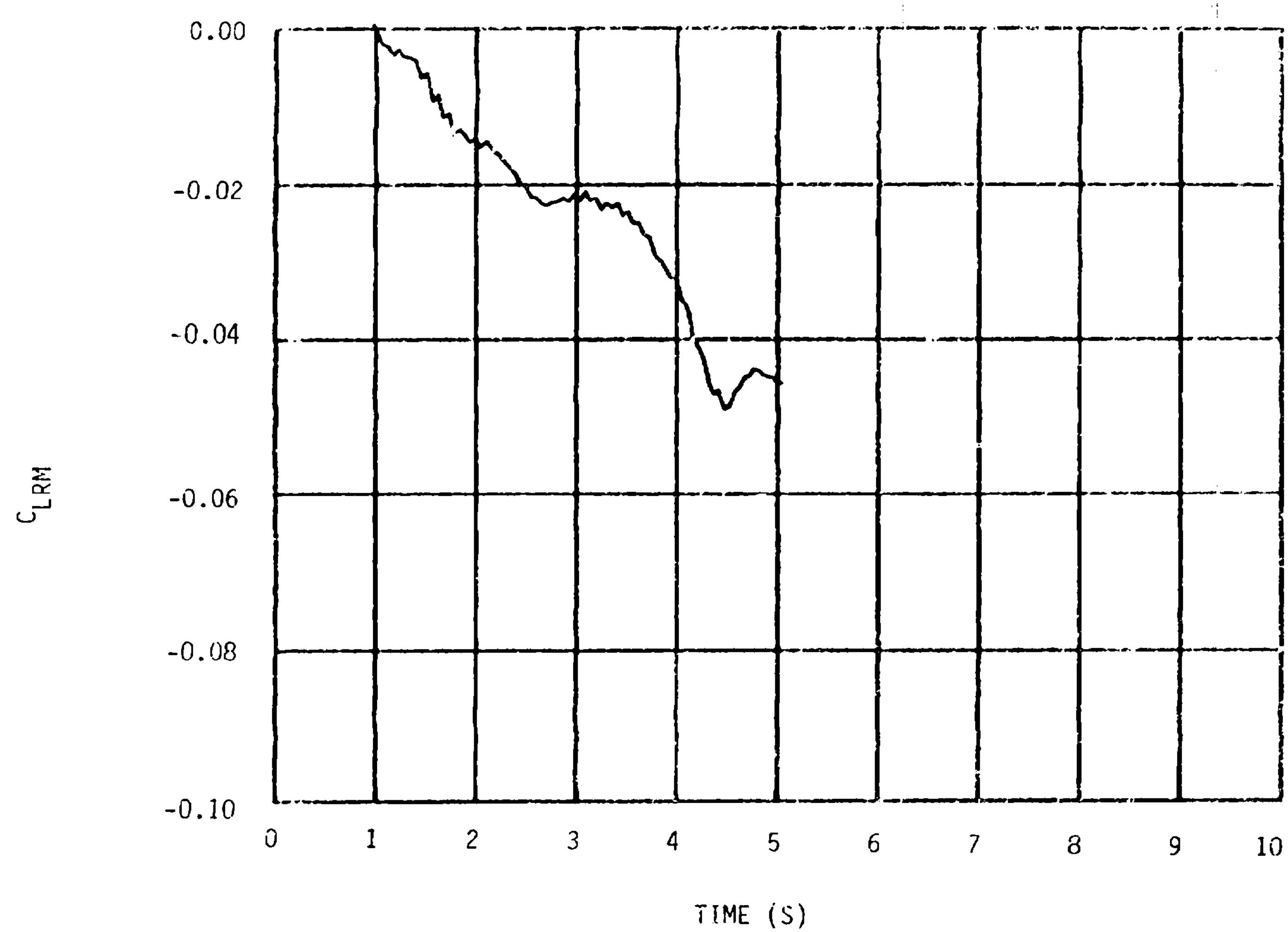

Figure 8d. Liquid Roll Moment Coefficient - BRL 1313.

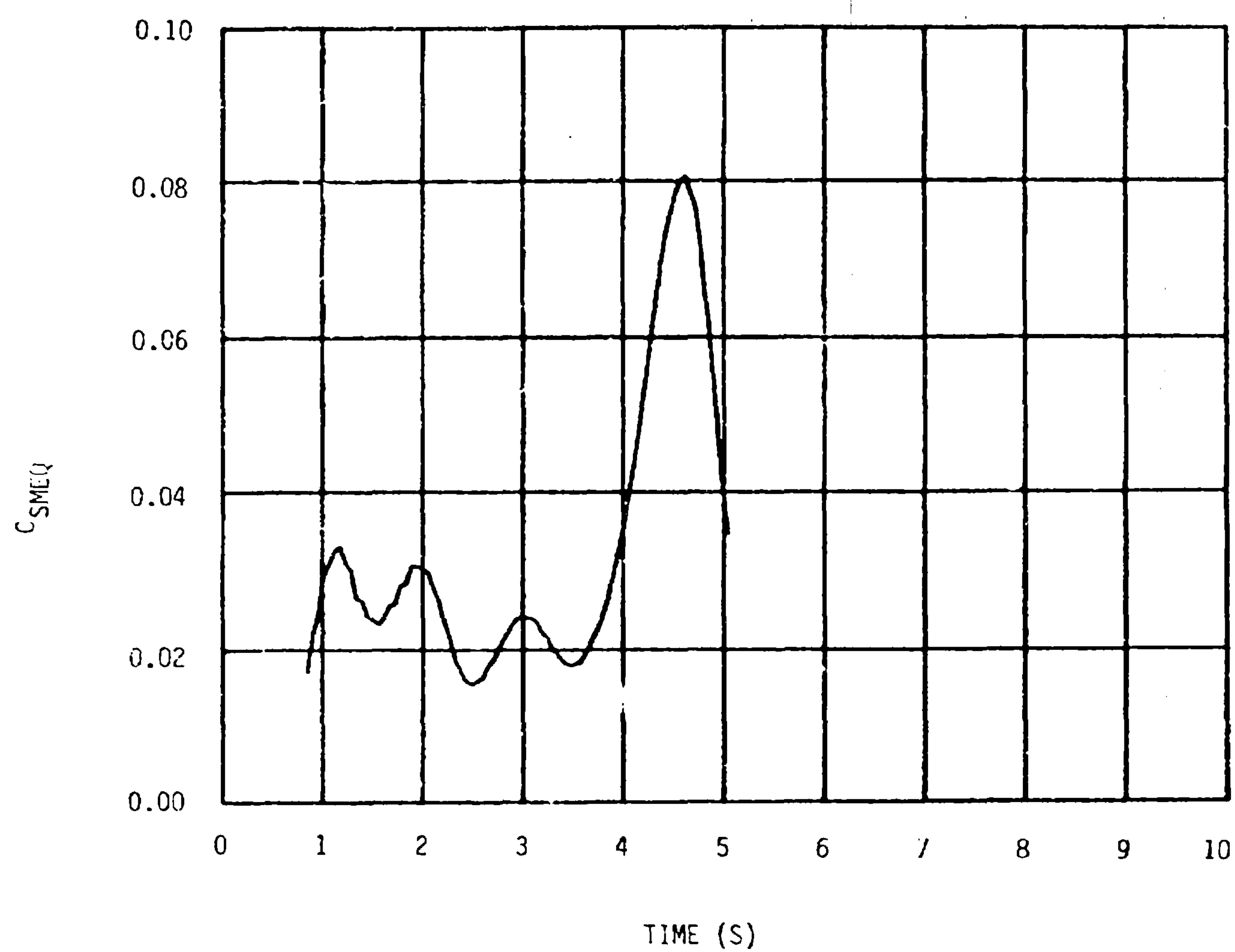

Figure 8e. Equivalent Side Moment Coefficient - BRL 1313.

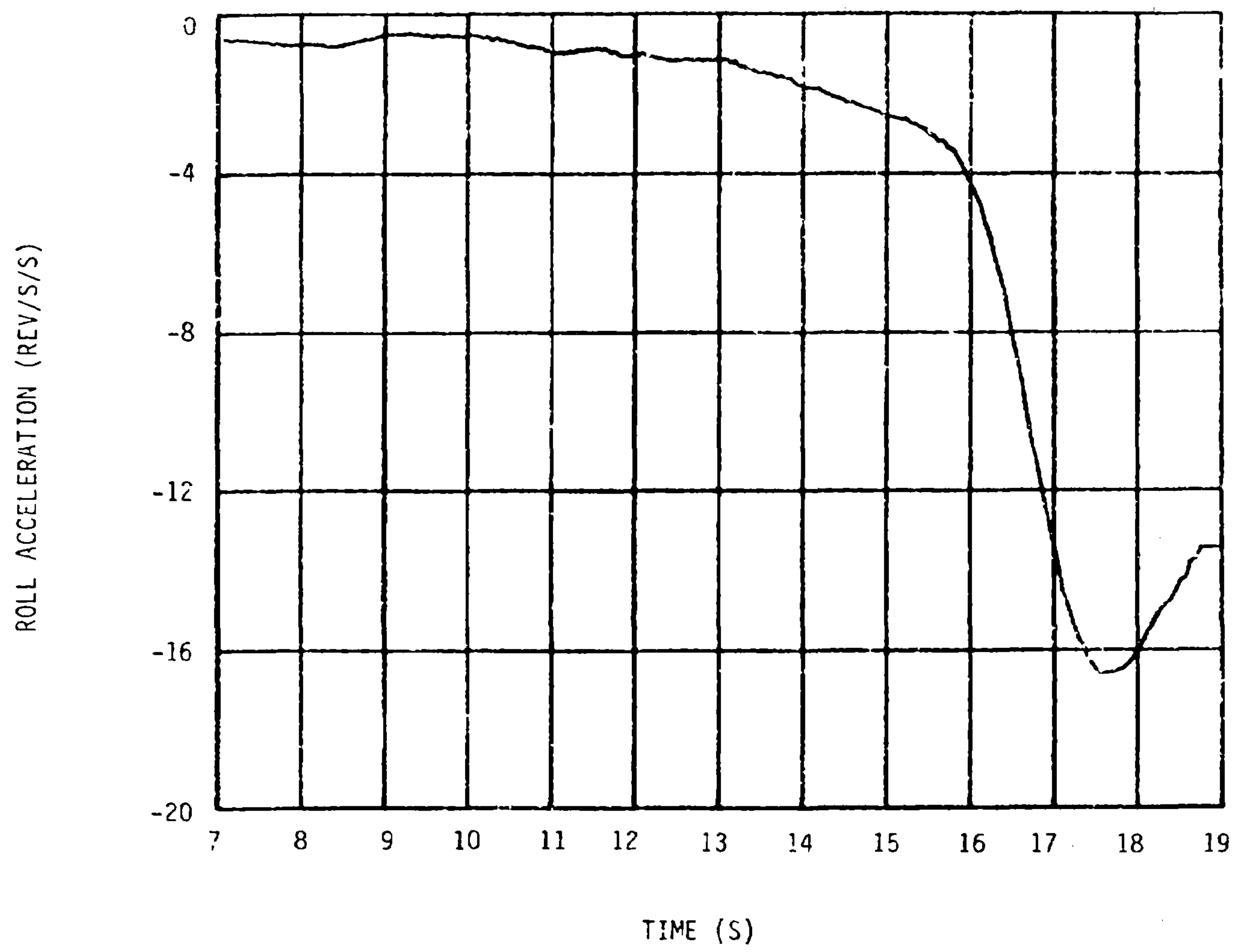

Figure 9a. Roll Acceleration - BRL 1585.

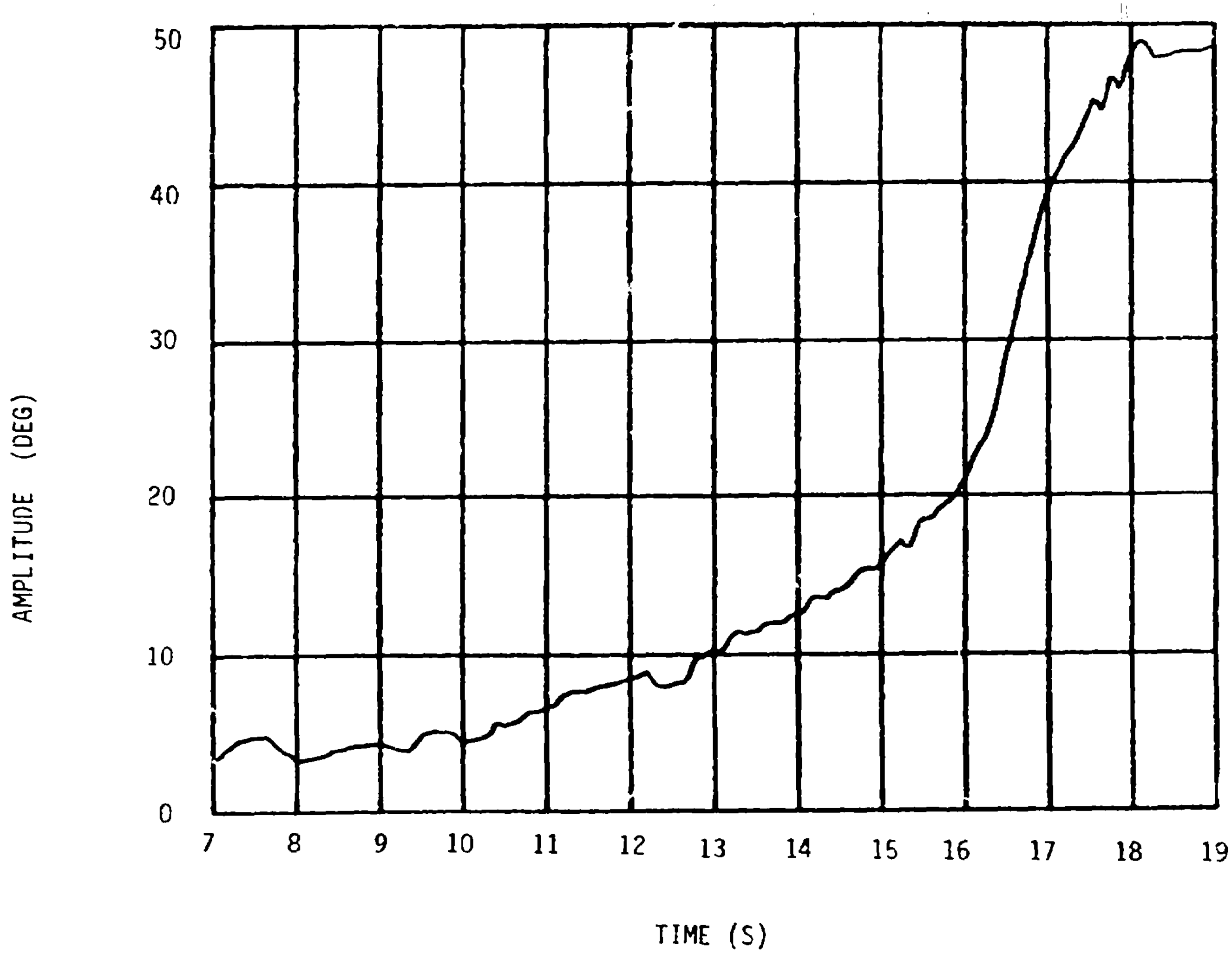

Figure 9b. Coning Amplitude - BRL 1585.

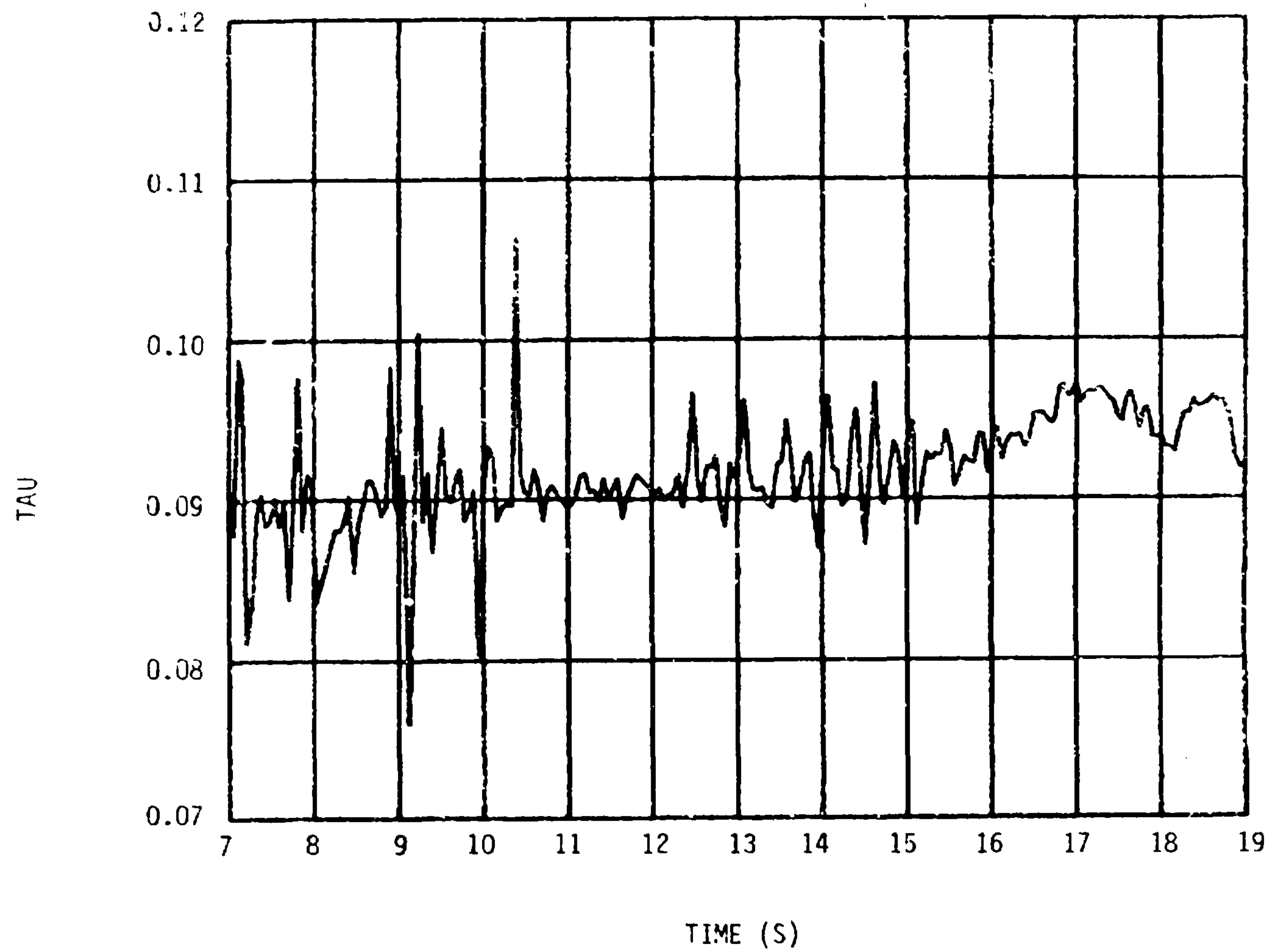

Figure 9c. **Nondimensional** Coning Frequency - BRL 1585.

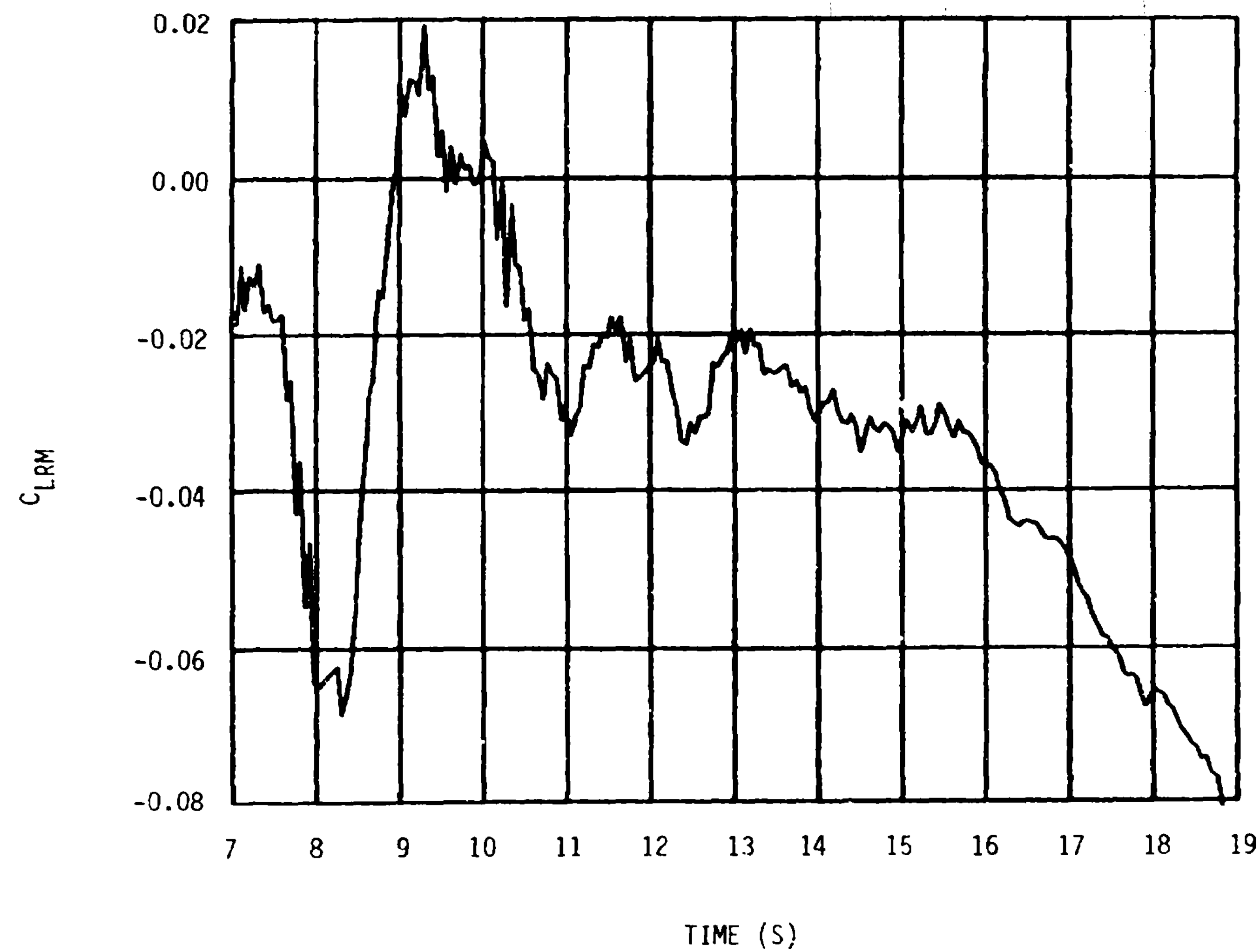

Figure 9d. Liquid Roll Moment Coefficient - BRL 1585.

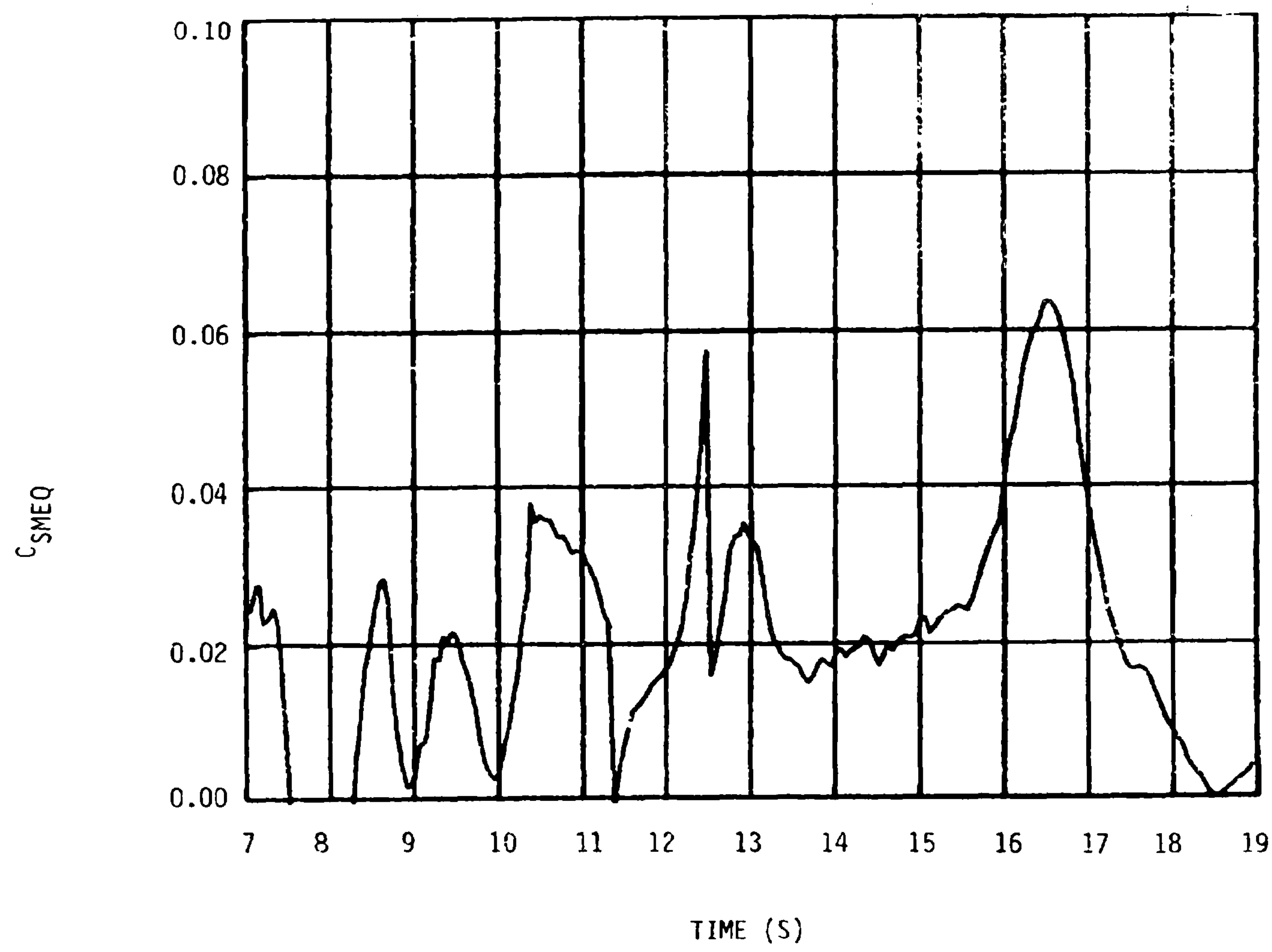

Figure 9e. Equivalent Side Moment Coefficient - BRL 1585.

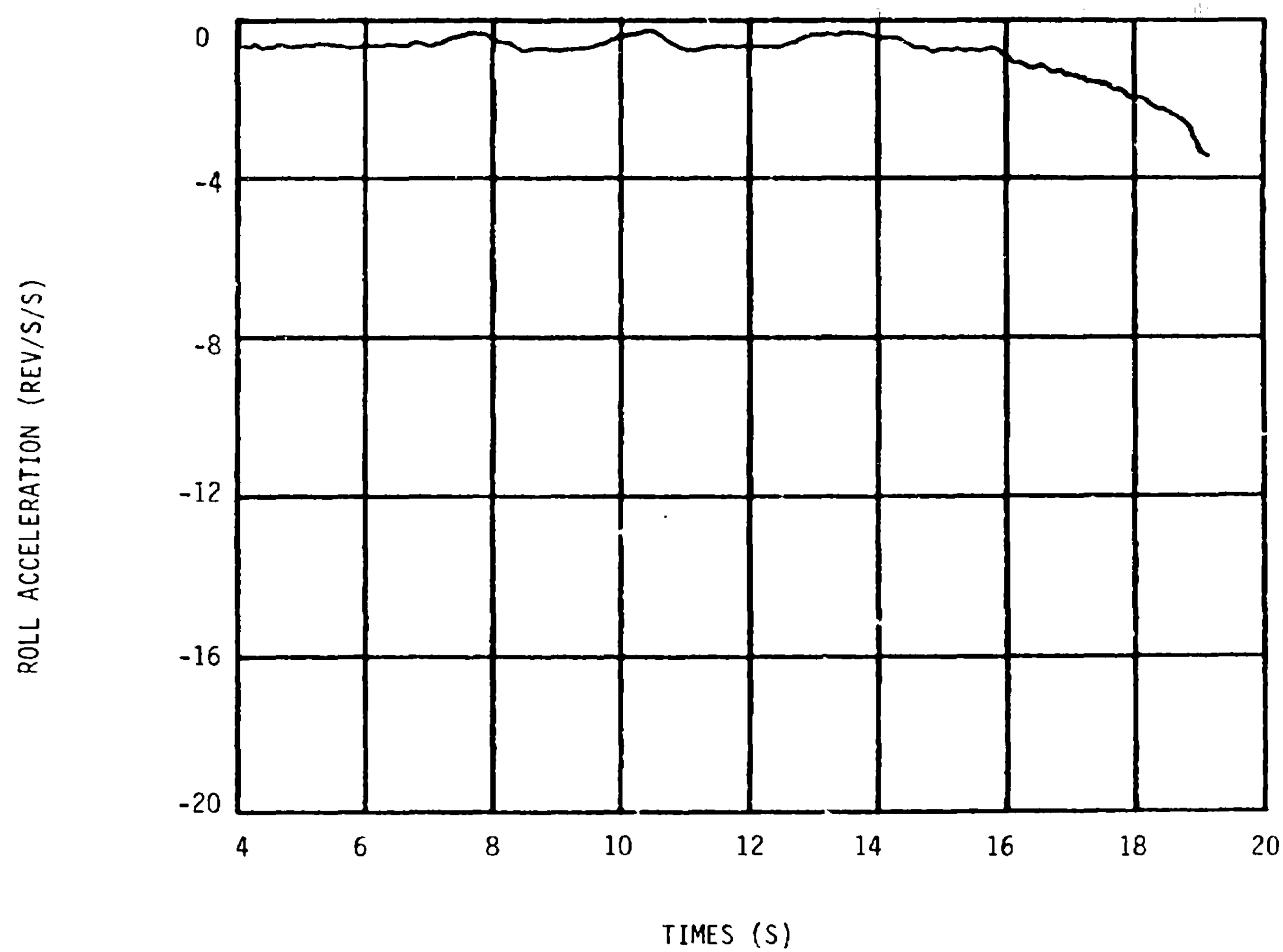

Figure 10a. Roll Acceleration - BRL 1587.

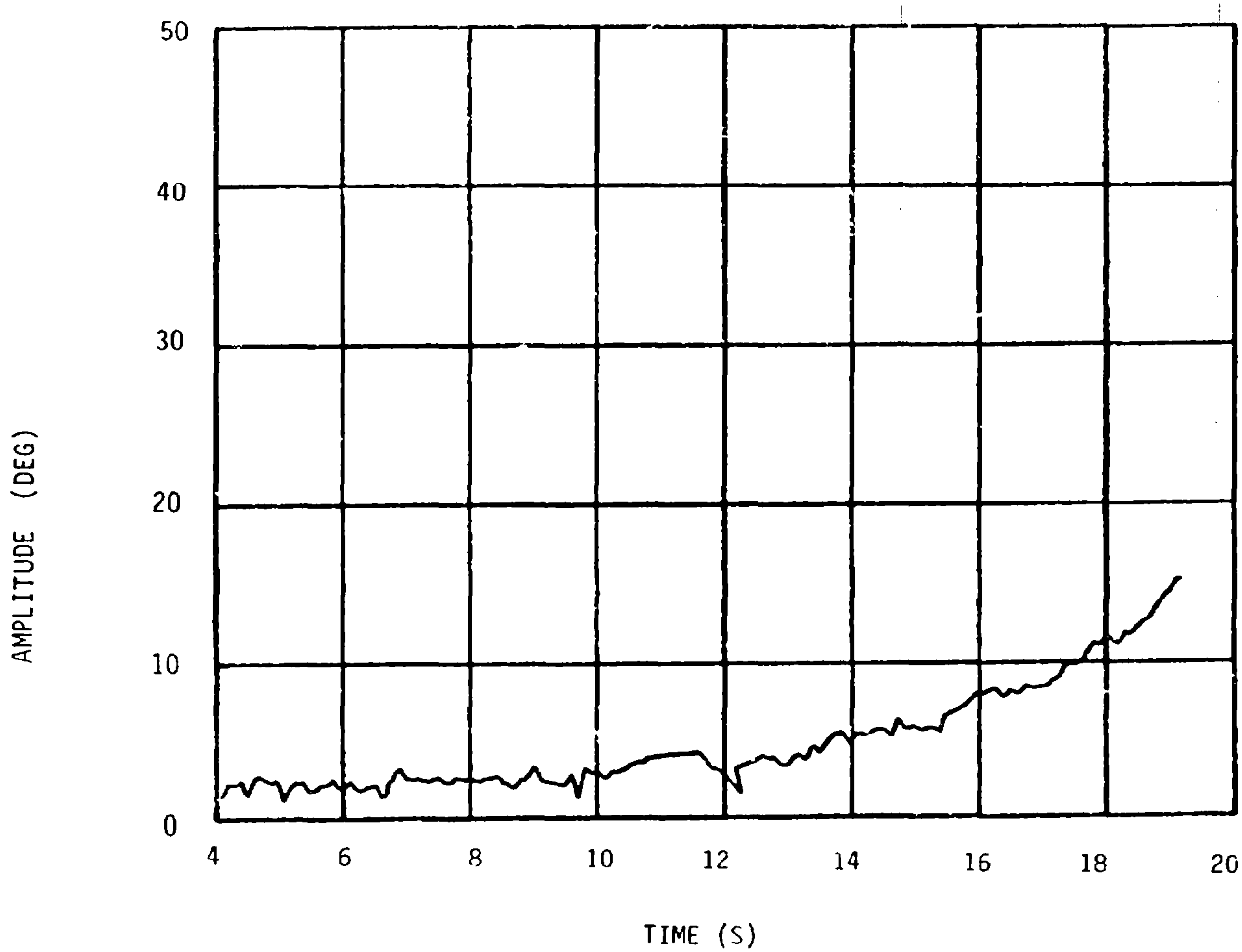

Figure 10b. Coning Amplitude - BRL 1587.

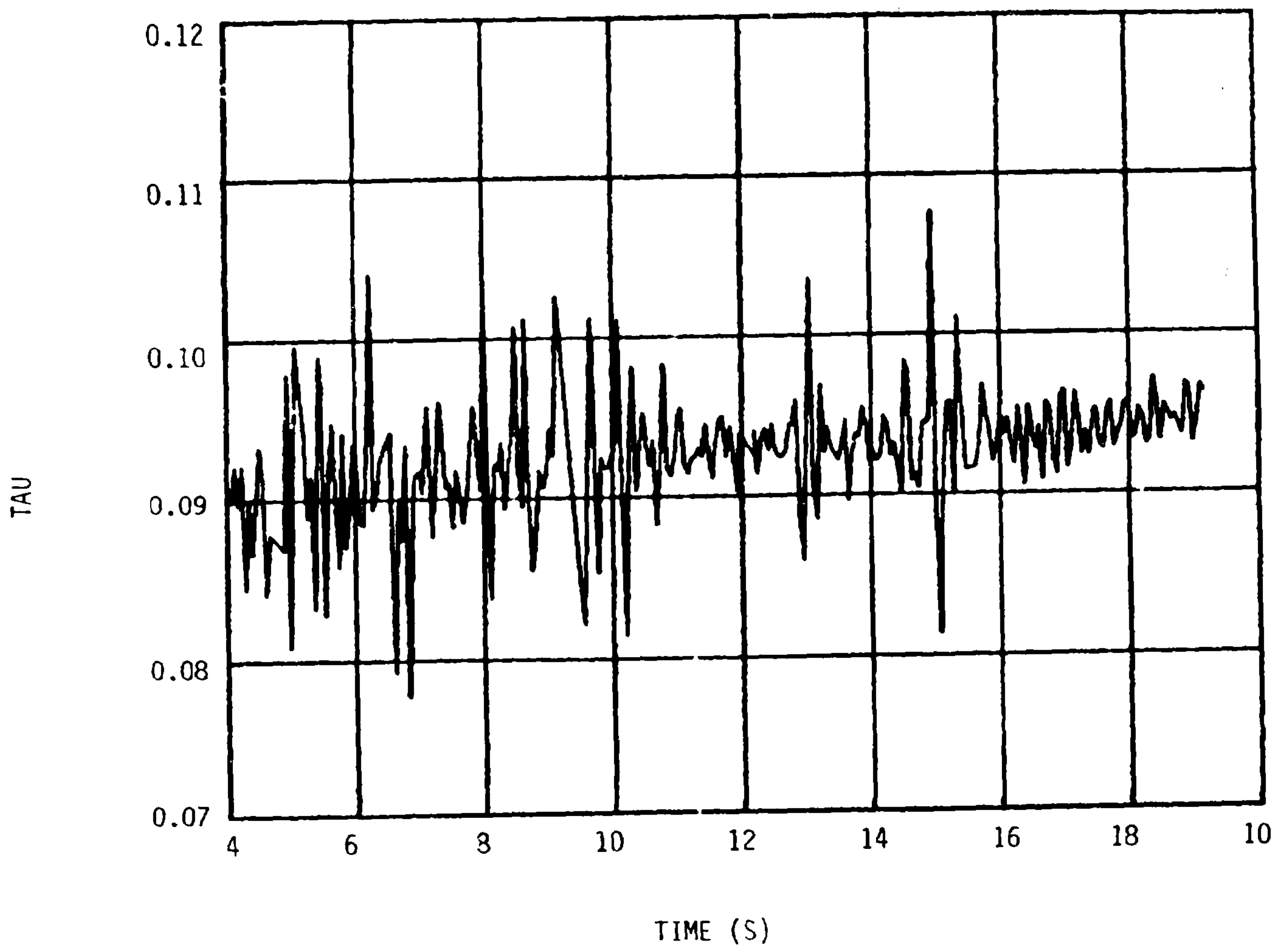

Figure 10c. Nondimensional Coning Frequency - BRL 1587.

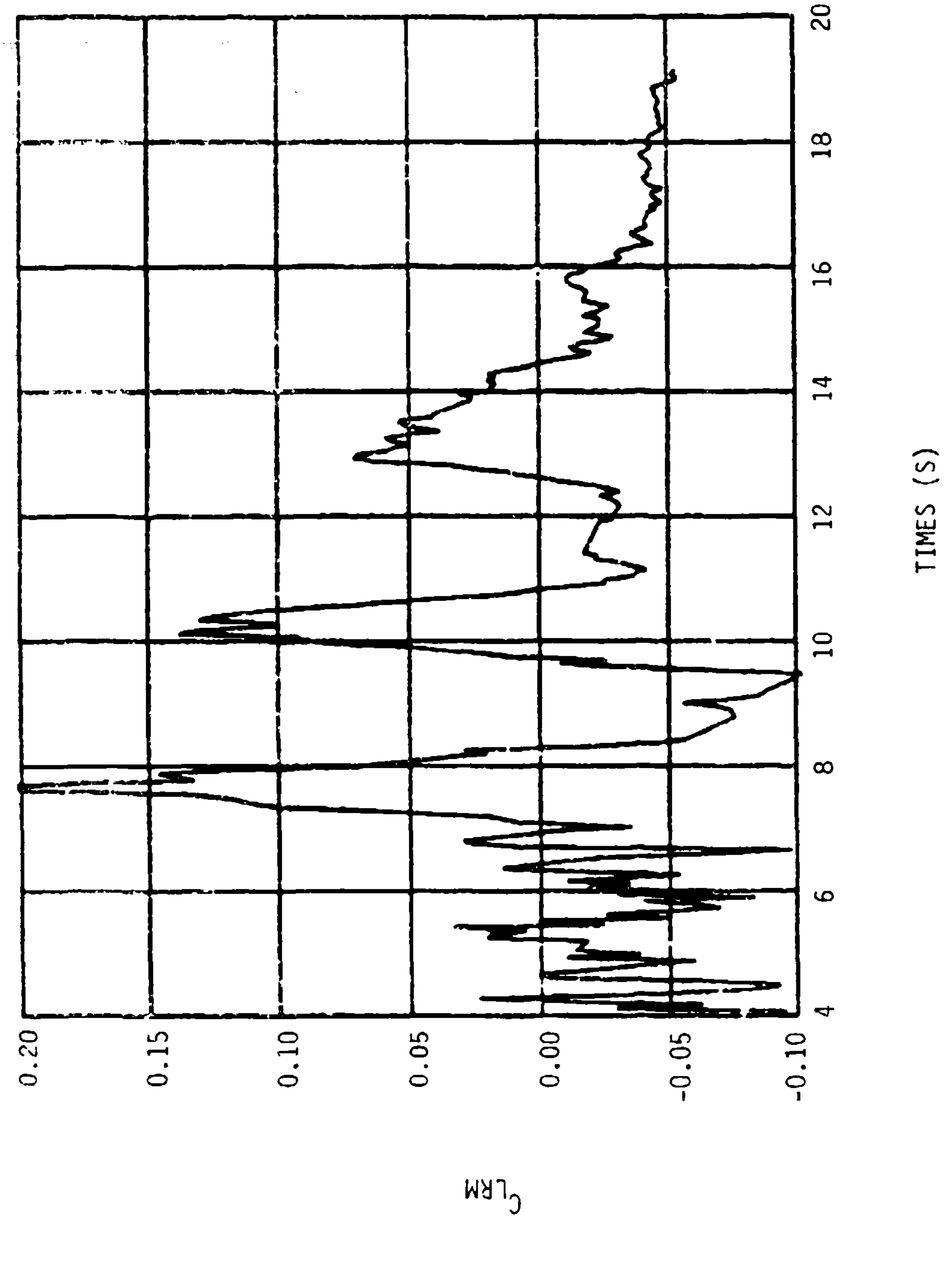

Figure 10d. Liquid Roll Moment Coefficient - BRL 1587.

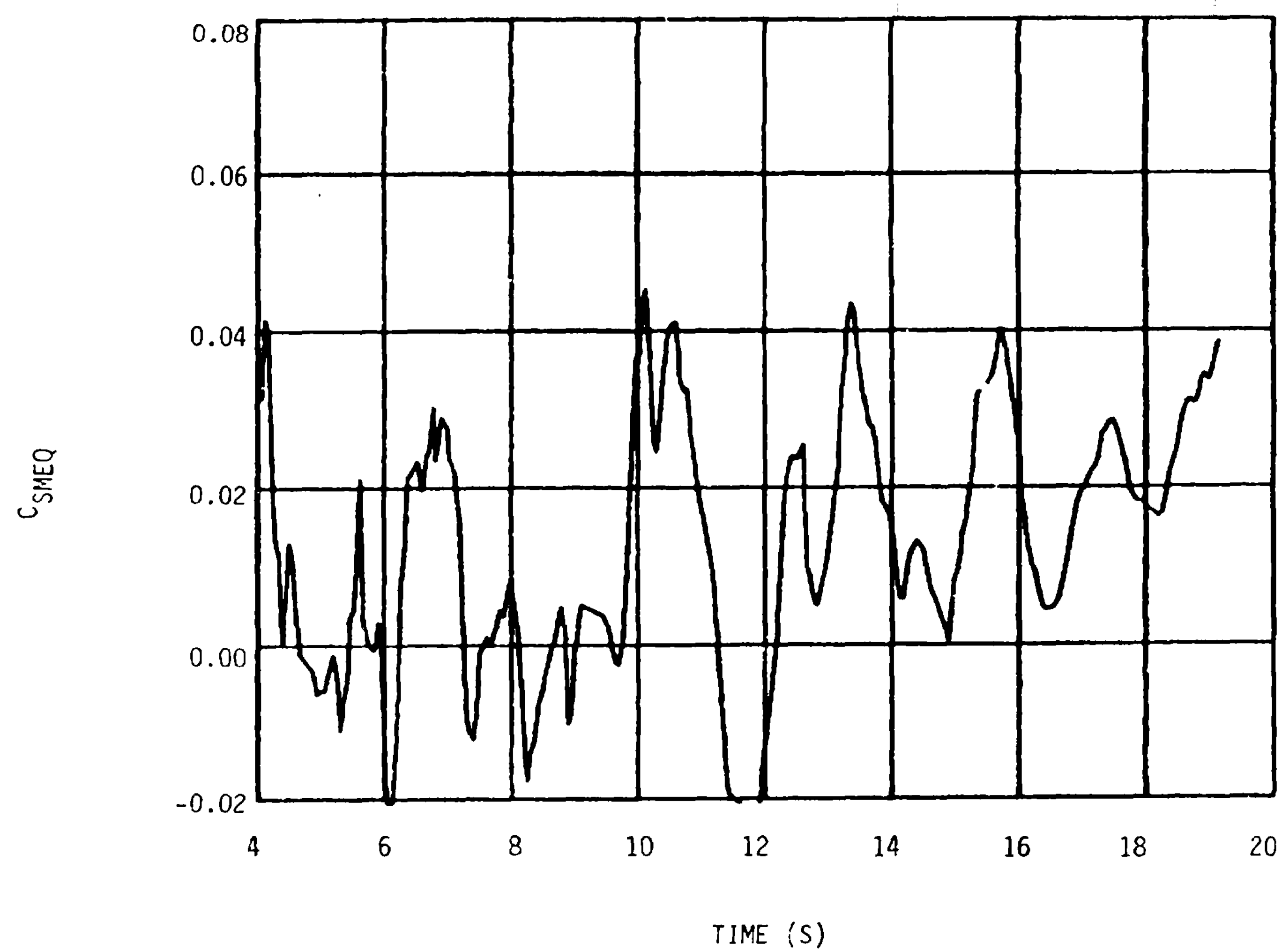

Figure 10e. Equivalent Side Moment Coefficient - BRL 1587.

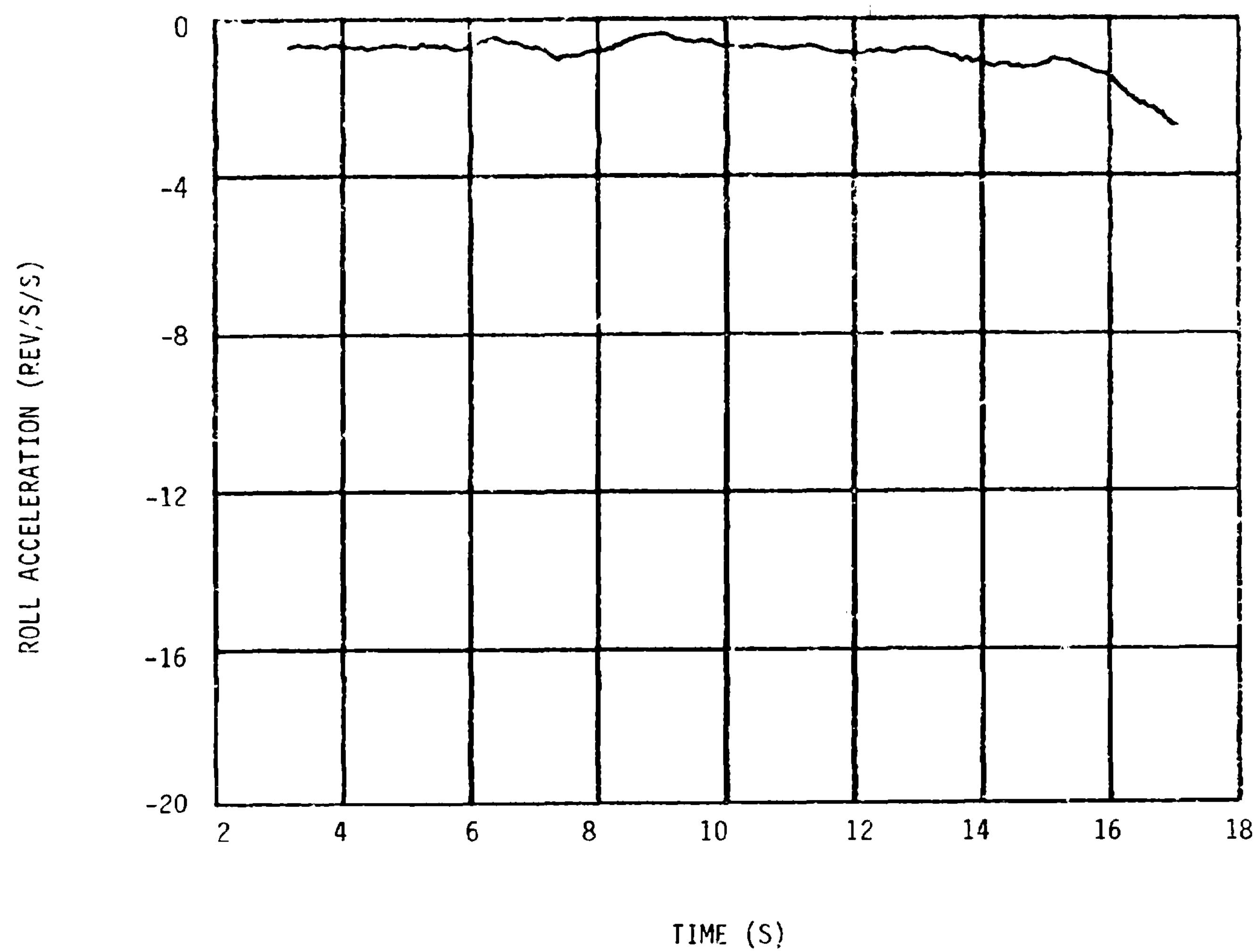

Figure 11a. Roll Acceleration - BRL 1588.

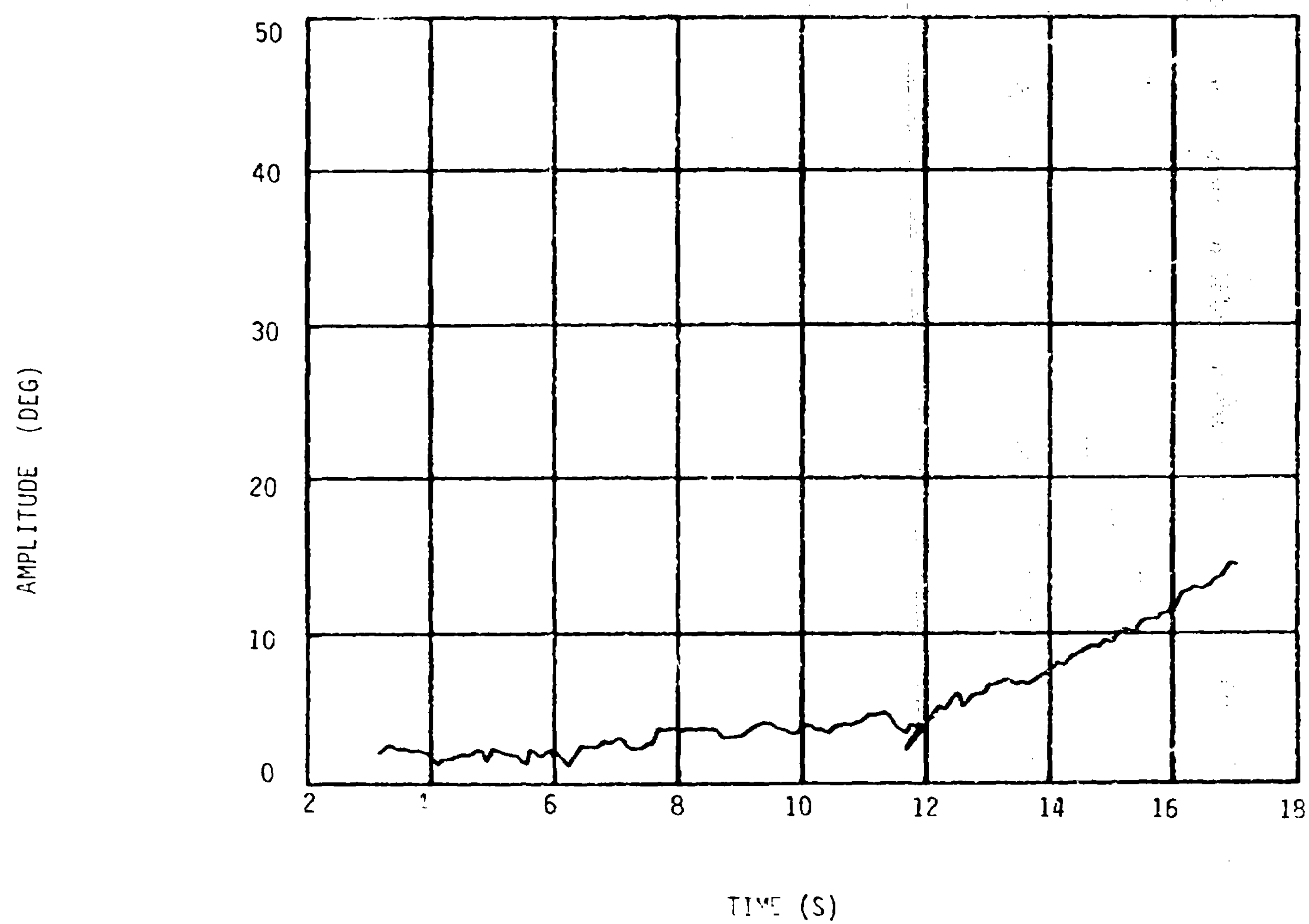

Figure 1[illegible]. Coning Amplitude - BRL 1588.

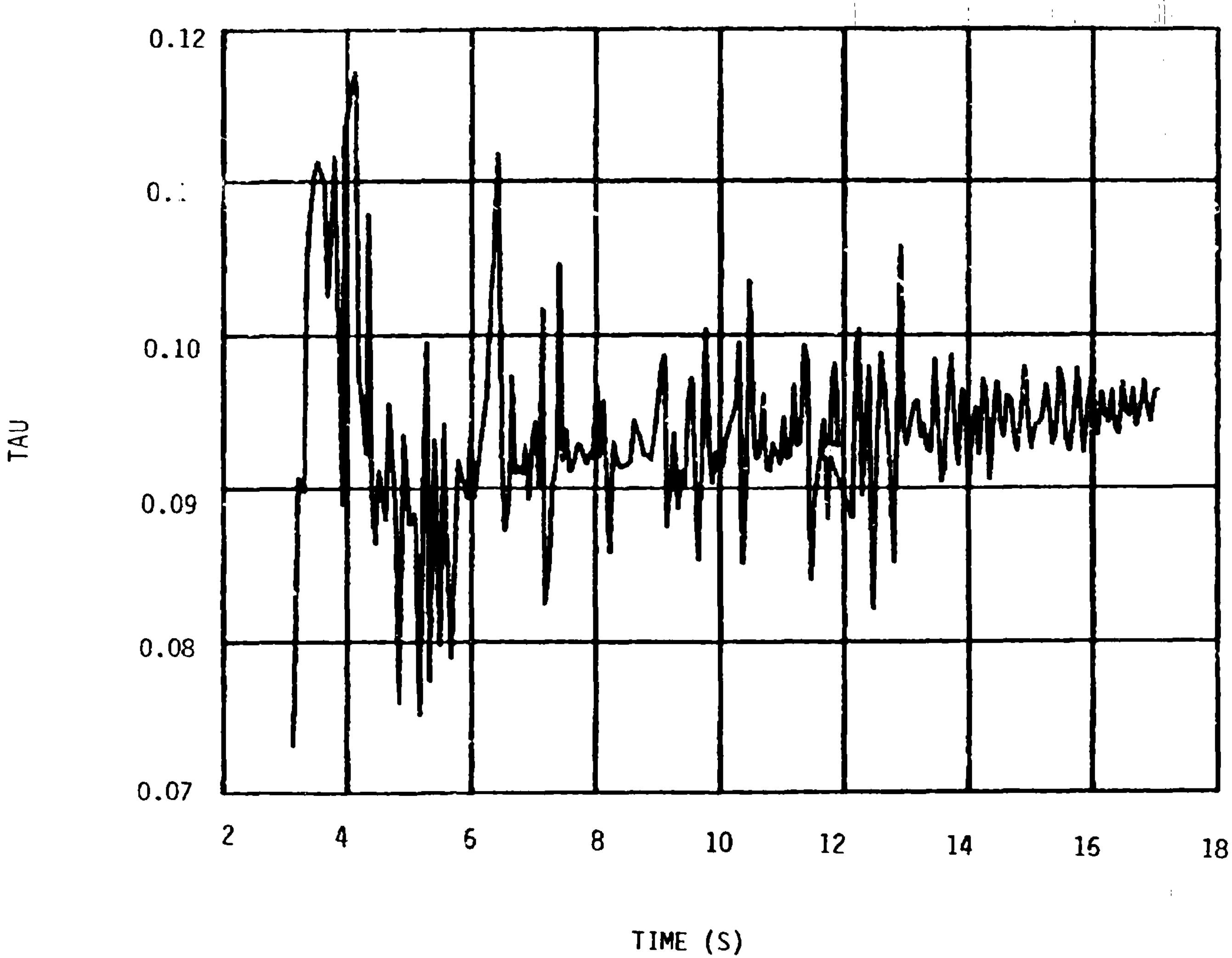

Figure 11c. Nondimensional Coning Frequency - BRL 1588.

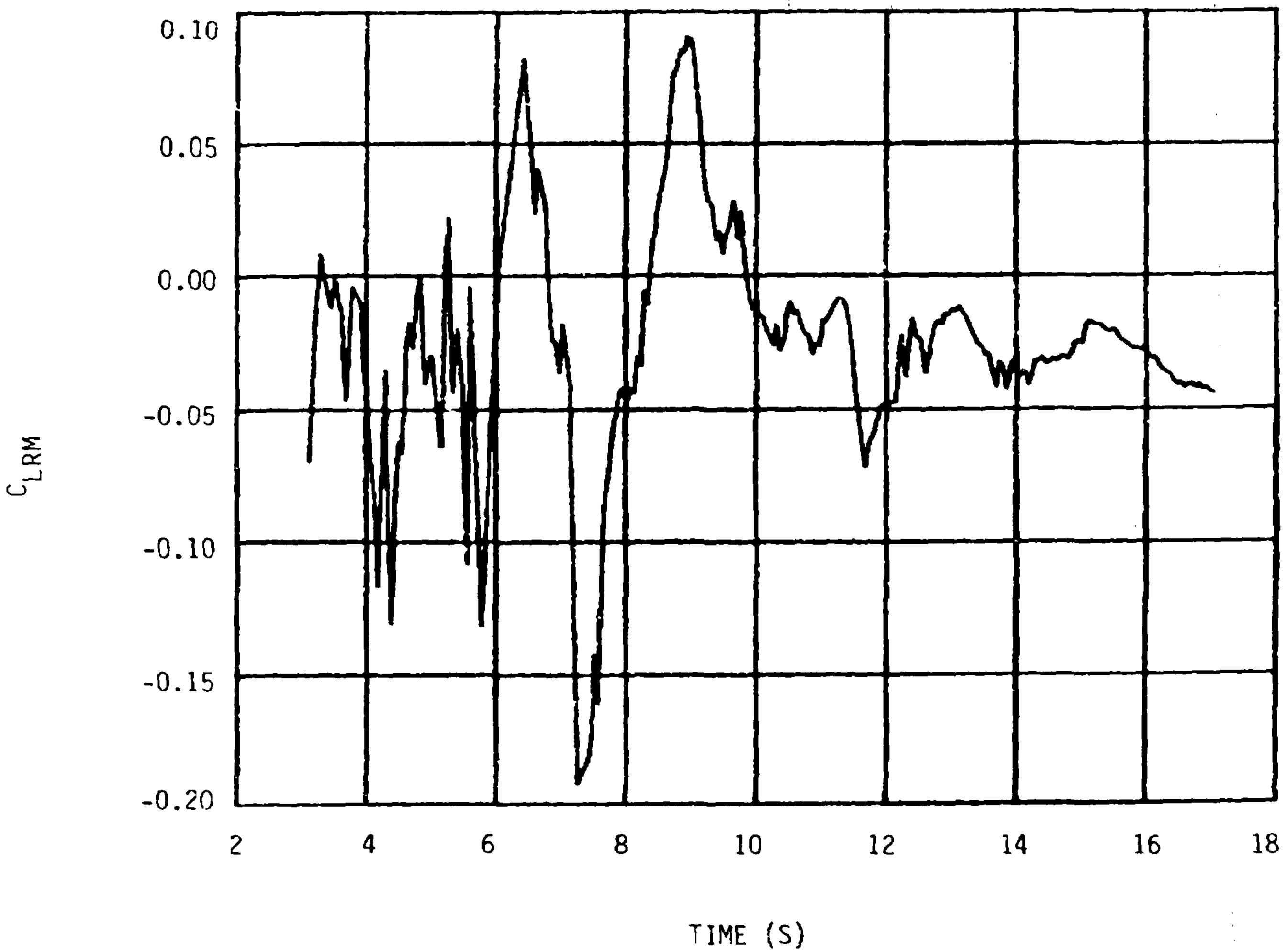

Figure 11d. Liquid Roll Moment Coefficient - BRL 1588.

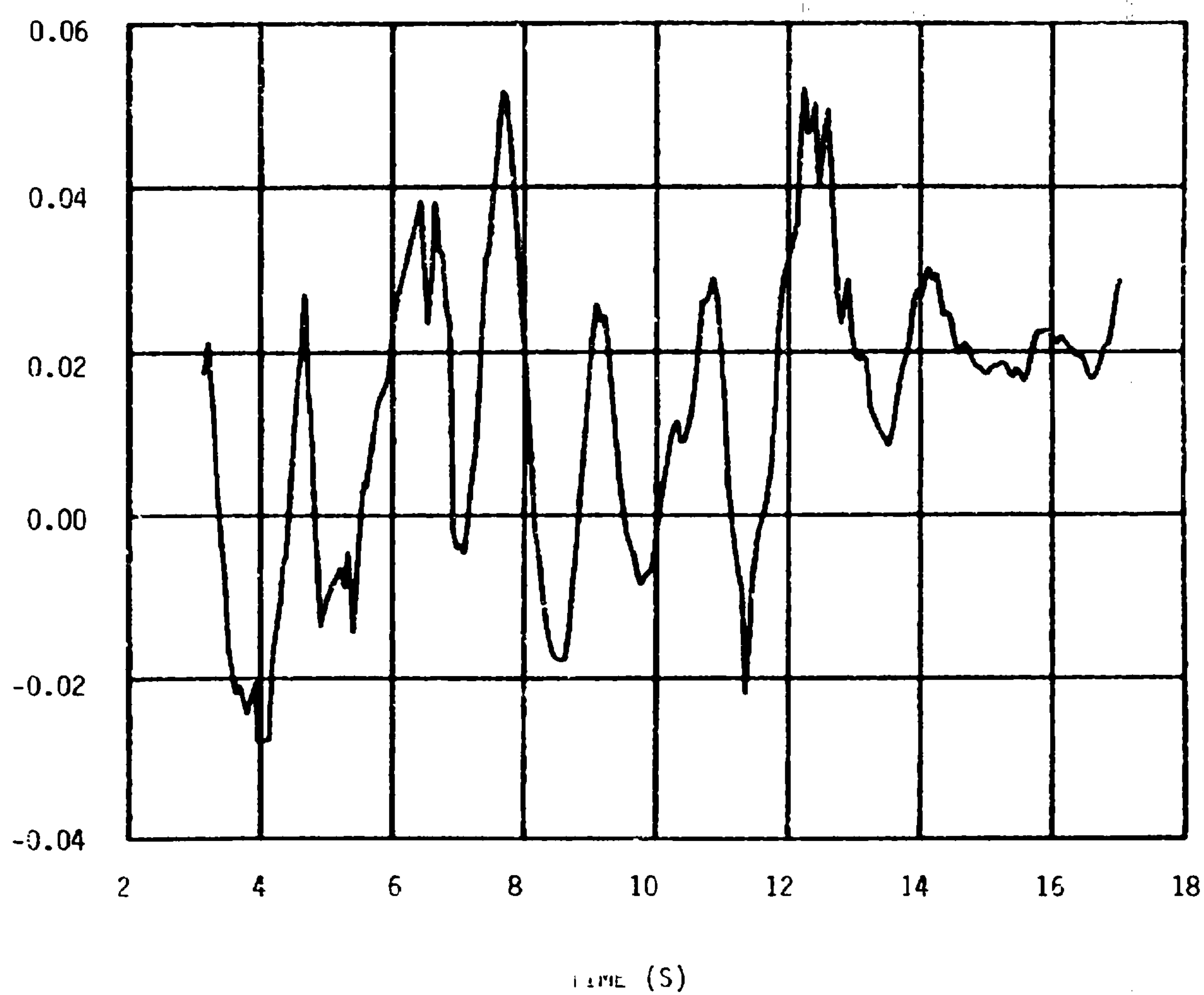

Figure 11a. Equivalent Side Moment Coefficient - BRL 1588.

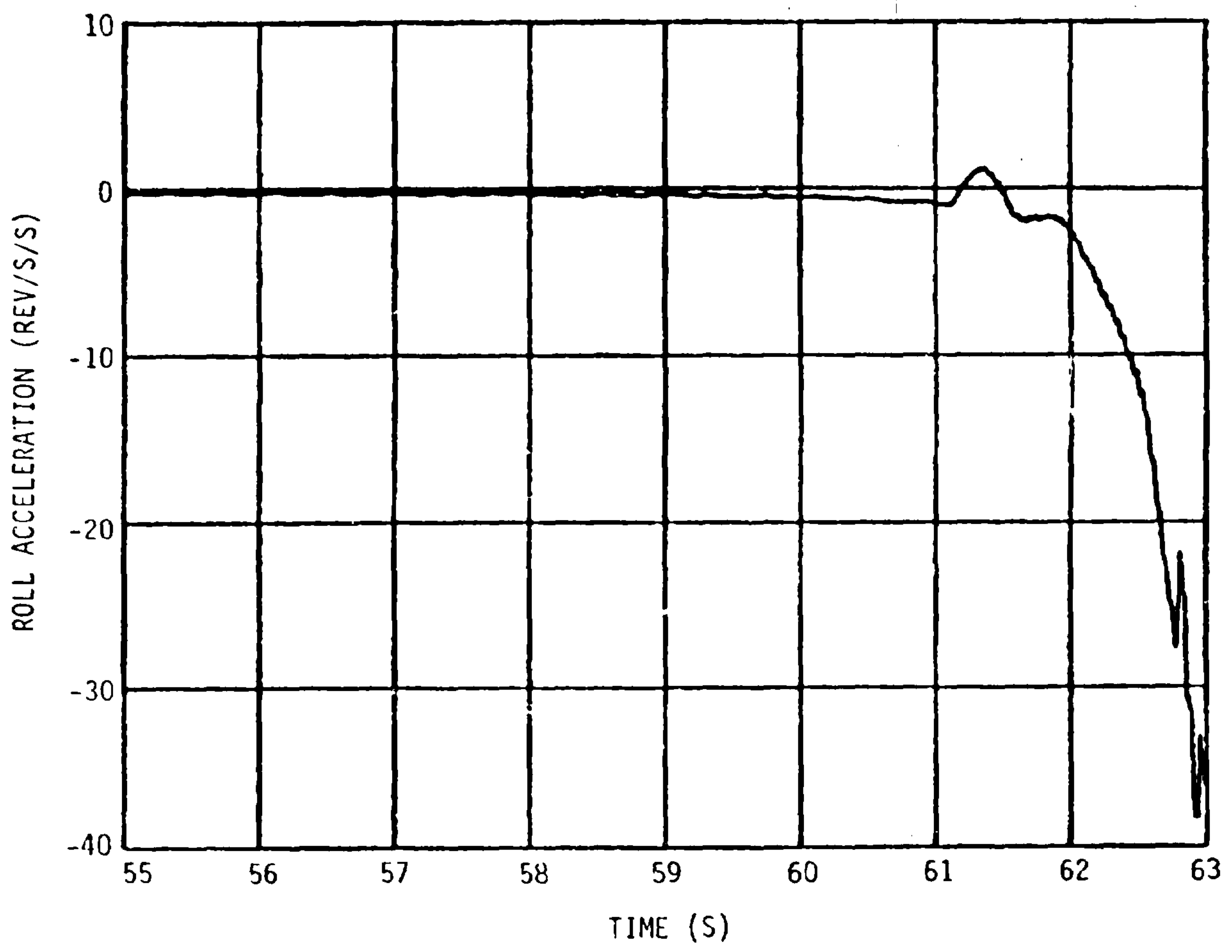

Figure 12a. Roll Acceleration - BRL 1693.

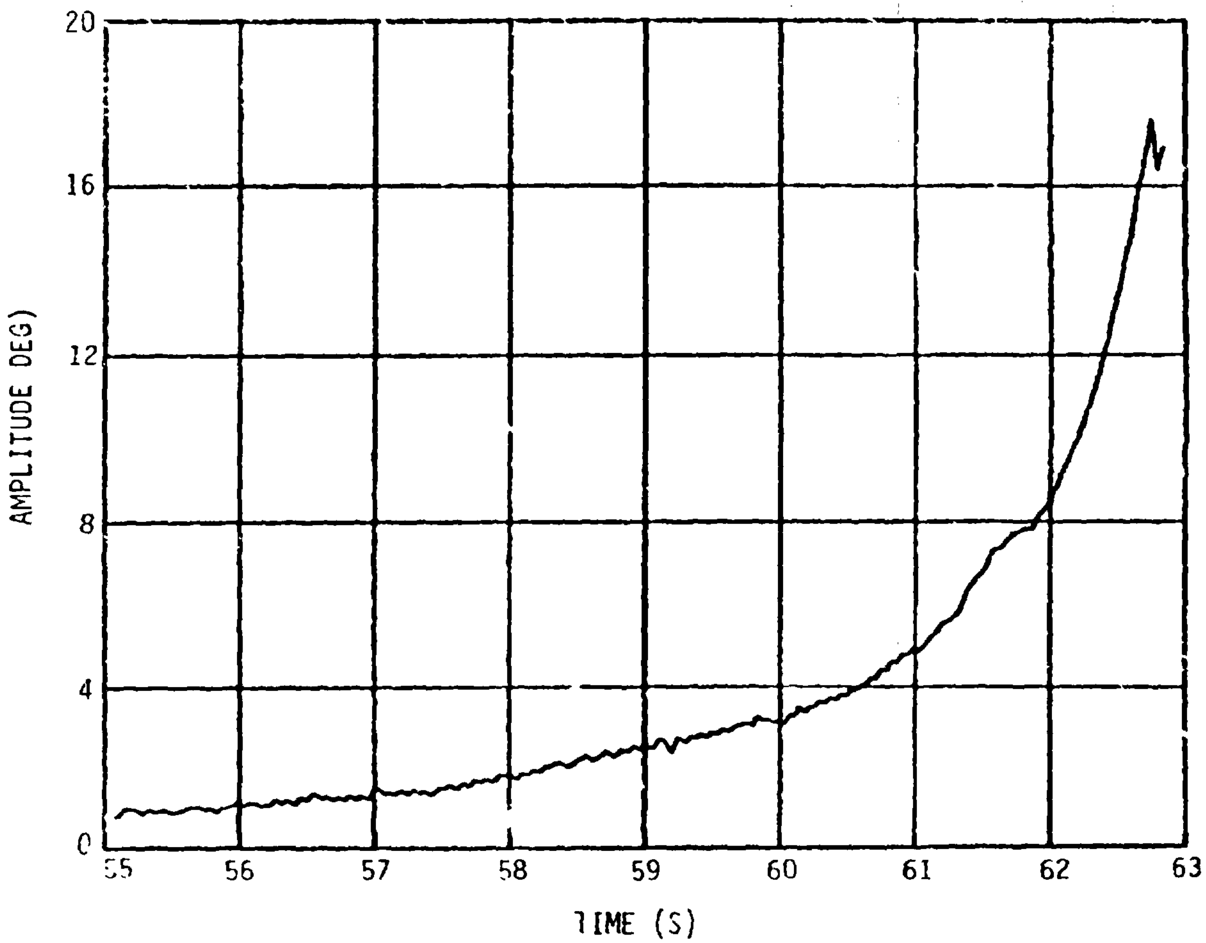

Figure 12b. Coning Amplitude - BRL 1693.

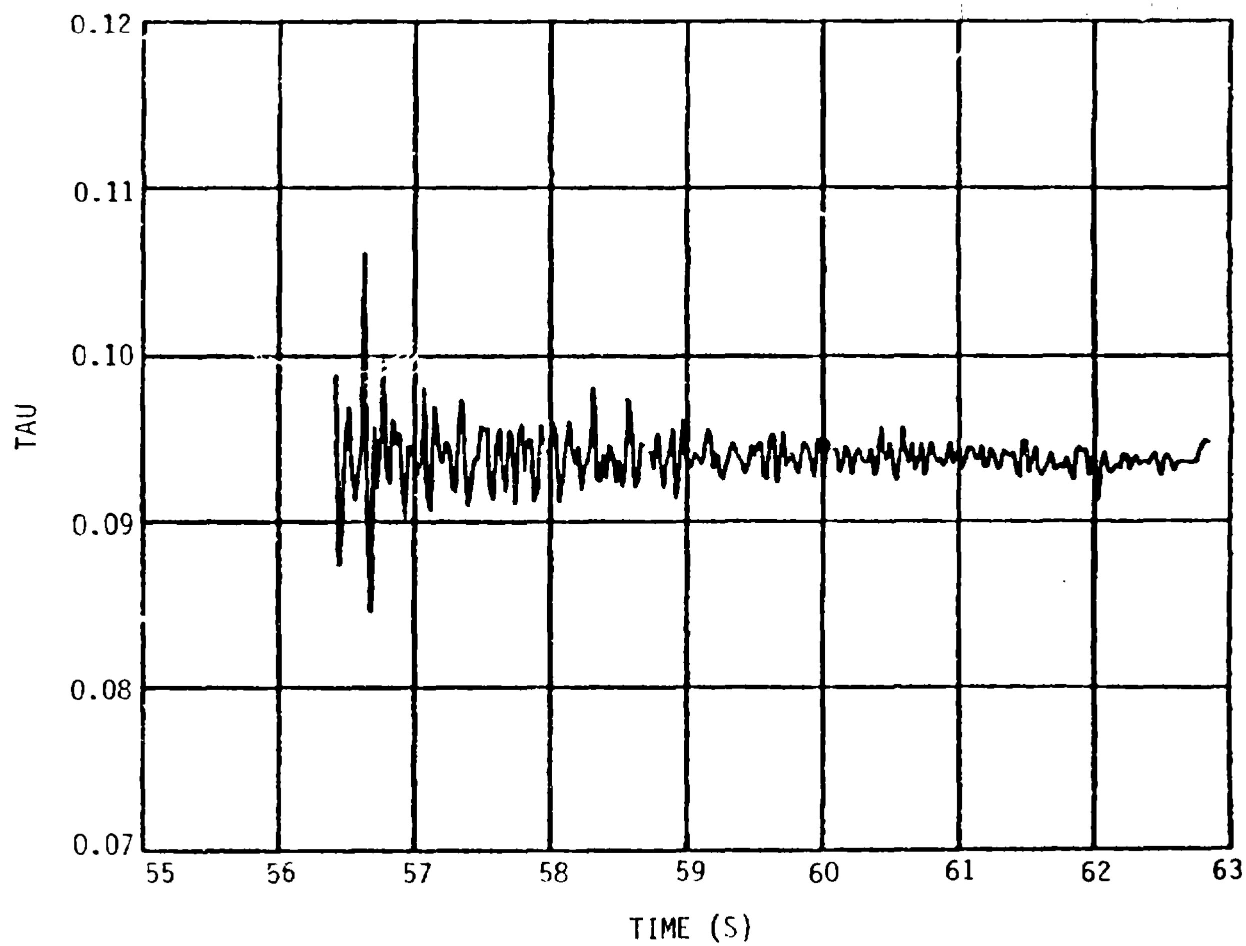

Figure 12c. Nondimensional Coning Frequency - BRL 1693.

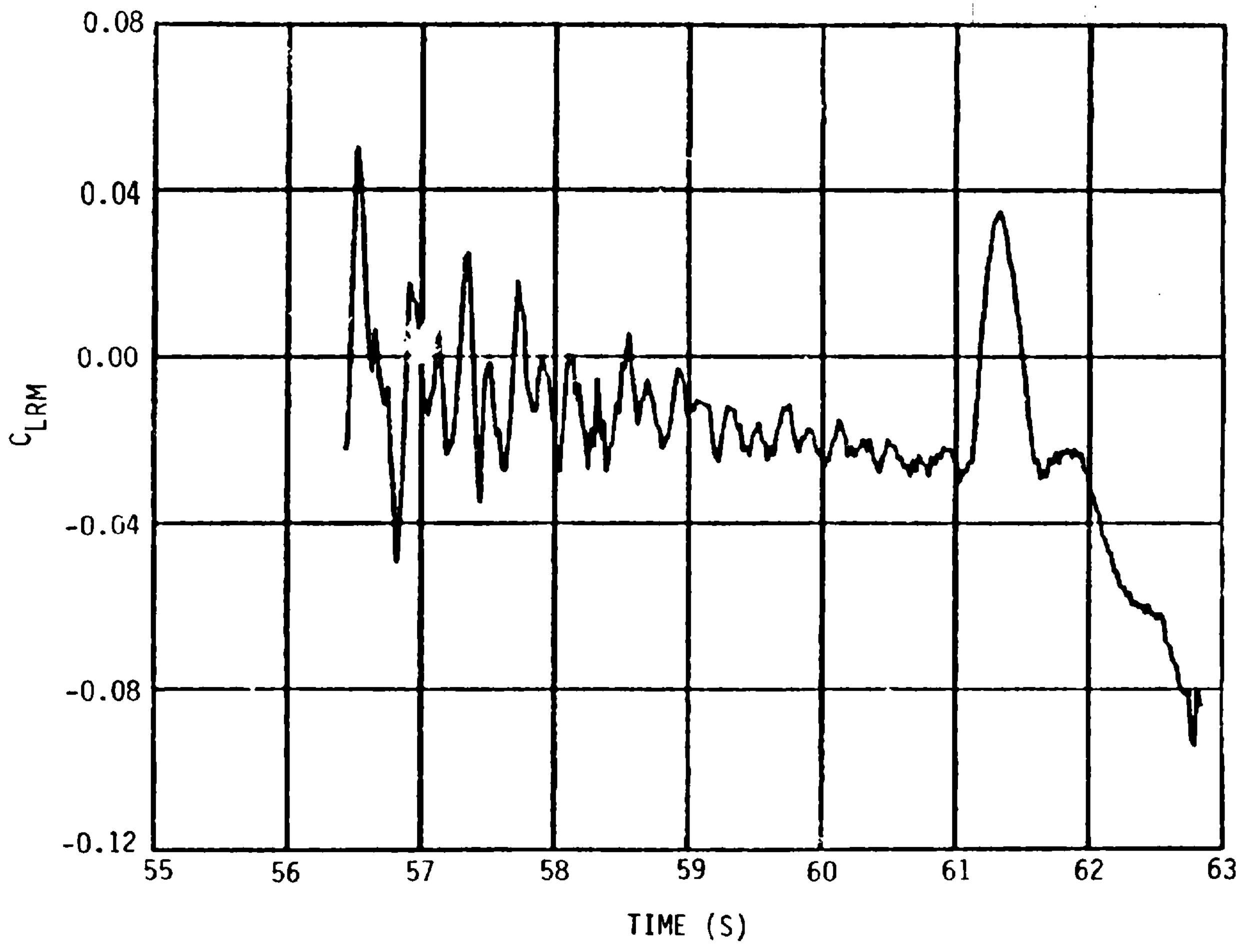

Figure 12d. Liquid Roll Moment Coefficient - BRL 1693.

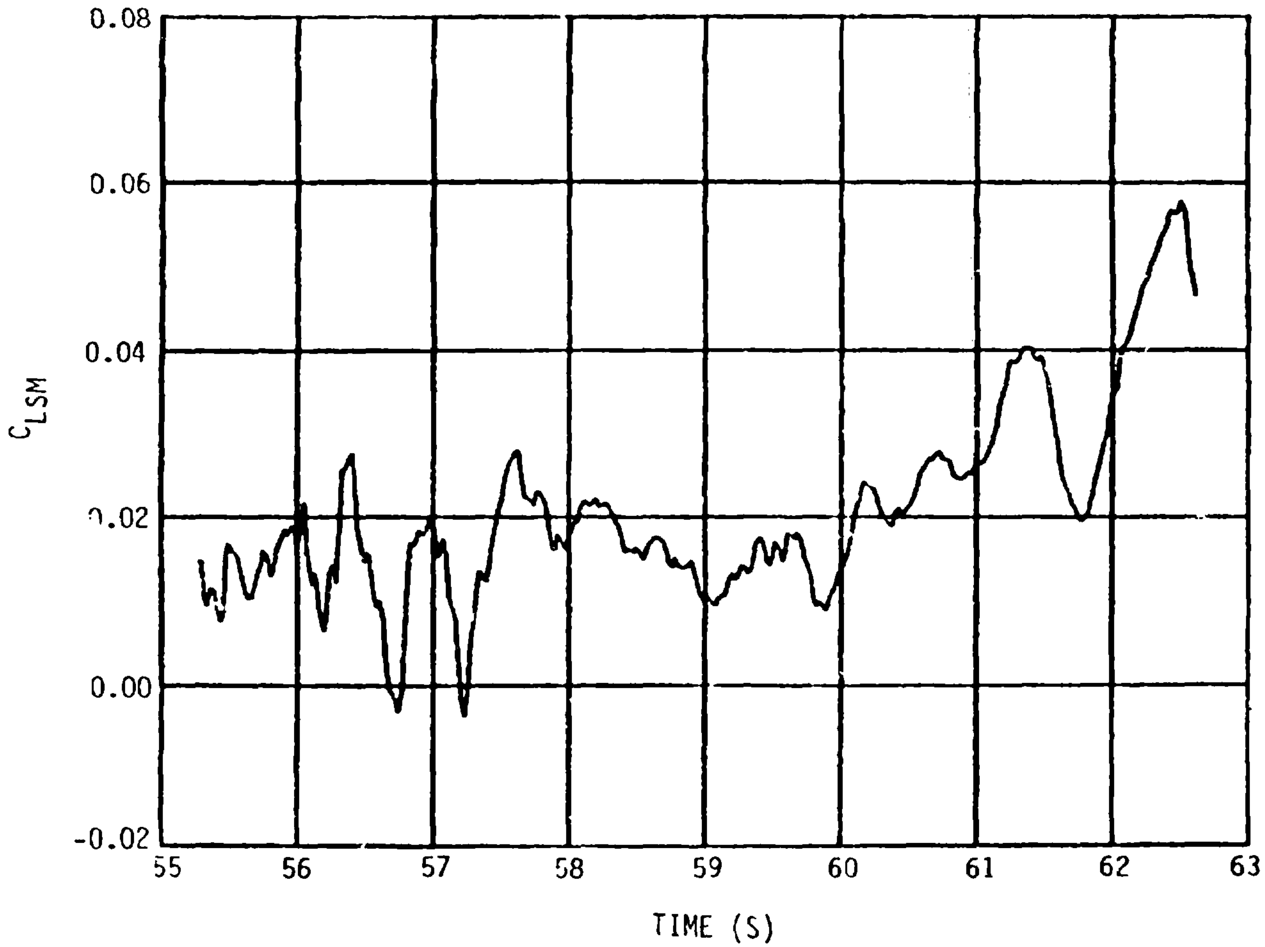

Figure 12e. Equivalent Side Moment Coefficient - BRL 1693.

REFERENCES

1. W. P. D'Amico, V. Oskay, and W. H. Clay, "Flight Tests of the 155mm XM687 Binary Projectile and Associated Design Modification Prior to the Nicolet Winter Test 1974-1975,"U.S. Ballistic Research Laboratory, Aberdeen Proving Ground, Maryland, BRL Memorandum Report ARBRL-MR-2748, May 1977 (AD B019693L).

2. W. P. D'Amico, W. H. Clay, and A. Mark, "Yawsonde Data for M687-Type Projectiles With Application to Rapid Spin Decay and Stewartson-Type Spin-Up Instabilities," U.S. Ballistic Research Laboratory, Aberdeen Proving Ground, Maryland, BRL Memorandum Report ARBRL-MR-03027, June 1980 (AD A089646).

3. W. P. D'Amico, W. H. Clay, and A. Mark, "Diagnostic Tests for Wick-Type Payloads and High-Viscosity Liquids," U.S. Ballistic Research Laboratory, Aberdeen Proving Ground, Maryland, BRL Memorandum Report ARBRL-MR-02913, April 1979 (AD A072812).

4. W. P. D'Amico and W. H. Clay, "High Viscosity Liquid Payload Yawsonde Data for Small Launch Yaws," U.S. Ballistic Research Laboratory, Aberdeen Proving Ground, Maryland, BRL Memorandum Report ARBRL-MR-03029, June 1980 (AD A088411).

5. W. P. D'Amico and R. J. Yalamanchili, "Yawsonde Tests of the 8-Inch XM877 Binary Projectile: Phase I," U.S. Ballistic Research Laboratory, Aberdeen Proving Ground, Maryland, BRL Memorandum Report in preparation.

6. W. P. D'Amico, "Aeroballistic Testing of the XM825 Projectile: Phase III, High Muzzle Velocity and High Quadrant Elevation," U.S. Ballistic Research Laboratory, Aberdeen Proving Ground, Maryland, BRL Memorandum Report ARBRL-MR-03196, September 1982 (AD B068511L).

7. C. H. Murphy, "Angular Motion of a Spinning Projectile With a Viscous Liquid Payload," U.S. Ballistic Research Laboratory, Aberdeen Proving Ground, Maryland, BRL Memorandum Report ARBRL-MR-03194, August 1982 (AD A118676). (See also Journal of Guidance, Control, and Dynamics, Vol. 6, No. 4, July-August 1983, pp. 280-286.)

8. C. H. Murphy, "Liquid Payload Roll Moment Induced by a Spinning and Coning Projectile," U.S. Ballistic Research Laboratory, Aberdeen Proving Ground, Maryland, BRL Technical Report ARBRL-TR-02521, September 1983 (AD A133684).

9. M. C. Miller, "Flight Instabilities of Spinning Projectiles Having Nonrigid Payloads," Journal of Guidance, Control, and Dynamics, Vol. 5, March-April 1982, pp. 151-157.

10. W. P. D'Amico and M. C. Miller, "Flight Instability Produced by a Rapidly Spinning, Highly Viscous Liquid," Journal of Spacecraft and Rockets, Vol. 16, January-February 1979, pp. 62-64.

REFERENCES (Continued)

11. C. H. Murphy, "Effect of Large High-Frequency Angular Motion of a Shell on the Analysis of its Yawsonde Records," U.S. Ballistic Research Laboratory, Aberdeen Proving Ground, Maryland, BRL Memorandum Report ARBRL-MR-2581, February 1976 (AD B009421L).

12. W. P. D'Amico, "Yawsonde Tests for Prototype 155mm Shell Using High Viscosity and Non-Newtonian Liquids," U.S. Ballistic Research Laboratory, Aberdeen Proving Ground, Maryland, BRL Memorandum Report in preparation.

LIST OF SYMBOLS

a	radius of liquid payload cavity
c	half-height of liquid payload cavity
C_{LRM}	liquid roll moment coefficient
C_{LSM}	liquid side moment coefficient
$C_{M_{p\alpha}}$	Magnus moment coefficient
$C_{M_q} + C_{M_{\dot{\alpha}}}$	pitch damping moment coefficient
C_{SMA}	aerodynamic equivalent side moment coefficient
C_{SMEQ}	total equivalent side moment coefficient
I_x	axial moment of inertia of projectile
K_1	magnitude of the coning motion
K_{10}	initial value of K_1
ℓ	reference length
m_L	mass of liquid in a fully filled payload cavity
p	roll rate in inertial axes
Re	$\equiv pa^2/\nu$, Reynolds number
S	reference area
t	time
V	magnitude of projectile's velocity
XYZ	inertial axes, X-axis tangent to trajectory
X'Y'Z'	sun fixed projectile axes, X'-axis along missile, X'Z' plane contains missile axis and the sun
α	incidence of projectile, cone semi-angle
$\dot{\gamma}$	coning rate in sun-fixed axes
Γ	$\phi_1 + \phi_A + \phi^*$
ε	growth rate/$\dot{\phi}_1$

ν	dynamic viscosity
ρ	air density
σ	ratio of axial to transverse moments of inertia
σ_L	$2\, m_L a^2 p / \rho S \ell^2 V$
σ_{NT}	complementary solar aspect angle of velocity vector
τ	$\dot{\phi}_1/p$, nondimensional coning rate
$\dot{\phi}$	roll rate, measured in sun fixed axes
$\dot{\phi}_A$	roll rate of sun fixed axes
$\dot{\phi}_1$	coning rate in inertial axes
ϕ^*	phase angle of coning motion, a function of sun position relative to the velocity vector

DISTRIBUTION LIST

No. of Copies	Organization
12	Administrator Defense Technical Information Center ATTN: DTIC-DDA Cameron Station Alexandria, VA 22314
1	Commander US Army Materiel Development and Readiness Command ATTN: DRCDMD-ST 5001 Eisenhower Avenue Alexandria, VA 22333
1	Commander US Army Armament, Munitions and Chemical Command ATTN: DRSMC-TDC(D) Dover, NJ 07801
2	Commander US Army Armament, Munitions and Chemical Command ATTN: DRSMC-TSS(D) Dover, NJ 07801
1	Commander US Army Armament, Munitons and Chemical Command ATTN: DRSMC-LC(D) Dr. J. T. Frasier Dover, NJ 07801
1	Commander US Army Armament, Munitions and Chemical Command ATTN: DRSMC-CAWS- (D) Mr. Della'erga Dover, NJ 07801
2	Commander US Army Armament, Munitions and Chemical Command ATTN: DRSMC-LCA-F(D) Mr. D. Mertz Mr. A. Loeb Dover, NJ 07801
1	Commander US Army Armament, Munitions and Chemical Command ATTN: DRSMC-LEP-L(R) Rock Island, IL 61299
1	Director ARDC, USA AMCCOM Benet Weapons Laboratory ATTN: DRSMC-LCB-TL(D) Watervliet, NY 12189
1	Commander US Army Aviation Research and and Development Command ATTN: DRDAV-E 4300 Goodfellow Blvd St. Louis, MO 63120
1	Director US Army Air Mobility Research and Development Laboratory Ames Research Center Moffett Field, CA 94035
1	Commander US Army Communications Research and Development Command ATTN: DRSEL-ATDD Fort Monmouth, NJ 07703
1	Commander US Army Electronics Research and Development Command Technical Support Activity ATTN: DELSD-L Fort Monmouth, NJ 07703
1	Commander US Army Missle Command ATTN: DRSMI-R Redstone Arsenal, AL 35898
1	Commander US Army Missile Command ATTN: DRSMI-YDL Redstone Arsenal, AL 35898

DISTRIBUTION LIST

No. of Copies	Organization
1	Commander US Army Tank Automotive Comma ATTN: . TA-TSL Warren, MI 48090
1	Director US Army TRADOC Systems Analysis Activity ATTN: ATAA-SL White S ds Missile Range NM 880
2	Director US Army Dugway Proving Ground ATTN: STEDP-MT Dugway, UT 84022
1	Commander US Army Yuma Proving Ground ATTN: STEYP-MTW MAJ. S. Thorlin Yuma, AZ 85365
1	Commandant US Army Field Artillery School ATTN: ATSF-CD-MW LT Bryan Ft. Sill, OK 73503
1	Commandant US Army Field Artillery School ATTN: ATZR-BD-WT CPT Dawson Ft. Sill, OK 73503
2	Commandant US Army Infantry School ATTN: ATSH-CD-CSO-OR Fort Benning, GA 31905
1	AFWL/SUL Kirtland AFB, NM 87117

No. of Copies	Organization
2	Director Sandia Laboratories ATTN: Mr. H. R. Vaughn Dr. W. Oberkampf Albuquerque, NM 87115

Aberd Proving Ground

No. of Copies	Organization
	Director, USAMSAA ATTN: DRXSY-D DRXSY-MP, Mr. H. Cohen
	Commander, USATECOM ATTN: DRSTE-TO-F DRSTE-CM-F Mr. Gibson (2 cys)
	PM-SMOKE, Bldg. 324 ATTN: DRCPM-SMK-M (MAJ Gober)
	Commander, USACRDC USA AMCCOM ATTN: DRSMC-CLN Mr. W. Dee Mr. G. Jeffers
	Commander, USACRDC USA AMCCOM ATTN: DRSMC-CLB-PA Mr. M. C. Miller DRSMC-CLJ-L DRSMC-CLB-PA DRSMC-CLN

USER EVALUATION OF REPORT

Please take a few minutes to answer the questions below; tear out this sheet, fold as indicated, staple or tape closed, and place in the mail. Your comments will provide us with information for improving future reports.

1. BRL Report Number ______________________

2. Does this report satisfy a need? (Comment on purpose, related project, or other area of interest for which report will be used.)

____

____

____

3. How, specifically, is the report being used? (Information source, design data or procedure, management procedure, source of ideas, etc.) ______________________

____

____

4. Has the information in this report led to any quantitative savings as far as man-hours/contract dollars saved, operating costs avoided, efficiencies achieved, etc.? If so, please elaborate.

____

____

5. General Comments (Indicate what you think should be changed to make this report and future reports of this type more responsive to your needs, more usable, improve readability, etc.) __________

____

____

____

6. If you would like to be contacted by the personnel who prepared this report to raise specific questions or discuss the topic, please fill in the following information.

Name: ______________________

Telephone Number: ______________________

Organization Address: ______________________

____

____

FOLD HERE

Director
US Army Ballistic Research Laboratory
ATTN: DRSMC-BLA-S (A)
Aberdeen Proving Ground, MD 21005

NO POSTAGE NECESSARY IF MAILED IN THE UNITED STATES

OFFICIAL BUSINESS
PENALTY FOR PRIVATE USE, $300

BUSINESS REPLY MAIL
FIRST CLASS PERMIT NO 12062 WASHINGTON, DC

POSTAGE WILL BE PAID BY DEPARTMENT OF THE ARMY

Director
US Army Ballistic Research Laboratory
ATTN: DRSMC-BLA-S (A)
Aberdeen Proving Ground, MD 21005

FOLD HERE